THE ROLE OF RAB GTPASES IN THE ENDOLYSOSOMAL SYSTEM OF *S. CEREVISIAE*

Daniel F. Markgraf

DISSERTATION

SUBMITTED TO THE

COMBINED FACULTIES FOR THE NATURAL SCIENCES AND FOR MATHEMATICS

OF THE RUPERTO-CAROLA UNIVERSITY OF HEIDELBERG, GERMANY

FOR THE DEGREE OF

DOCTOR OF NATURAL SCIENCES

presented by

Diplom-Biologe Daniel Frank Markgraf

born in Berlin, Germany

Oral examination:

THE ROLE OF RAB GTPASES IN THE ENDOLYSOSOMAL SYSTEM OF *S. CEREVISIAE*

Referees: Prof. Dr. Michael Brunner

Prof. Dr. Christian Ungermann

Declaration

I herewith declare that I wrote this thesis independently and used no other sources and aids than those indicated.

October 16th, 2008

_____

(Daniel Markgraf)

„…I revise my record of these adventures once more. Not a fact has been omitted, not a detail exaggerated. It is a faithful narrative of this incredible expedition in an element inaccessible to man, but to which Progress will one day open a road “

—*Jules Verne in „20.000 Leagues under the sea“*

Acknowledgments

Life can take many different routes. I was so far lucky to pick one of the right ones, which I define as one that prevents me from any harm and which allows for a desirable, independent life. I am aware that this is a privilege and that judging the track that lies behind you is strongly influenced by the people that joined you on your way. In this regard, again, I think that I chose one of the right routes when I decided to join Christian's lab and started my PhD in Heidelberg. I would like to thank Christian for his constant support that allowed me to develop my skills and to regard science as a noble, pure and honest subject far beyond daily bench work. I want to thank also my colleagues, especially the "old" Heidelberg-crew, a colourful mixture of characters that made my PhD an enjoyable part of life. All this couldn't have been achieved without the ongoing support of my family. My optimistic view results from their strong believe in me, my skills and the decisions I make. Finally, the path I took became exceptionally valuable since I follow it together with my wife Vesna and our daughter Lea Ava. The fortune of having them at my site makes me looking ahead with a smile.

Table of Contents

Summary

The evolution of the eukaryotic cell was accompanied by the development of an elaborate endomembrane system. Maintenance of distinct features of each organelle is achieved by transport vesicles that constantly bud from donor membranes and fuse with target membranes. Rab GTPases together with tethering factors mediate first specific contact between membranes destined for fusion. Whereas components of the vacuolar tethering system have been identified in the endolysosomal system, little is known about tethering of prevacuolar, endosomal structures. In my research, I focused on the endosomal Rab5 homolog Vps21 and its interplay with the putative endosomal tethering complex CORVET. I was able to show that the hexameric CORVET complex interacts with the endosomal Rab GTPase Vps21. Whereas the whole complex binds the active form of Vps21, its inactive, GDP-bound form is preferentially recognized by the CORVET subunit Vps3. Further binding studies showed that the CORVET subunit Vps8 directly binds to Vps21-GTP, revealing its identity as effector subunit of CORVET. Consistent with this, the correct localization of Vps8 clearly depends on Vps21 and is regulated by the nucleotide binding state of this GTPase. Based on an *in vivo* approach that allows monitoring of late endosomal tethering events, I could show that Vps8 and Vps21 functionally interact to mediate endosomal tethering. Furthermore, Vps8 and Vps21, together with two other subunits of the CORVET complex, Vps3 and Vps16, were shown to be the minimal molecular requirement for tethering of late endosomal membranes. The results presented in this study indicate that the sequential recruitment of Vps8 to Vps21-positive late endosomes initiates tethering and leads to further assembly of the CORVET complex that dictates successive fusion events.

Zusammenfassung

Die Evolution der eukaryotischen Zelle wurde durch die Entwicklung eines umfassenden Endomembransystems begleitet. Die Aufrechterhaltung der spezifischen Eigenschaften jedes einzelnen Organells wird durch Transportvesikel, die sich fortwährend von Donorkompartimenten abschnüren und mit Zielkompartimenten fusionieren, gewährleistet. Rab GTPasen, zusammen mit Tethering-Faktoren, vermitteln den ersten spezifischen Kontakt zwischen Membranen („Tethering“) vor dem eigentlichen Fusionsprozess. Während im endolysosomalen System Komponenten der vakuolären Tethering-Maschinerie identifiziert wurden, ist nur wenig über Tethering von prevakuolären, endosomalen Strukturen bekannt. In meiner Forschungsarbeit habe ich die Funktion der Rab5 homologen GTPase Vps21 und deren Wechselwirkung mit dem mutmaßlichen Tethering Komplex CORVET untersucht. Ich konnte zeigen, daß der hexamere CORVET Komplex mit der endosomalen Rab GTPase Vps21 interagiert. Während der gesamte Komplex mit der aktiven Form von Vps21 interagiert, wird die inaktive GDP-Form vorzugsweise von der CORVET Untereinheit Vps3 gebunden. Weitere Bindungsstudien haben gezeigt das die CORVET-Untereinheit Vps8 direkt mit Vps21-GTP interagiert. Vps8 konnte so als Vps21-Effektoruntereinheit des CORVET Komplexes identifiziert werden. In Übereinstimmung mit diesen Ergebnissen ist die korrekte Lokalisierung von Vps8 abhängig von Vps21 und wird über die alternierende Bindung der Nukleotide GDP oder GTP reguliert. Basierend auf *in vivo* Experimenten, die die Beobachtung von endosomalen Tethering Prozessen ermöglichen, konnte gezeigt werden, daß Vps8 und Vps21 auch funktional interagieren und dadurch Tethering von endosomalen Strukturen bewerkstelligt wird. Weiterhin zeigte sich, daß

Vps8 und Vps21, zusammen mit den CORVET Untereinheiten Vps3 und Vps16, die minimal erforderlichen molekularen Komponenten des endosomalen Tethering Systems darstellen. Die in dieser Studie vorgestellten Daten lassen darauf schließen, daß Tethering durch die sequentielle Rekrutierung von Vps8 an Vps21-positive späte Endosomen initiiert wird und die weitere Assemblierung des CORVET Komplexes die folgenden Fusionsprozesse determiniert.

List of Publications/Manuscripts

Markgraf, D.F., Peplowska, K., Mari, M., Griffith, J., Reggiori, F., and Ungermann, C. (2008) Direct interaction of the CORVET subunit Vps8 and the Rab5 GTPase Vps21 tethers late endosomal compartments. In revision for *The Journal of Cell Biology*

Peplowska, K., Markgraf, D.F., Ostrowicz, C.F., Bange, G., and Ungermann, C. (2007) The CORVET tethering complex interacts with the yeast Rab5 homolog Vps21 and is involved in endo-lysosomal biogenesis. *Dev. Cell* **12**, 739-750

Markgraf, D.F**.**, Peplowska, K., and Ungermann, C. (2007) Rab cascades and tethering factors in the endomembrane system. *FEBS Lett* **581**, 2125-2130

Hou, H., Subramanian, K., LaGrassa, T.J., Markgraf, D., Dietrich, L.E.P., Decker, N., and Ungermann, C. (2005) The DHHC protein Pfa3 affects vacuole-associated palmitoylation of the fusion factor Vac8. *Proc Natl Acad Sci USA* **102**, 17366-17371

1 Introduction

The diversity of life that allows organisms to populate a variety of ecological niches on this planet originates from the strong capability of cells to adapt and develop according to environmental needs. A remarkable step during evolution was the emergence of the eukaryotic cell, which finally led to the separation of single cell and multi cellular organisms. Distinct from bacteria and archae that make up the two domains of prokaryotes, eukaryotic cells have a membrane-enclosed nucleus and cytoplasmic organelles. This study is devoted to the endomembrane system of the eukaryotic cell and aims to understand how certain transport processes within this system are regulated on a molecular level.

1.1 The endomembrane system of the eukaryotic cell

Eukaryotic cells are composed of pleiomorphic organelles that divide the cell into functionally and structurally distinct compartments. Each of these organelles is enclosed by a lipid bilayer, which can be characterized by a distinct lipid composition[1] [2]. As shown in Figure 1, the main components of the endomembrane system include the endoplasmic reticulum (ER), the Golgi apparatus, the yeast vacuole/mammalian lysosome, the multivesicular body (MVB) and the plasma membrane. The high grade of complexity, compared to the simpler organisation of prokaryotes, allows cells to separate e.g. molecular synthesis, storage and transport, to specialized compartments that are optimized for each individual function. Along with their various functions, intracellular compartments possess a huge variety of different proteins and lipids.

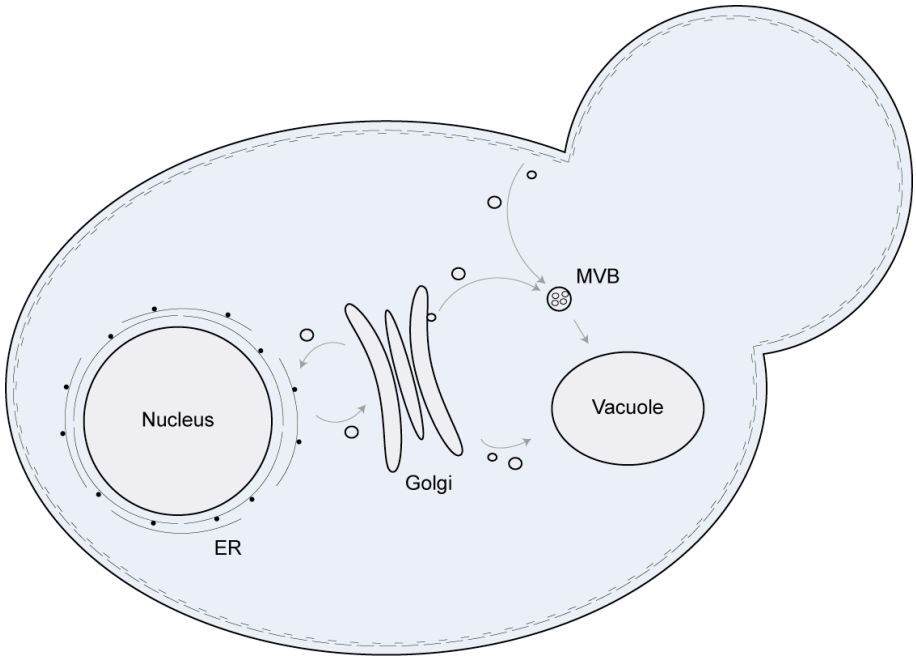

Figure 1 The endomembrane system of the eukaryotic cell
A schematic view of the endomembrane system of yeast, *S.cerevisiae*. Intracellular organelles highlighted are the nucleus, forming a continuous membrane system with the endoplasmic reticulum, the Golgi apparatus, the multivesicular body (MVB), the yeast vacuole and transport vesicles.

1.1.1 Intracellular organelles

In contrast to prokaryotes, DNA in eukaryotes is clearly separated from the cytosol by a continuous membrane system that comprises the nuclear envelope and the endoplasmic reticulum. Within the nucleus DNA replication and transcription takes place, whereas newly synthesized, secretory and plasma membrane proteins are co-translationally translocated into the lumen of the ER or inserted into the ER membrane. Lumenal chaperones within the ER recognize incorrectly folded proteins as well as protein subunits that have not yet assembled and thus support proper folding of these proteins. Most of the newly synthesized soluble and membrane-bound proteins in the ER are N-glycosylated. Recent efforts have shown that elaborate systems within the ER

i) ensure proper folding of newly synthesized proteins ii) coordinate the response to varying levels of unfolded proteins[3] (UPR; unfolded protein response) and iii) subsequently dispose misfolded proteins by handing them over to the cytosolic proteasome system[4] (ERAD; ER-associated protein degradation). Besides being the entrance for proteins into the secretory pathway (see section 1.4) the endoplasmic reticulum also has a central role in lipid biosynthesis.

The Golgi apparatus was identified in 1897 by an Italian physician named Camillo Golgi. In mammalian cells, it consists of a stack of flattened, membrane-enclosed cisternae and is located near to the cell nucleus. The Golgi apparatus is divided into the *cis*-Golgi, facing the endoplasmic reticulum and the *trans*-Golgi facing the plasma membrane. Both are associated with tubular and cisternal structures: the *cis*-Golgi network (CGN) and the *trans*-Golgi network (TGN)[5]. This organelle plays an important role as sorting station for proteins that, in addition, become successively modified (N-glycosylation) during their passage through the different Golgi cisternae[5-7]. Noteworthy, the yeast Golgi apparatus is not organized as stacked compartment.

The yeast vacuole is analogous to the mammalian lysosome and serves as the main storage and degradative organelle. It is the final station of several transport pathways and thus is constantly receiving cargo[8 9]. Vacuoles contain a variety of hydrolytic enzymes, i.e. nucleases, phosphatases, lipases and proteases that are active under acidic conditions (pH approx. 5) prevailing in the vacuolar lumen. By degrading receptor proteins of the plasma membrane that are delivered to the vacuole, this organelle plays an important role in the down regulation of these receptors and thus in regulating signalling processes. Vacuoles are highly dynamic compartments. They undergo fission and fusion processes in response to osmotic stress to balance homeostasis of the cell[10]. In addition, the morphology of the vacuole is coordinated with

the cell cycle[11]. During G1, vesicular-tubular structures emanates from the vacuole of the mother cell, move into the emerging daughter cell where they fuse and thereby regenerate the vacuole. The highly dynamic nature of this organelle, together with its simple purification procedure make it a perfect model for studying membrane fusion that underlies vesicular transport[12]. Membrane enclosed vesicles are much smaller in size than all other organelles. They perform the crucial task of maintaining the different compartments by shuttling proteins and lipids between them.

1.1.2 Cellular membranes

Lipids, besides proteins are one of the major building blocks of life. Being composed of polar headgroups and hydrocarbon chains, these molecules are water-insoluble and tend to form thin molecular bilayers in aqueous solutions[13]. Membranes create essential boundaries between intracellular organelles and the cytoplasm as well as between whole cells and the surrounding environment. As shown in Figure 2, the modification of the main three classes of lipids results in a variety of lipids. Studying lipids in more detail revealed a role for these molecules beyond being the structural basis of cellular membranes[14]. Consistent with their emerging, diverse cellular functions, lipids are not equally distributed throughout membranes of the endomembrane system[13]. Sterols, sphingolipids and saturated glycerolipids are enriched in the plasma membrane.

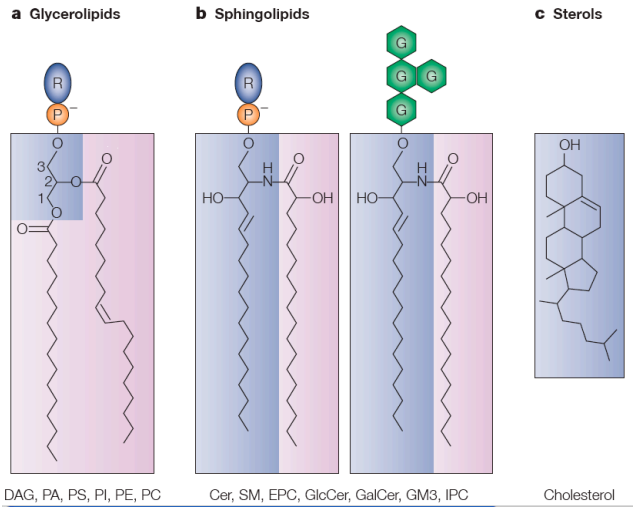

Figure 2 Membrane lipids of the eukaryotic cell
(a) Glycerolipids; Two C16-C18 fatty acid chains are bound to glycerol via an esther bond (diacylglycerol, DAG). The third –OH group is linked to a phosphate group (phosphatidic acid, PA) which itself can be bound to serine (PS), inositol (PI) ethanolamine (PE) or choline (PC). (b) Sphingolipids; The C18 sphingosine backbone is amide linked to a C16-C26 saturated fatty acid whereas its headgroup (R) either can be phosphocholine (sphingomyelin SM), phosphoethanolamine (EPC). Headgroups of glycosphingolipids can be glucose (glucoseceramide GlcCer) or galactose (galactoseceramide GalCer). Further addition of monosaccharides creates a variety of glycosphingolipids (e.g. GM3). (c) Sterols; A planar four-ring-structure. Cholesterol in mammals, Ergosterol in fungi. Adapted from Holthuis and Levine[13].

Their high packaging density explains its impermeability, an important feature of a membrane that serves as barrier to the extracellular space. Interestingly, lipids of the plasma membrane are asymmetrically distributed between the two leaflets of the bilayer. The aminophospholipids phosphatidylserine and – ethanolamine are mainly found in the cytosolic leaflet, whereas the exoplasmic leaflet is mainly composed of sphingolipids[15 1]. Energy-driven lipid translocases, so called flippases, maintain the asymmetry of the plasma membrane[16], and loss of the imbalance between the bilayer leaflets results in severe defects in cellular processes. Contrary, the endoplasmic reticulum membrane shows a symmetric distribution of lipids and consists mainly of

unsaturated glycerophospholipids. This flexible membrane therefore allows insertion of newly synthesized proteins[1].

Phosphoinositides (PtdIns), phosphorylated derivatives of phosphatidylinositol (PI), play an important role in membrane trafficking[17 18]. The phosphorylation of the inositol head group at different positions leads to a huge variety of derivatives that localize to distinct intracellular compartments (Figure 3).

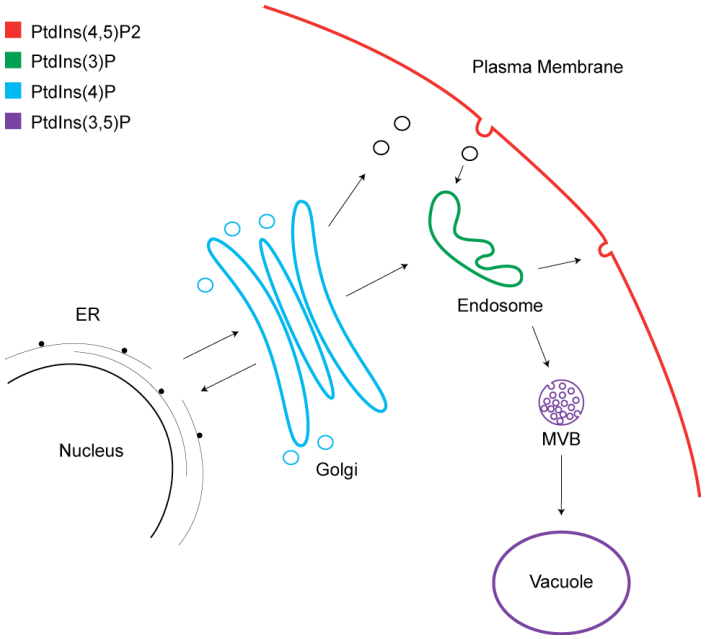

Figure 3 Cellular distribution of phosphoinositides
Different species of PtdIns characterize membranes of distinct organelles. PtdIns(4)P is the major phosphatidylinositol derivative found at the Golgi whereas PtdIns(4,5)P_2 is detected mainly at the plasma membrane. PtdIns(3)P is concentrated on early endosomes. Multivesicular bodies and the vacuole are enriched in PtdIns(3,5)P_2. Small amounts of phosphoinositides are found in the ER and the nucleus, though their precise role there is not known.

Important for the understanding of the regulative function of PtdIns in membrane trafficking was the identification of specific PtdIns binding domains within proteins required for membrane trafficking. The pleckstrin homology (PH) domain preferentially binds to PtdIns(4,5)P_2, found at the plasma membrane, whereas the phox (phagocyte

oxidase) homology domain, PX domain, mediates binding of proteins to PtdIns(3)P, the major PtdIns on endosomes[19]. Membrane binding of proteins containing either of these PtdIns binding domains depends on lipid binding as well as protein-protein interactions. Another domain that binds to PtdIns(3)P is a type of Zn^{2+} finger, the FYVE domain[20]. It is mostly found in proteins that function in endocytosis and localizes these to endosomes. ENTH (epsin1 NH_2-terminal homology) domains represent another domain that binds to PtdIns(4,5)P_2. Initially identified in epsin1, this domain was found in many proteins with known roles in endocytosis[21]. Interestingly, binding of the ENTH domain to PtdIns(4,5)P_2 leads to the insertion of an amphipathic helix into the lipid bilayer, thereby generating membrane curvature which is required for budding of vesicles from the plasma membrane[22]. The strong impact of PtdIns distribution on the recruitment of proteins to specific sites of the endomembrane system leads to the question how certain PtdIns domains themselves are generated and maintained. It is now clear that a number of phosphatidylinositol modifying enzymes play an important role in this process. Specific kinases, PI 3-, PtdIns 4-, PtdIns 5-kinases, phosphorylate different PI or PtdIns substrates[23]. In yeast, the PI 3-kinase Vps34 forms a membrane associated complex with Vps15 and generates PtdIns(3)P on endosomal membranes. Both proteins were shown to be essential for sorting of proteins to the yeast vacuole[24]. At the vacuole, the PtdIns(3)P 5-kinase Fab1, converts PtdIns(3)P into PtdIns(3,5)P_2. Its kinase activity is essential for the maintenance of the vacuole[25]. It is not surprising that PtdIns are not only generated by phosphorylation but are also dephosphorylated and thus interconverted through the action of phosphatases. In summary, the precise regulation of PtdIns generation, maintenance and thus distribution plays an important role in keeping the organelle identity and ensures proper membrane trafficking by recruiting proteins of specific trafficking steps.

1.1.3 Transport pathways

To maintain compartmentalization, cells have evolved elaborate transport pathways to ensure that proteins are delivered to their specific target organelles. This section will give an overview about transport pathways between components of the endomembrane system.

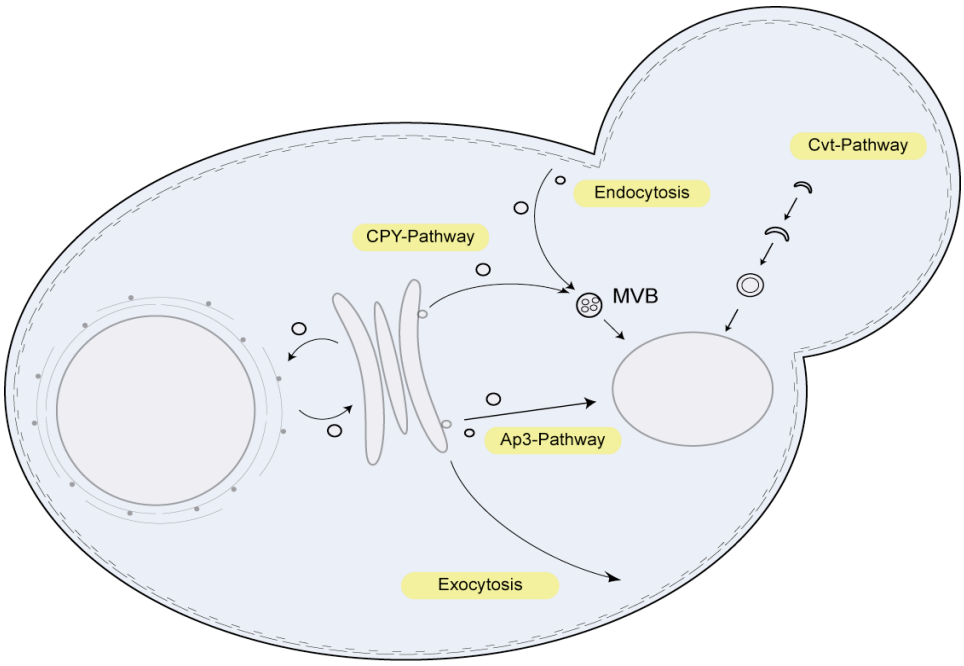

Figure 4 Transport pathways within the eukaryotic cell
Newly synthesized proteins enter the secretory pathway at the ER. COPI and COPII vesicles mediate anterograde- and retrograde transport between the ER and the Golgi. From the Golgi, proteins are transported to the vacuole either via the CPY-pathway, an indirect route via endosomal carriers, or via the AP3-pathway, which displays a direct transport route to the vacuole. Nutrients or plasma membrane proteins are transported to the vacuole via the endocytic pathway, whereas Golgi to PM transport occurs via the exocytic pathway.

ER – GOLGI TRANSPORT – Proteins destined for entering the secretory pathway are translocated into the ER lumen or inserted into the ER membrane. After having successfully passed the quality control system of the ER, these proteins are further transported to the Golgi apparatus[26]. Exit of COPII (coat protein complex II) coated

vesicles, specific carriers that mediate anterograde transport to the Golgi, takes place at ER exit sites[27 28 29 30] (ERES). Retrograde transport from the Golgi to the ER via COPI vesicles ensures that ER resident proteins that escaped via COPII vesicles are transported back to their appropriate place of action.

EXOCYTOSIS – Contrary to endocytosis, cells also transport secretory or plasma membrane proteins to the plasma membrane and the extracellular space, respectively[31]. Exocytic vesicles bud from the TGN and are directed to the PM via a direct transport route.

CPY-PATHWAY – Named after the carboxypeptidase Y (CPY), a soluble vacuolar hydrolase that led to the identification of this transport route, this pathway transports cargo from the TGN to the vacuole via an endosomal prevacuolar compartment (PVC)[32]. CPY is recognized in the TGN by a specific receptor, Vps10, and subsequently delivered to the PVC[33 34]. After arrival, Vps10 is recycled back to the TGN[35] and CPY is further transported to the vacuole by fusion of the PVC with the vacuole. Details of this step will be discussed in section 1.4.

ALP-PATHWAY – An alternative route from the TGN to the vacuole is used by the alkaline phosphatase (ALP)[36]. This direct route bypasses the prevacuolar compartment, as revealed by studies showing that ALP sorting is not affected by mutants that block PVC to vacuole transport[37]. Typical cargo proteins that take this route to the vacuole include the SNARE protein Vam3 and the casein kinase Yck3[38 39 40]. Because of the involvement of the adaptor protein complex AP-3, this pathway is alternatively referred to as the AP-3 pathway[38].

ENDOCYTOSIS – Transport of vesicles, originating at the plasma membrane by inward budding is a widely used way of cells to take up extracellular nutrients or to internalize membrane receptors to regulate signalling[41]. Endosomes mature into late endosomal structures and converge with carriers from the TGN at the level of the PVC before being further delivered to the vacuole.

CVT-PATHWAY – Cytosol-to-vacuole transport (Cvt) occurs independently from the secretory pathway[32]. The cytosolic precursor of aminopeptidase I (prAPI) oligomerizes into homodecamers and is packed into de novo forming double-membrane enclosed vesicles[42]. The source of the newly forming membrane still remains unclear. Cvt vesicles are delivered to the vacuole and after fusion release their content into the vacuolar lumen where prAPI is processed and gains full activity. The Cvt pathway is specific, saturable and constitutively active. Autophagy, a delivery pathway used to transport proteins and organelles to the vacuole for degradation uses a similar machinery, but is non-specific and only induced under starvation conditions[32 43].

1.2 Membrane Trafficking

To maintain identity and functionality of the various organelles, cells have evolved an elaborate transport system to shuttle cargo between individual compartments. The basic transport unit in this system are membrane enclosed vesicular carriers that are generated at a donor compartment and fuse with an appropriate acceptor compartment. Vesicular transport, however, is a complex process, which can be dissected into multiple sub-processes. This section will describe general principles of vesicular transport.

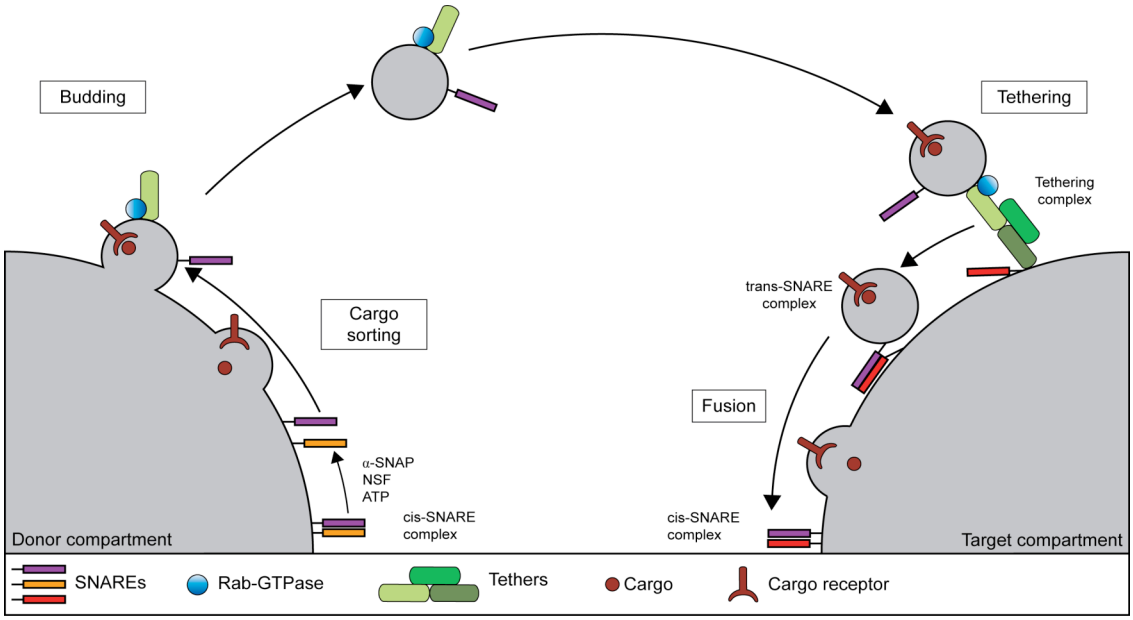

Figure 5 General principles of vesicular transport
Vesicular transport can be dissected into sub-processes. Cargo is sorted into newly forming vesicles at the donor compartment. Budding involves coat proteins that interact with sorting signals on cytoplasmic domains of transmembrane cargo proteins or on membrane receptors of soluble cargo proteins. After transport to its target compartment, first specific contact between vesicle and target membrane (membrane tethering) is mediated by Rab GTPases and tethering factors. SNARE proteins of opposing membranes form *trans*-complexes and thus drive fusion of the vesicle with the target membrane.

1.2.1 Cargo sorting

The underlying aim of membrane trafficking is the transport of soluble and membrane proteins as well as lipids between organelles of the endomembrane system. Thus, an important step preceding vesicle formation is the correct sorting of cargo into emanating vesicles. Two models of how cargo proteins exit compartments have been discussed intensively. In a first scenario, proteins leave a compartment via transport vesicles at their prevailing concentration (bulk flow), whereas in a second scenario proteins are concentrated in forming vesicles. These two ways of sending proteins differ with regards to the machinery that is required to load vesicles.

BULK FLOW – Several studies have addressed passive sampling of cargo proteins. By measuring the rate of secretion of a glycosylated acyltripeptide, Wieland et al.[44] proposed that secretory proteins are nonselectively transported out of the ER. However, the analysis of three independent markers of bulk flow from the ER (glycosylated acyltripeptide, ER-lumenal GFP and total phospholipids) revealed that in the absence of an ER exit signal, only up to 2% of the cargo analysed was captured into COPII vesicles[45]. The nonselective, passive transport from the ER thus turns out to be very inefficient, but nevertheless is used by some proteins.

ENRICHMENT OF CARGO – In contrast to passive cargo transport, many proteins are selectively concentrated into forming vesicles. Studies on a soluble secretory protein, glycosylated pro-alpha-factor (gpα-F) revealed that it was enriched 20fold in forming vesicles leaving the ER, compared to bulk flow markers[45]. Interestingly, gpα-F packaging into vesicles was as inefficient as for bulk flow markers in the absence of Erv29, a membrane protein that was implicated in gpα-F transport[46] [45]. This result nicely demonstrates the basic principle underlying selective cargo transport. Enrichment of cargo is achieved by interactions of sorting signals on cargo proteins with a cytoplasmic coat that covers vesicles. Sorting signals are located in the cytoplasmic domain of transmembrane cargo proteins or in the cytoplasmic domain of membrane proteins that act as receptors for soluble cargo proteins[47]. In the following section I will discuss the current knowledge about sorting signals. Vesicle coats, that interact with these signal sequences are also involved in vesicle budding and will be discussed in detail in the next section.

SORTING SIGNALS – Within the endomembrane system, cargo has to be delivered to specific target compartments. Proteins destined for secretion, for example, start their

journey at the ER, similar to vacuolar hydrolases that enter the biosynthetic pathway at this compartment. Nevertheless both kinds of proteins are separated at the TGN. How is the decision whether to continue the journey to the PM or to the vacuole made? The answer is given by sorting signals, degenerated motifs of four to seven residues[48]. Especially in the field of endolysosomal transport, many questions about signal-mediated sorting could be answered.

Early studies on trafficking in the endolysosomal system revealed that sorting of proteins occurs at specialized membrane areas. These regions differ from the rest of the organelle surface in that they are covered with a proteinaceous coat. It is now well accepted that the coat proteins directly interact with sorting signals on cargo proteins. Considering the huge variety of cargo, it is not surprising that different sorting signals have been identified, which interact with different coat proteins. Sorting signal-sequences can be grouped in tyrosine-based and dileucine based sorting signals. NPXY-type sorting signals are tyrosine-based signals that mediate internalization of type I integral membrane proteins, e.g. LDL (low density lipoprotein) receptors of different species, integrin β and in the β-amyloid precursor protein (APP)[47 48]. YXX∅-type signals represent a second type of tyrosine based sorting signal, in which the ∅-position can be assigned to bulky hydrophobic side chains. Being more widely involved in cargo transport than NPXY motifs, they are found in endocytic receptors, for example the transferring receptor, lysosomal membrane proteins, LAMP-1 and LAMP-2, and proteins from the TGN, like TGN38[48]. NPXY-containing proteins are mainly internalized via clathrin-coated pits, whereas YXX∅-containing proteins are also sorted by non clathrin-coated vesicles. Clathrin is composed of three large (CHC) and 3 small (CLC) subunits that form a “triskelion” structure, which assembles into a basketlike frame of hexagons and pentagons that covers the vesicular surface[49]. The amino

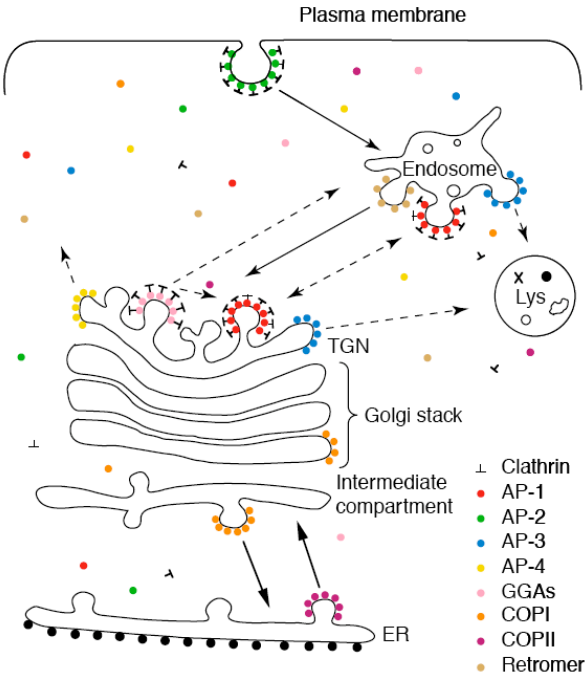

Figure 6 Coat proteins and their adaptors
Adapted from Robinson[50].

terminus of each CHC binds to adaptor proteins. As shown in Figure 6, clathrin is involved in different transport steps in the cell. Interestingly, different adaptor proteins complexes (AP-1, AP-2, GGAs) are required to recruit clathrin to different stages in the endomembrane system[50]. At the plasma membrane the AP-2 complex is situated between the clathrin lattice and the membrane (Figure 6, 7) and it was shown that this complex interacts with FXNPXY, as well as with YYX∅-containing proteins[51]. Consistent with the broader cellular distribution of YYX∅-containing proteins, this sorting signal was shown to bind also to the μ2-subunits of AP-1, AP-3 and AP-4 complexes[52] [53] [54]. These coat adaptor protein complexes act at the TGN and partially at endosomes (Figure 6) and with the exception of AP-1 are parts of non-clathrin coats.

Dileucine-based sorting signals were identified after the discovery of tyrosine-based signals and can be grouped into [DE]XXXL[LI] and DXXLL-motifs[48] [50]. [DE]XXXL[LI]-signals are conserved from yeast to mammals and are found on many type I, type II and multispanning transmembrane proteins.

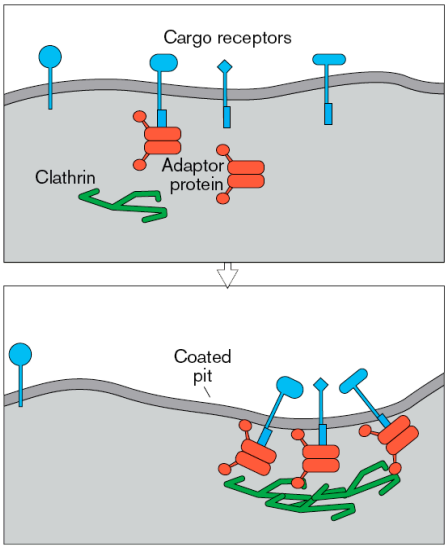

Figure 7 Cargo capturing by AP complexes and clathrin
Adaptor protein complexes bind to cargo proteins via specific signal sequences. Clathrin binds to AP-1 and AP-2 complexes, which leads to further crosslinking of the adaptor proteins and concentration of cargo proteins in the forming vesicle. Adapted from Jackson[55].

Like the tyrosine-based YYX∅-sequence, [DE]XXXL[LI]-proteins are internalized at the plasma membrane and targeted to endolysosomal compartments[48]. Consistent with the functional similarities between these two types of signals, [DE]XXXL[LI] containing proteins were shown to interact with different AP-complexes[56]. The DXXLL-sequence resembles a second type of dileucine-sorting signal. It is present in transmembrane receptors, such as the cation-independent as well as the cation-dependent mannose 6-phosphate receptor that shuttle lysosomal enzymes between the TGN and endosomes[57]. Unlike the previously mentioned signal sequences, the DXXLL-motif interacts with GGAs (Golgi-localized, γ-ear-containing, ARF-binding proteins), alternative adaptor proteins of clathrin. GGAs are found on TGN and endosomal membranes[58]. The fact that adaptor proteins like the four AP complexes and GGAs have distinct cellular distribution pattern, together with their ability to bind to specific sorting signals, explains how cargo proteins are selected into distinct types of vesicles.

The role of ubiquitin (Ub) as sorting signal that regulates internalization of plasma membrane proteins and biosynthetic delivery to the vacuole/lysosome, will be discussed in detail in section 1.4.

1.2.2 Vesicle budding

The process of vesicle budding is tightly connected to cargo sorting by a complex interplay between proteins, adaptor- and coat-proteins, involved in both steps. Here I will describe how COPI, COPII, and clathrin-coated vesicles are generated. Despite the differences between these vesicles that facilitate transport at various positions within the cell, general principles apply for the formation of all of them. As described before, vesicles of different transport routes are covered with a proteinaceous coat. Each type of coat requires the active form of a small GTPase to be recruited, and consists of two layers. The inner layer binds to the GTPase, cargo proteins, in some cases to phosphoinositides and to the outer layer. The outer layer stabilizes the inner layer and thus the overall assembly structure, allowing the vesicle to bud. Despite the similarities between these systems differences exist with regard to the composition of different layers and especially between the ways how membrane curvature in generated.

CLATHRIN-COATED VESICLES – Clathrin is the main coat protein involved in endocytosis and several transport processes originating at the TGN[59]. As described above its composition of 3 CHC and 3 CLC forms a triskelion that assembles into remarkable basket-like structures (Figure 8). The small GTPase Arf6 recruits the AP-2 adaptor complex to the plasma membrane[60], whereas Arf1 recruits AP-1 at the TGN[61]. Both adaptor complexes interact with clathrin and sorting signals of cargo proteins (see 1.2.1). In case of clathrin-mediated endocytosis, sorting signals are also recognized by the accessory adaptor proteins Dab2, ARH, epsin, Eps15, AP180/CALM and HIP1/R. With exception of Eps15 these endocytic adaptors bind to PtdIns(4,5)P_2[62 22], the main phosphatidylinositol derivative found at the plasma membrane. Clathrin forms the outer layer of the coated vesicles by binding to the adaptor complexes.

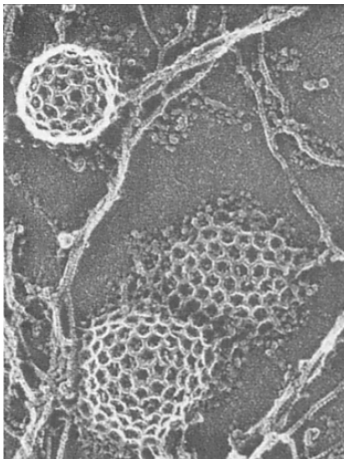

Figure 8 Formation of Clathrin-coated vesicles
Clathrin lattices at the inner surface of chicken fibroblast. Adapted from Heuser and Anderson[63].

Though it was shown that clathrin is essential for invagination of endocytic structures, the energy of clathrin polymerization into the curved polyhedral structure is not sufficient to bend the membrane. Epsin, a protein that inserts an amphipathic helix upon binding of its ENTH domain to PtdIns(4,5)P_2 might act together with clathrin to bend membranes[64 65 66]. Additional proteins that are discussed to be involved in membrane bending are EFC/F-BAR proteins[67]. These proteins were shown to induce membrane tubulation *in vitro* and *in vivo* and are required for endocytosis[68 69]. Scission of the emerging vesicles involves the GTPase dynamin and components of the actin cytoskeleton. Dynamin forms a contractile ring around the neck and its nucleotide dependent contraction, accompanied by twisting is supposed to mediate fission of the vesicle. Myosin motors that link actin filaments to the endocytic machinery add to this process by a pulling mechanism[70].

COPI AND COPII TRANSPORT – Transport between the first compartments of the secretory pathway, the ER and the Golgi occurs bidirectional. Anterograde transport is mediated by COPII-[71 72 73], whereas retrograde transport, to retrieve ER resident proteins and recycle the vesicle formation and fusion machinery, is mediated by COPI vesicles[74 75 79]. In both cases, coat proteins are recruited by active GTPases. Inactive Arf1 (COPI) and Sar1 (COPII) are cytosolic and expose an amphipathic helix upon activation, which leads to their membrane recruitment. The COPII coat assembles sequentially. Active Sar1 recruits the heterodimers Sec23/24 onto which the outer layer

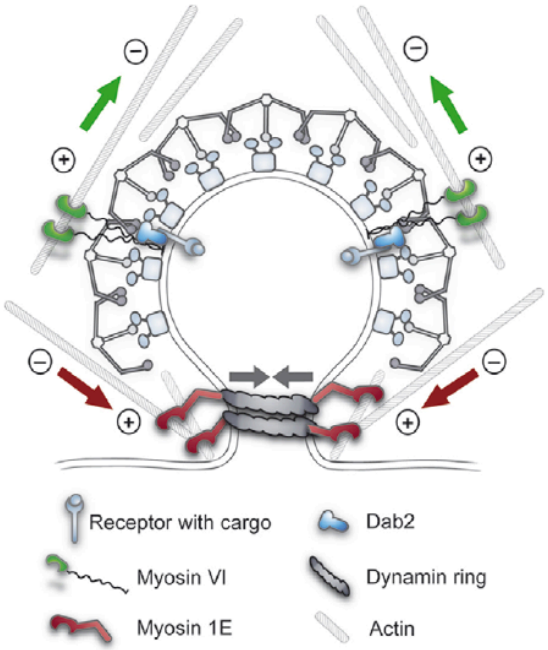

Figure 9 Scission of clathrin-coated vesicles
Scission of clathrin-coated vesicles is mediated by the concerted action of the GTPase dynamin and components of the cytoskeleton. Adapted from Ungewickel and Hinrichsen[70].

composed of Sec13/31 dimers assembles. Contrary, the COPI coat, which is structurally related to the AP complexes, is recruited by Arf1 as preassembled unit[76]. Coat disassembly after vesicle formation is achieved by the activity of GTPase activating proteins (GAPs). Transferring the coat recruiting GTPases into their inactive, cytosolic state destabilizes the overall coat structure and finally leads to disassembly. In case of the COPII coat, the Sec23 subunit exhibits GAP activity towards Sar1[77] whereas cytosolic ArfGAP1 inactivates Arf1. ArfGAP1 was shown to specifically bind to highly curved membranes, thereby coupling coat disassembly to fully generated vesicles[78].

1.2.3 Vesicle Transport

Newly formed vesicles are delivered to their target compartment by transport along fibres of the cytoskeleton[80]. Movement of vesicles along actin-filaments or microtubules is mediated by specific motor proteins, such as myosins, dyneins and kinesins[81 82 83]. Interestingly, these motor proteins are connected to vesicles via a certain class of vesicle associated GTPases, Rab GTPases, that play an important role in the

process of membrane tethering (1.2.4). Thus, the consecutive steps of transport and tethering are coupled by the same factors residing on the vesicular surface

1.2.4 Membrane Tethering

The specific fusion of transport vesicles with specific target compartments is a fundamental feature of vesicular transport. How is first specific contact between membranes destined for fusion achieved and what are the factors that control this? It has been postulated that SNARE proteins, responsible for the final fusion of the vesicle with the target membrane (discussed in 1.2.5) provide specificity[84]. However, studies have shown that the disruption of SNARE function and thus fusion does not block tethering[85]. In addition, the increasing number of studies, focusing on Rab GTPases and specific tethering factors led to the now well accepted model of tethering being mediated by a complex interplay between these two factors. Membrane tethering is a reversible process. Rab GTPases as well as tethering factors are specific for individual organelles and thus for specific fusion processes. A detailed description of Rab GTPases and tethering factors will be given in section 1.3.

1.2.5 Vesicle Fusion

After being successfully transported and tethered to the correct target compartment, the vesicular membrane is in close proximity to the target membrane. Spontaneous lipid bilayer mixing is prevented by a high-energy barrier resulting from repulsive membrane charges. In addition, a tight protein network on the membrane surface does not allow for optimal contact between the two bilayers. The identification of SNARE (soluble N-ethylmaleimide-sensitive factor attachment protein receptor) proteins was a hallmark in understanding of how membrane fusion occurs. SNARE proteins contain an evolutionary conserved SNARE motif and various folded N-terminal domains. These

N-terminal domains can be grouped into i) elongated domains consisting of antiparallel three-helix bundles, ii) domains having profiling-like folds (longin domains) and iii) short and unfolded domains[86 87]. SNAREs, with only few exceptions, are anchored to membranes via a transmembrane domain. Alternative membrane anchors used by SNAREs are lipid modifications. The exocytic SNARE SNAP-25, for example is anchored to membranes by a palmitate anchor[14] and the highly conserved SNARE Ykt6 is dually palmitoylated and farnesylated[88]. The yeast vacuolar SNARE protein Vam7 contains a PX domain that mediates membrane binding via an interaction with PtdIns(3)P[89 90].

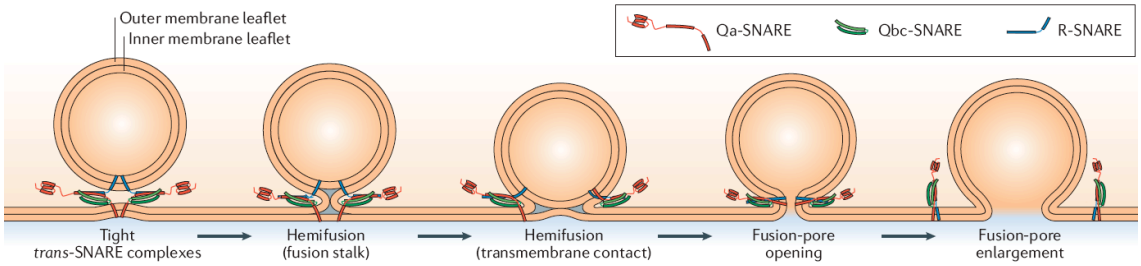

Figure 10 Stages of SNARE mediated membrane fusion
Q-SNAREs are grouped into Qa, b or c, depending on different N-terminal domains. Fusion is driven by complex formation between SNARE motifs of Qa, b, c and an R-SNARE from the opposing membrane. It occurs via a hemifusion state that is followed by fusion pore opening. Adapted from Jahn and Scheller[86].

Membranes fuse upon complex formation between the SNARE motifs of SNAREs residing in opposing membranes (Figure 10). These motifs form a stable, energetically favoured four-helix bundle, thereby overcoming the energy barrier[91]. SNAREs are separated into Q- and R-SNAREs depending on a conserved glutamine- or arginine residue at the 0-layer within the helical SNARE motif. It was shown that SNARE complexes are formed by three Q-SNAREs from one, and one R-SNARE from the opposing membrane[86]. The directed zippering of the parallel-arranged SNARE motifs,

from N- to the C-terminus drives the fusion process. As shown in Figure 10, fusion occurs via a hemifusion state in which only the two "outer" leaflets of the membranes merge. This step is followed by the opening of a fusion pore, which finally leads to the overall fusion of vesicular and target membrane. To make SNARE proteins available for further fusion events, postfusion SNARE complexes are disassembled by the action of NSF, an AAA-ATPase and its co-factor α-SNAP[92 93 94]. SNAREs can be assigned to specific fusion events within the endomembrane system and by themselves are regulated by accessory proteins. Well-described regulatory proteins include the Sec1/Munc18 (SM) family proteins. SM proteins bind to the syntaxin group of SNAREs, which contain an N-terminal three-helix bundle. Interestingly, the N-terminal domain of yeast and mammalian syntaxins involved in exocytosis can fold back on the SNARE motif thereby adopting a closed conformation[95 96]. The binding of SM proteins to SNARES that do not necessarily adopt a "closed conformation" (e.g. Tlg2, Pep12, Vam3) is arranged by the supportive activity of an N-terminal peptide residing in the SM protein[97 98 99]. Despite the consensus about the regulatory role of SM proteins in SNARE function, the precise mechanism is still under debate and differences seem to exist between SM proteins of different systems. In mammalian cells, the closed conformation of syntaxin is unable to participate in SNARE complex formation. Binding of the SM protein Munc18 to the closed conformation[100] thus inhibits fusion and exhibits a regulatory function in SNARE assembly. In contrast, Sec1-like proteins in yeast were described to positively regulate SNARE complex formation[101 102]. Unlike mammalian Munc18, yeast Sec1 recognizes and binds to Sso1 (syntaxin ortholog) in context of the respective preassembled exocytic SNARE complex[103]. Similarly, the SM protein Vps45, involved in endosome to Golgi and cytosol to vacuole transport associates with the SNARE Tlg2 and facilitates assembly of the corresponding SNARE

complex[101]. The Sec1 like protein Vps33 is a component of the vacuolar tethering complex HOPS and was shown to interact with the unpaired form of the vacuolar SNARE Vam3[104]. However, proofreading activity of the vacuolar HOPS tethering complex, by which membrane fusion based on mismatch SNARE-complexes is inhibited does not require the Vam3 N-terminal domain[105].

1.3 Rab GTPases and tethering factors

Membrane tethering is a highly regulated process and relies on the concerted interplay between Rab GTPases and tethering factors. This section will introduce and explain basic characteristics of either of these factors and finally describes the complex interplay between them.

1.3.1 Rab GTPases

Rab GTPases (Ras-like proteins in brain) form the largest branch of the Ras superfamily of small monomeric GTPases. So far, eleven Rab GTPases (Ypt/Sec4) have been described in yeast, whereas over 60 Rab proteins are known in mammalian cells[106]. The C-terminus of Rabs is posttranslationally modified (Figure 11)[107]. Rab escort proteins (REPs) present newly synthesized Rabs to a geranylgeranyltransferase, which covalently attaches two geranylgeranyl groups to two cysteine residues[108]. These highly hydrophobic groups serve as membrane anchors for the GTPase[109]. After the transfer, REPs function as chaperones that keep the prenylated Rab soluble and deliver it to the appropriate membrane. Each intracellular compartment can be characterized by specific Rab GTPases.

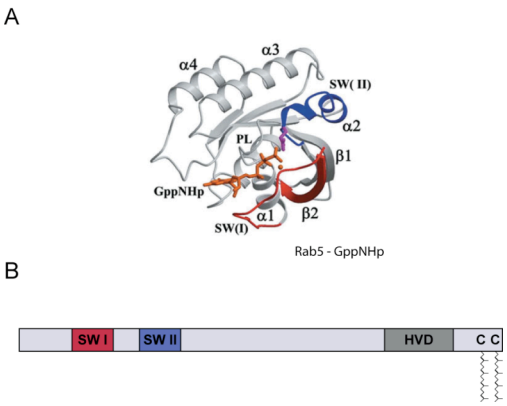

Figure 11 Structure and domain organization of Rab GTPases
A) Protein structure of the GppNHp bound, mammalian, endosomal Rab GTPase Rab5. The G domain (gray) contains the nucleotide-binding pocket and two switch regions (SWI, II) that undergo major conformational changes upon nucleotide exchange. Adapted from Zhu et al.[110] B) Domain structure of Rab GTPases. The two switch regions (SWI, II) and a hypervariable domain (HVD) are shown. Two geranylgeranyl-moieties are attached to C-terminal cysteines.

Rab GTPases are important regulators of vesicular transport and, as all GTPases, function as molecular switches. Cycling between the inactive and the active state is tightly connected to their subcellular distribution. The inactive, GDP bound form mainly resides in the cytosol where it is bound to a GDP-dissociation inhibitor (GDI; Figure 12)[111]. GDIs mask the prenyl anchor and prevent Rabs from random membrane association[112 113]. Release of the Rab from its cytosolic escort is mediated by a GDI-displacement factor (GDF), which extracts GDP bound Rab and thus allow its binding to membranes (Figure 12)[114]. In order to prevent subsequent membrane re-extraction the GTPase has to be transferred into its GTP bound state. Small G proteins bind nucleotides with high affinity and thus require additional factors to exchange GDP for GTP in order to function at physiologically required rates. Guanine exchange factors (GEFs) catalyze the dissociation of GDP. They lower the nucleotide affinity by modifying the nucleotide-binding site such that GDP is released[115]. As a result of the ten times higher cellular levels of GTP compared to GDP, the empty nucleotide-binding site is loaded with GTP. This activation of the Rab GTPase is accompanied by a conformational change, occurring mainly in the two switch regions, switch I and II, that surround the nucleotide-binding site[116](Figure 11). The active, GTP bound form provides the

structural prerequisite to interact with specific effector proteins. Among the many different effector proteins of individual Rab GTPases, tethering factors represent key interaction partners during the process of membrane tethering.

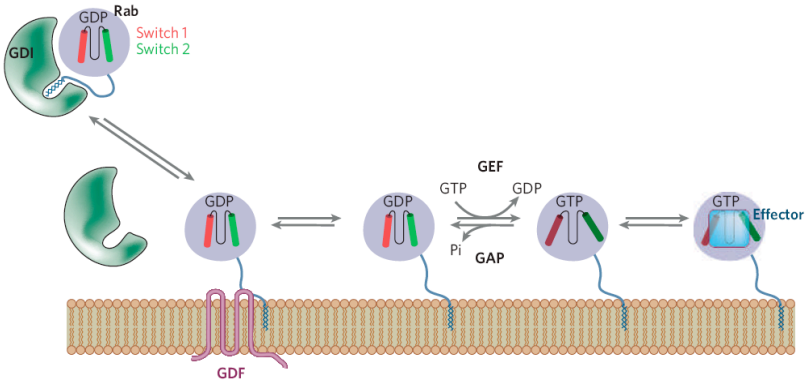

Figure 12 Dynamic cycling of Rab GTPases
Inactive, cytosolic Rab is bound to GDI. Displacement from the GDI is mediated by GDF and leads to the membrane recruitment of the Rab. After its activation by a GEF, GTP bound Rab interacts with effector proteins. GAP proteins, stimulate GTP hydrolysis and transfer the Rab GTPase into its inactive, GDP bound state, which is prone to extraction by GDI. Adapted from Behnia and Munro[117].

In order to terminate processes initiated by active Rabs, these GTPases have to be inactivated. Because of the low intrinsic GTP-hydrolysis rate, Rabs require GTPase activating proteins (GAPs) that accelerate this process by several orders of magnitude[115]. Thus, a complex interplay between Rabs, activating (GEF) and inactivating (GAPs) proteins regulate GTPase activity as well as localization.

1.3.2 Tethering factors

Important assistance for Rab GTPases during membrane tethering comes from specific tethering factors. These factors are heterogeneous in sequence and structure, with only little similarities between them. Nevertheless, many tethering factors are highly conserved with homologues being described in all eukaryotes so far examined[118].

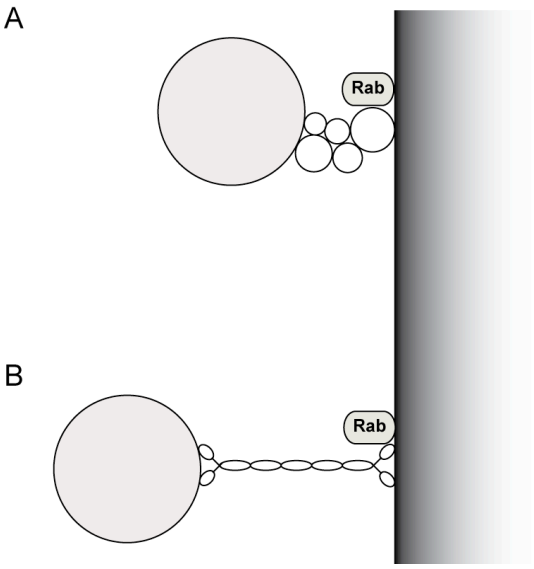

Figure 13 The two classes of tethering factors
Vesicles are tethered to the appropriate target membrane by the concerted interplay between Rab GTPases and either A) multisubunit protein tethering complexes, or B) long rod shaped, monomeric tethering factors.

Tethering factors can be grouped in two classes: long range tethers, coiled-coil proteins like EEA1 and p115/Uso1[119 120 121] and multisubunit complexes[122].

Most of the coiled-coil proteins involved in tethering events are peripheral membrane proteins and have been identified on the Golgi and endosomes. They form homodimers that are thought to capture transport vesicles in proximity of an organelle[123]. A variety of Golgi associated coiled-coil proteins, the Golgins, exist and, besides tethering, they are also thought to be involved in creating a structural meshwork that maintains the typical architecture of this organelle. Studies of Drin et al.[124] nicely demonstrated how the human Golgin GMAP-210 tethers COPI vesicles. GMAP-210 binds to active Arf1 on the flat Golgi membrane and to the vesicle surface via a curvature dependent lipid-binding motif. This ALPS (ArfGAP lipid packaging sensing) motif was initially described in ArfGAP1 and directs it to highly curved membranes of vesicles[79]. By this mechanism, Arf1 is inactivated at fully formed vesicles, leading to its membrane extraction and thus also to coat disassembly[125]. The dual binding mode of GMAP-210 thus leads to asymmetric tethering of flat and curved lipid membranes. However, this is just one example of how coiled-coil tethers work and the precise function of many others remains still unknown

In contrast to the monomeric coiled-coil tethers, multi-subunit tethering complexes are found on most organelles[126]. A number of tethering complexes, which operate at different organelles, have been identified over the last years. The COG complex operates at the Golgi[127], the GARP complex is required for endosome-Golgi transport[128], the exocyst at the Golgi-plasma membrane interface[129 130] and the Class C Vps/HOPS complex in the late endocytic pathway[131 132]. All complexes consist of multiple subunits with limited sequence identity[126]. However, structural analysis of some exocyst subunits revealed that the subunits share similar folds, which might be the basis for functional assembly during tethering[133]. Two additional complexes that seemingly do not bind Rab-GTP fall into the tethering complex family: the Dsl complex, which operates between Golgi and ER[134], and the TRAPP complex required for Golgi biogenesis[135]. For the Dsl complex, a corresponding Rab has not been identified, and TRAPP appears to be a large GEF, which cooperates with other proteins during tethering[136].

1.3.3 Rab cascades and tethering factors

The comprehensive analysis of several tethering processes revealed that maturation of organelles of the secretory/biosynthetic pathway and the endolysosomal system is often coupled to cascades of Rabs and their effectors. Within these cascades, effector proteins serve as linker between Rabs of consecutive tethering systems.

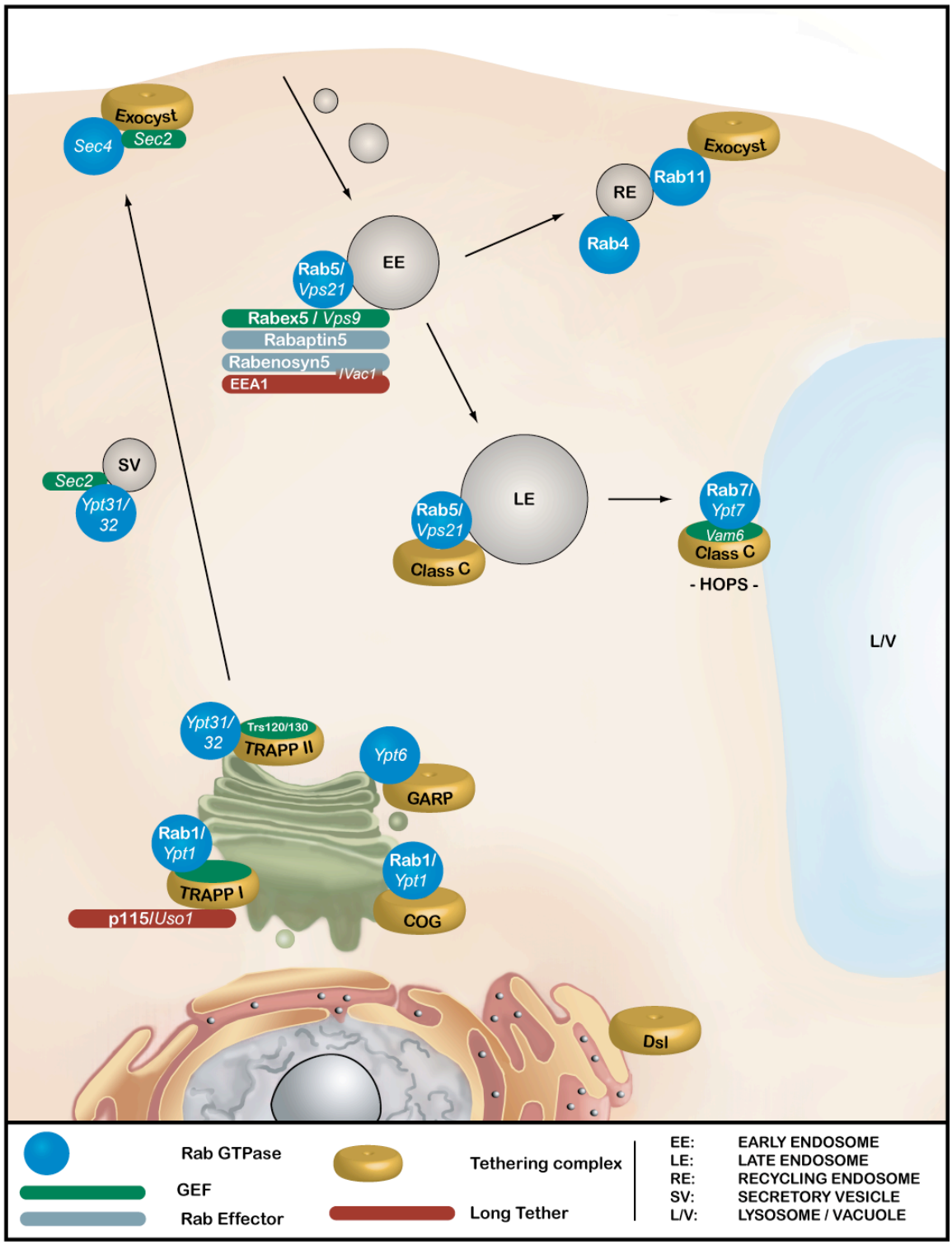

Figure 14 Intracellular distribution of Rabs, Tethering factors and effectors
Yeast genes are in italics. Adapted from Markgraf et al.[122]

ER TO TRANS-GOLGI NETWORK – Anterograde transport from the ER to the Golgi is mediated by COPII vesicles. Rab1/Ypt1, the Rab GTPase that operates in tethering processes at the Golgi is present on these vesicles and, in its active form, interacts with several effector proteins, e.g. Uso1/p115 and the COG complex[137 138]. According to a current model of tethering at the Golgi by the Sacher lab[139], Rab1/Ypt1 undergoes a repetitive cycle of activation/ inactivation during the tethering process. In a first step, p115, a large protein that belongs to the group of coiled-coil tethers interacts with ER derived vesicles in a Rab1/Ypt1-GTP dependent manner[140]. The GEF that activates Rab1/Ypt1 at the vesicular surface is so far not known. Inactivation of Rab1/Ypt1 on vesicles could lead to a conformational change of p115 allowing it to interact with the Golgi proteins GM130 and GRASP65[141 142]. Rab1/Ypt1 then would be activated again by the multisubunit complex TRAPP I, which resides at the Golgi. A possible effector of Rab1/Ypt1 at this stage could be the COG complex[138]. This octameric complex was described as tethering factor for retrograde transport from the endosome to the Golgi[127] and in addition is required for ER to Golgi transport *in vivo* and *in vitro*[143 144]. An interesting GEF switch, coupling consecutive Rab systems, is proposed for the TRAPP complex. TRAPP subunits are found in two different complexes, TRAPP I and II[145 146]. TRAPP I is composed of eight subunits, whereas TRAPP II has two additional subunits (Trs120, Trs130) and acts as GEF for the Ypt31 and Ypt32 (Ypt31/32) GTPases in Golgi to endosome transport. Recent studies showed that both complexes exhibit distinct GEF activities for Ypt1 and Ypt31, respectively[146]. It seems very likely that the TRAPP II specific subunits Trs120 and Trs130 change the GEF activity from Ypt1 towards Ypt31/32, and indeed, inactivation of Trs130 leads to mislocalization of Ypt31/32[146].

TGN TO PLASMA MEMBRANE – On secretory vesicles, activated Ypt32 recruits Sec2, which is a GEF for the Rab GTPase Sec4[147]. In a next step, Sec2 recruits Sec4 to exocytic vesicles and by activating this GTPase it initiates exocytosis. Sec4-GTP binds to the exocyst, an eight-subunit complex that tethers vesicles to the plasma membrane. Sec15, an exocyst subunit and direct effector of Sec4 could then displace Ypt32-GTP from Sec2, which consequently changes the identity of the exocytic vesicle and prepares it for fusion with the plasma membrane[148 149]. In sum, the connection of Rabs to GEFs and effectors is an underlying principle of the secretory pathway.

THE ENDOCYTIC PATHWAY – The endocytic pathway can be dissected into three distinct Rab-specific stages; the (early) endosome (Rab5), the sorting endosome (Rab4, Rab11), and the lysosome/vacuole as the target organelle for degradation (Rab7)[150]. Clathrin coated-vesicle (CCV) mediated transport in the early endocytic pathway is regulated by Rab5, a GTPase which is required for CCV-endosome and homotypic endosome fusion, whereas recycling processes, during which internalized material is transported back to the plasma membrane, are regulated by Rab4 at the level of the early endosomes and Rab11 on recycling endosomes[151 152]. During recycling, cargo transits through several compartments positive for two Rabs, e.g. Rab5/Rab4 and Rab4/11, indicating that Rab domains on organelles are not static, but merge in a dynamic manner during protein transport[106 153]. These processes depend on a complex network of Rab regulators and effectors. In the case of Rab5, a positive feedback-loop, mediated by a GEF-effector complex, is responsible for generating stable, Rab5 positive endosomal structures. Upon membrane recruitment, Rab5 gets activated by the Rabex-5 exchange factor. Rab5-GTP is then able to interact with its effector Rabaptin5, which forms a complex with Rabex-5. Interestingly, the effector stimulates the exchange

activity of Rabex-5 on Rab5[154], thereby recruiting more Rab5 and generating a Rab5-enriched domain. Rab5 also recruits phosphoinositide kinases like hVps34[155], thus promoting binding of effectors with phosphoinositide binding domains like EEA1 and Rabenosyn5, which in turn can promote early endosome fusion[121].

TRANSITION BETWEEN ENDOSOME AND VACUOLE/LYSOSOME- Internalized material destined for degradation diverges from the endosomal recycling route, regulated by Rab4 and 11. Cargo, e.g. epidermal growth factor receptor EGFR, is first internalized into Rab5 positive endosomes and is then transported to late endosomes, carrying Rab7[156 157]. Finally, proteolysis takes place in lysosomes, which can be identified by the presence of Rab7. The yeast Rab7 homolog Ypt7 has been shown to be involved in the tethering/docking process of homotypic vacuole fusion and interacts with the vacuolar tethering factor HOPS complex (homotypic vacuole fusion and vacuole protein sorting) in its GTP bound form[131]. The HOPS complex consists of four Class C proteins, Vps11, Vps16, Vps18, and the Sec1p homolog Vps33, and the two additional subunits, Vps39/Vam6 and Vps41/Vam2[131 132]. Among these subunits, Vps39/Vam6 binds the GDP-bound form of Ypt7 and stimulates nucleotide exchange on this GTPase[132]. Binding of Ypt7-GTP to the HOPS complex suggests that the complex acts as Ypt7 effector, although precise binding studies have to be performed to identify the binding interface between GTPase and effector.

Focusing on the dynamic transport of material destined for degradation leads to the question whether cargo is transferred from stable Rab5-positive endosomes to stable, Rab7 carrying late endosomes. Alternatively, Rab5 might get dynamically lost from maturing endosomes and could be replaced by Rab7 and its effectors. Zerial and colleagues showed that the endosomes can mature to lysosomes[158]. Using live-cell imaging they demonstrated that Rab5 positive organelles grew in size over time, then

lost Rab5 and its effector EEA1, but at the same time acquired Rab7. This Rab-conversion reaction seemed to be mediated by the binding of Rab5 to the lysosomal HOPS complex. Indeed, the authors showed that hVps39 was binding to Rab5-GDP. This would suggest that Rab-exchange is actually driven by a GEF with specificity for Rab5 and Rab7, since yeast Vps39 is a Rab7-specific GEF and does not bind the Rab5 homolog Vps21[132]. It is therefore likely that additional factors control the specificity of hVps39 to mediate endosome–lysosome transition in mammalian cells. Importantly, these data indicate that a Rab cascade is the basic mechanism for Rab conversion between organelles of the late endocytic pathway. Whether such a transition is also operating in yeast will be an important issue for future studies. The Class C proteins have been shown to interact with another protein, Vps8, at the endosome[159], and Vps8 has been linked to the Rab5 homolog Vps21[160]. How the Class C complex can operate at two different organelles is still an unresolved issue.

In summary, the endocytic pathway is regulated by several Rab GTPases, creating different Rab effector-domains, and as in the case of Rab5, even altered membrane composition. Nevertheless it becomes clear that during dynamic trafficking processes, Rab domains get into contact via their effectors, generating directional Rab cascades which can result in Rab conversion accompanying cargo transport and organelle maturation.

1.4 The yeast endolysosomal system

Transport processes comprising the biosynthetic route from the Golgi apparatus to the vacuole (CPY pathway) and the endocytic pathway from the plasma membrane to the vacuole, are referred to as the endolysosomal transport system (Figure 15).

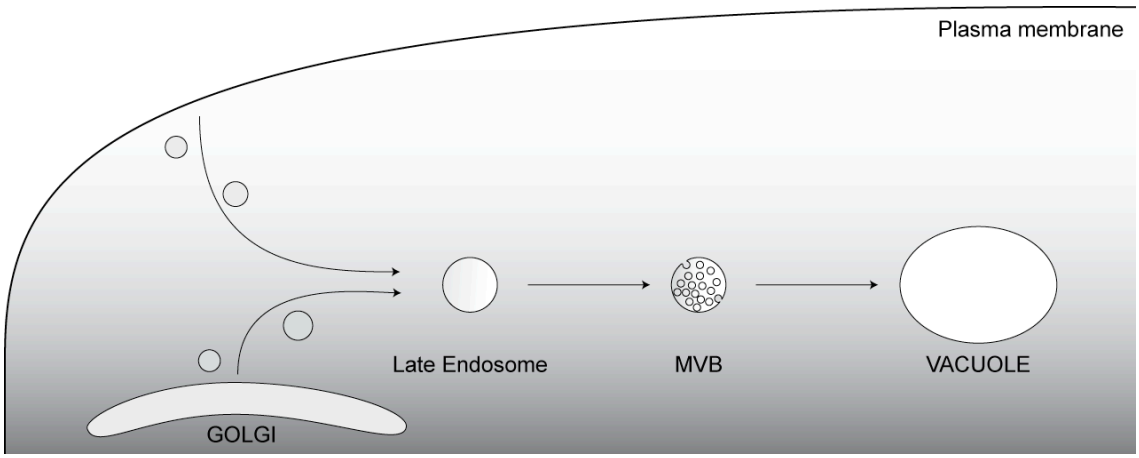

Figure 15 The endolysosomal system
Transport processes to the vacuole, originating at the TGN or the plasma membrane, together with their respective machinery, resemble the endolysosomal system. Both transport routes converge at the level of the late endosome/ multivesicular body and end at the vacuole.

1.4.1 Ubiquitin dependent sorting to the vacuole

Although originating at different sites, vesicular carriers of both pathways converge at the level of the late endosome / multivesicular body. How is the union of cargo of both pathways into one transport intermediate achieved? The identification of ubiquitin (Ub) as key signal for sorting of cargo into the proteolytic interior of the vacuole/lysosome helped to unravel the mechanism underlying TGN/PM-to-vacuole transport[161]. Ubiquitin is a small (76 amino acids), highly conserved protein, found only in eukaryotes. Within the cell it is either monomeric or covalently bound to proteins via an isopeptide bond between the carboxy-group of its C-terminal glycine and the amino-group of a lysine residue of a protein. The ubiquitination of proteins is mediated by the sequential action of three proteins. A ubiquitin-activating protein (E1) prepares Ub for the conjugation to substrate proteins. In an ATP-dependent process, Ub is first bound to E1 via a thiolesther bond and then transferred to an Ub-conjugating enzyme (E2). In

complex with the accessory ubiquitin ligase E3, which recognizes signals in target proteins, E2 transfers Ub to the substrate. Two different kinds of E3 ligases have been described. E3s, containing a HECT (Homologous to the E6-AP Carboxyl Terminus) domain are ubiquitinated themselves by E2 and thus serve as final Ub-donor whereas RING (really interesting new gene) domain containing E3 ligases only assist in transferring the ubiquitin to the substrate[162]. E3s specify to which substrate the Ub is transferred and thus are the key regulatory determinant. Interestingly, the fate of the ubiquitinated protein differs depending on the kind of its Ub-modification. Attachment of polyubiquitin chains onto a substrate leads to its degradation by the proteasome, an ATP dependent protease[163]. In contrast, monoubiquitination or the attachment of short Ub chains, serves as signal for the sorting to the vacuole/lysosome[164], which I will focus on here.

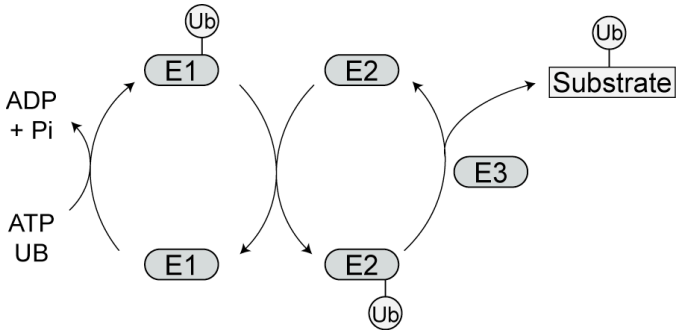

Figure 16 Mechanism of ubiquitination
Proteins are ubiquitinated by a concerted action of an ubiquitin-activating proteins (E1), an ubiquitin-conjugating enzyme (E2) and an ubiquitin ligase (E3).

In the endocytic pathway, ubiquitin was shown to act as internalization and endosomal sorting signal at the plasma membrane. For example, signal-transducing receptors as well as transporters and channels become rapidly internalized and sorted to the vacuole upon ubiquitination[165]. Furthermore, newly synthesized proteins arriving at the TGN are

directed to the vacuole by an Ub signal[166]. One way how cells interpret and transmit ubiquitin signals is through proteins that recognize Ub. Several Ub-binding motifs have been identified so far: UBA (ubiquitin-associated), UIM (ubiquitin-interacting motif), UEV (ubiquitin conjugating enzyme E2 variant) and CUE or NZF (Npl4zinc finger) domains[167]. UIM and UBA containing proteins act in endocytic vesicle budding events from the plasma membrane. For example, epsins (Eps15-interacting proteins) and Eps15 carry two and three UIM domains, respectively[21,168]. Since epsins contain two clathrin/AP-2 interaction motifs they are excellent candidates to link ubiquitinated cargo to the endocytic machinery. At the TGN, GGAs, were reported to bind to Ub via a GAT domain, thereby linking the Ub-signal to this particular transport machinery[169]. In sum, Ub targets cargo from the PM and the TGN to the vacuole. But how do the two pathways intersect?

1.4.2 MVB formation

After cargo recognition and formation of endosomal carriers, these vesicles undergo homotypic (endocytic vesicles) as well as heterotypic (endocytic and biosynthetic vesicles) fusion and thereby generate a late endosomal structure that resembles the concourse of both pathways. In a next, essential step, the membrane of the late endosome invaginates, pinches off, and thereby generates intralumenal vesicles that carry, for example transmembrane cargo proteins[170 171]. This new structure is referred to as the multivesicular body. After heterotypic fusion of the MVB with the vacuole, the intralumenal vesicles are released into the vacuolar lumen where they are degraded. A block of intralumenal vesicle formation leads to the missorting of transmembrane cargo proteins to the vacuolar membrane. Interestingly, ubiquitin-dependent sorting and especially the formation of MVB vesicles depend on the function

of a set of conserved proteins. These Class E Vps (vacuolar protein sorting) proteins were initially identified in a screen in yeast as being involved in transport processes to the vacuole[37 165]. Deletion of Class E genes leads to the missorting of transmembrane proteins to the limiting vacuolar membrane and to the accumulation of endosomal cargo proteins to a large aberrant structure, the Class E compartment[172]. Most of the Class E proteins are components of the ESCRT machinery that drives intralumenal vesicle formation[171].

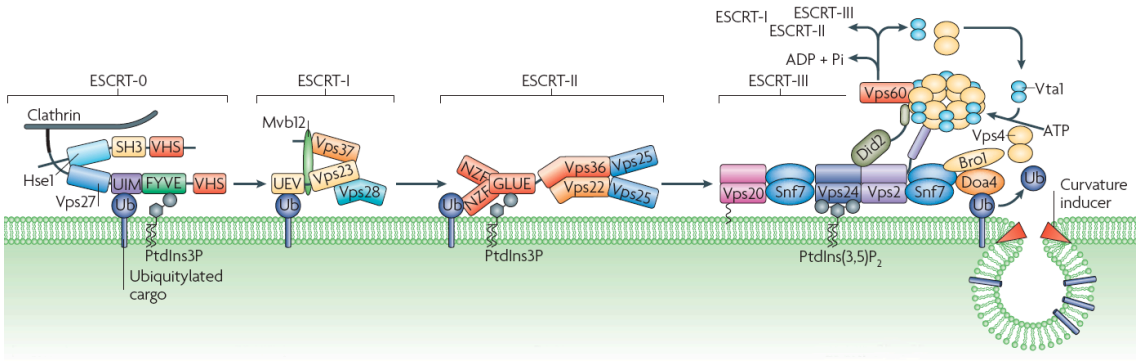

Figure 17 The ESCRT machinery at the MVB
The majority of Class E proteins are organized in ESCRT complexes 0 to III. Ubiquitinated cargo is captured by ubiquitin binding domain containing subunits and sorted into intralumenal vesicles after removal of Ub by the deubiquitinating enzyme Doa4. The ESCRT machinery is disassembled by the AAA-ATPaseVps4. Adapted from Williams and Urbé[173].

Proteins of the ESCRT machinery are highly conserved and organized in three distinct complexes, ESCRT I, -II and -III. An additional complex, consisting of Vps27 and Hse1 in yeast (Hrs, STAM1, 2 in mammals) is referred to as ESCRT-0 complex. UIM domains in both proteins are thought to recruit ubiquitinated cargo to the pathway[174 175]. Ubiquitin binding domains have also been described in subunits of the ESCRT I and II complexes[176]. In addition, several ESCRT proteins contain PtdIns(3)P binding domains that contribute to proper targeting to endosomal carriers (Figure 17)[170]. The precise

mechanism by which ESCRTs mediate sorting of cargo and generate intralumenal vesicle is not fully understood and currently two models of ESCRT function are discussed[177]. According to the "conveyor belt model", MVB sorting is initiated by ESCRT 0, which recognizes ubiquitinated cargo and thus introduces it into the pathway. In a sequential order, the remaining ESCRT complexes are recruited by interactions between consecutive complexes. Cargo is passed from ESCRT 0 to ESCRT III in a linear order and finally sorted into intralumenal vesicles. However, comprehensive interaction studies revealed a triangular network between ESCRT I, II and III, questioning the strict linearity of complex recruitment[178]. Furthermore, studies showing that small interfering RNA-mediated knockdown of ESCRT-II in HeLa cells does not affect epidermal growth factor (EGF) degradation[179] and interruption of the ESCRT 0 to ESCRT I interaction causes no defect in cargo sorting[180] argues against sequential and linear complex recruitment and activity. The alternative "concentric circle model" tries to integrate these results and explains ESCRT function to be initialized by the simultaneous and concentric assembly of ESCRT0, -I and –II around an ESCRT 0 hub. This arrangement of complexes allows concentration of ubiquitinated cargo and the subsequent assembly of ESCRT III subunits into ESCRT III lattices on the endosomal surface[181]. The release of the ESCRT 0, -I, -II core, could then lead to the recruitment of the deubiquitinating enzyme Doa4 via Bro1 and the ESCRT III subunit Snf7. Doa4 removes Ub from cargo proteins to regulate free Ub levels. In a last step, the AAA-ATPase Vps4, which forms dodecameric oligomers is recruited to the MVB and disassembles the remaining ESCRT components[182 183]. As shown by Kieffer et al.[184], recruitment of mammalian Vps4 is mediated by interactions between MIT (microtubule interacting and transport) domains of Vps4 and recognition helices within subunits of ESCRT III that are termed MIT interacting motifs (MIM). In an appealing model, Vps4

is suggested to remove individual ESCRT III subunits, leading to constriction of the ESCRT rings surrounding cargo and finally to inward budding of the endosomal membrane.

1.4.3 Dynamic conversion of endolysosomal tethering systems

Tethering processes accompanying transport processes in the endolysosomal system are only partially understood. Whereas several studies addressed the function of the vacuolar HOPS complex and its functional interplay with the vacuolar Rab GTPase Ypt7 (see 1.3.3), little is known about membrane tethering at prevacuolar, endosomal stages. At early endosomes EEA1, the mammalian homolog of yeast Vac1, was described to be required for endosome tethering[121]. This coiled-coil protein interacts with the active form of Rab5[121 185] and thus is considered as tethering factor, though additional studies are required to gain more insight into the precise mechanism. In yeast, the Rab5 homolog Vps21 was shown to be activated by Vps9, a homolog of Rabex5[186 187 188]. Consistent with studies in mammalian cells, active Vps21 interacts with the EEA1 homolog Vac1[189]. However, Vac1 mediated tethering of endosomes has not been described in yeast so far.

According to studies of Rink et al.[158], transport to the vacuole is mediated by maturation of Rab5 positive endosomes into Rab7 carrying late endosomal structures that finally fuse with the vacuole (Figure 18). Though the vacuolar HOPS complex was discussed to mediate Rab conversion by dual binding to Rab5 and Rab7, the underlying mechanism of conversion is by far not understood. The Class C core of the HOPS complex was shown to interact with Vps8[159], a protein required for endosome to vacuole transport, indicating a function of the Class C core distinct from tethering at the vacuole.

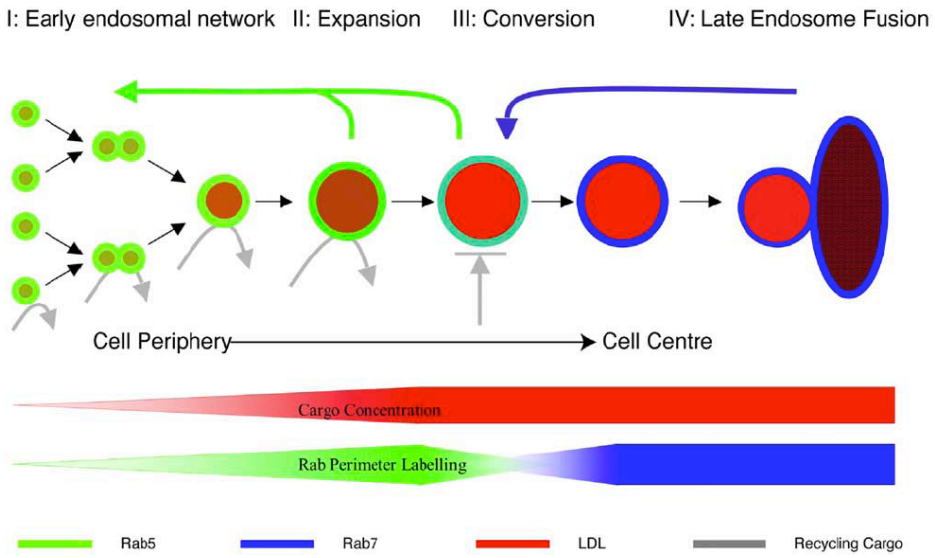

Figure 18 Rab conversion and endosome dynamics in the endolysosomal system
Endosome dynamics, symbolized at the left, and transport to the vacuole via the late Endosome/MVB are depicted. Identity of vesicle structures is indicated by green (Rab5) and blue (Rab7) boundaries, respectively. Cyan colour illustrates transient co-localization of Rab5 and Rab7. Gray arrows represent fusion of cargo vesicles. Red colour illustrates concentration of cargo (LDL). Adapted from Rink et al.[158]

Since Vps8 was shown to functionally interact with Vps21[160], it would be interesting to investigate whether the interplay between the Class C core and Vps8 and Vps21 reflects a function in late endosome tethering, distinct from early endosome tethering mediated by EEA1/Vac1 or if the Class C core just provides a Rab exchange platform at a prevacuolar compartment. In summary, the current knowledge about membrane tethering in the endolysosomal system is restricted mainly to vacuolar tethering events with little information about tethering at the level of endosomes. However, deciphering the endosomal tethering system would shed light onto the initiation of Rab conversion accompanying endosomal maturation.

2 Rationale

An important aspect of vesicular transport is the question of how vesicles recognize their appropriate target membrane. It is now well accepted that Rab GTPases together with tethering factors mediate the first specific contact between membranes that are destined for fusion. Within the endolysosomal system of yeast, tethering, which precedes fusion processes with the vacuole, requires the vacuolar HOPS complex and the Rab GTPase Ypt7[131 132]. However, little is known about tethering processes at the level of endosomes. Homotypic early-endosome fusion and fusion of endosomes with the late endosome are processes that are still poorly understood.

Based on studies in the mammalian system, some information is available about the endosomal Rab GTPase Rab5 that is discussed to be involved in endosomal tethering processes[190]. Nevertheless, its precise function during tethering is not solved yet, especially because tethering factors could not be identified yet.

This study aims to unravel endosomal tethering. By employing the yeast *Saccharomyces cerevisiae*, the precise function of the endosomal Rab5 homolog Vps21 will be analyzed. The understanding of Vps21-dependent endosomal tethering was strongly promoted by the identification of the CORVET complex by Peplowska et al.[191]. Its striking similarity to the vacuolar HOPS complex made it appealing to believe that the missing endosomal tethering complex has been found. However, a role of CORVET in membrane tethering remains highly speculative since it was mainly based on its similarity to the HOPS complex.

Based on the identification of CORVET and the strong indication for Rab5/Vps21 being involved in endosomal tethering processes, the following questions were addressed in this study in order to shed light onto endosomal membrane tethering:

I. What is the Rab GTPase that interacts with the putative tethering complex CORVET – a role for the Rab5 homolog Vp21?
II. Do CORVET and Rab GTPases functionally interact to mediate membrane tethering?
III. What are the sequential events that lead to tethering of endosomal membranes?
IV. Does CORVET mediate tethering in an assembled state or can tethering be assigned to distinct subunits?
V. How can CORVET and its associated Rab GTPase be placed into the model of Rab-conversion accompanying endosome-to-vacuole-maturation?

3 Results

3.1 The vacuolar tethering system

Membrane tethering preceding homotypic vacuole fusion and heterotypic fusion of MVBs with the vacuole requires the HOPS tethering complex and the Rab GTPase Ypt7[192 131]. Consistent with their function at the vacuole, GFP-tagged versions of Ypt7 and the two HOPS subunits Vam2 and Vam6 localize to the vacuolar rim, as shown by fluorescence microscopy (Figure 19). GFP-fusion proteins of these tethering components co-localize with the lipophilic dye FM4-64, which becomes endocytosed and transported to the vacuole.

3.1.1 The Ypt7 – HOPS interaction network

As shown by Wurmser et al.[132], the HOPS subunit Vam6 has guanine exchange activity and specifically converts Ypt7-GDP into its GTP form. The activated GTPase is able to bind the whole HOPS complex, revealing the identity of the latter as Ypt7-effector. In order to identify and characterize a putative, so far unknown endosomal tethering system, crucial techniques had to be established to identify interacting partners of endosomal Rab GTPases. Since the vacuolar tethering system was described before, Rab pull-down experiments were conducted to verify the established method.

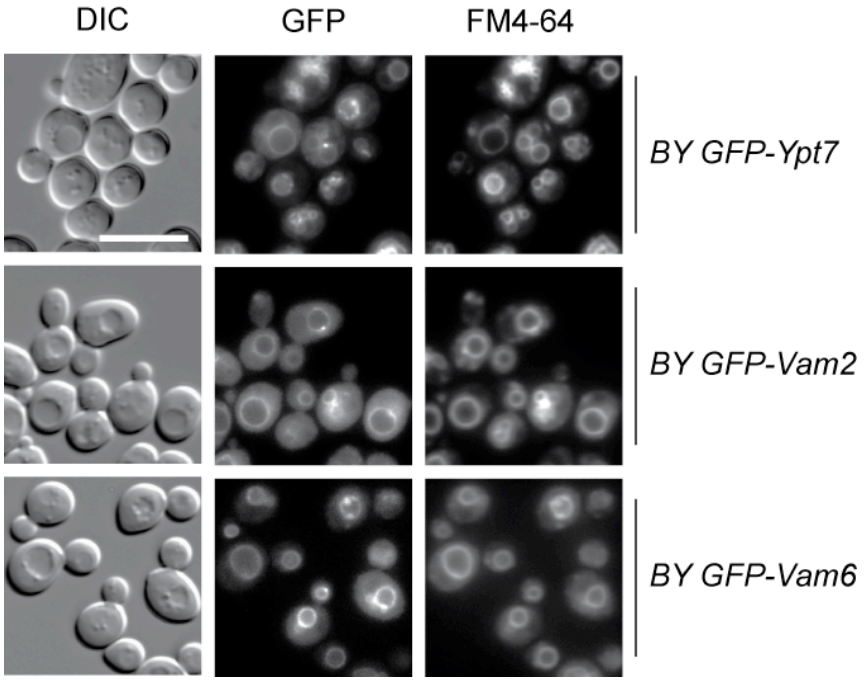

Figure 19 Localization of vacuolar tethering components
Cells expressing GFP-tagged Ypt7, Vam2 or Vam6 were grown to logarithmic phase in glucose containing medium, stained with FM4-64, harvested, washed once with PBS buffer and analyzed by fluorescence microscopy. Size bar = 10µm

In a first approach, purified yeast vacuoles were lysed and loaded onto Rab GTPases, which were preloaded with GDP, GTPγS, or left nucleotide-free. As shown in Figure 20, Vam6 specifically interacts with Ypt7-GTP, which is consistent with previous reports by Seals et al.[131]. No interaction with the endosomal Rab GTPase Vps21 was observed. However, Vam6 interacts with the active form of the Vps21 homologs, Ypt52 and Ypt53. This different binding pattern of Vps21 and its two homologs might indicate that unique functions can be assigned to each of these Rab GTPases. The interaction of Vam6 with Ypt7-GTP is most likely mediated by the HOPS complex since GEFs were described to bind only to the nucleotide-free and GDP form of GTPases[115]. To test whether the HOPS subunit Vam2 also interacts with active Ypt7, a prerequisite for a

putative function as direct Ypt7 effector, further Rab pull-down experiments were conducted.

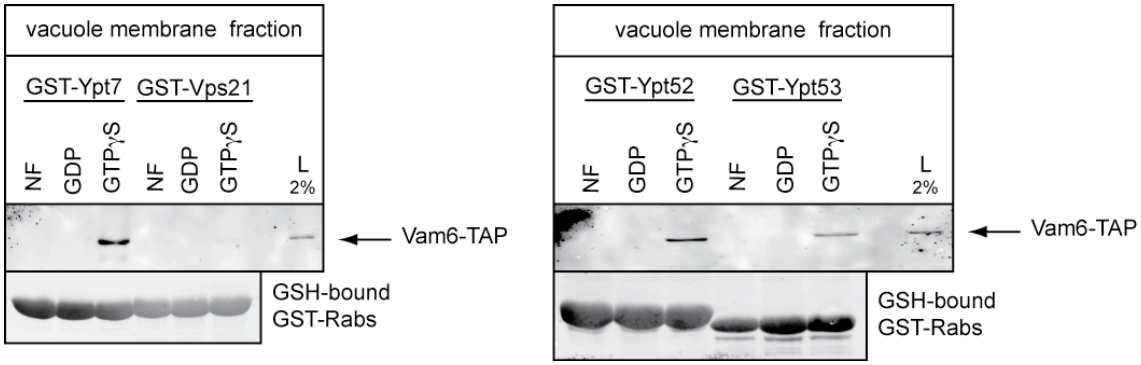

Figure 20 Interaction of the HOPS subunit Vam6 with endolysosomal Rab GTPases
Detergent lysate of purified vacuoles was applied to immobilized GST-Ypt7, Vps21, Ypt52 and Ypt53, which were preloaded with the indicated nucleotide (NF, nucleotide-free). Bound protein was eluted by EDTA/high salt, TCA precipitated, and analyzed by SDS-PAGE and western blotting using Protein A-peroxidase. Rab GTPases were eluted by boiling beads in sample buffer and analyzed as above.

An interaction between Vam2 and Ypt7-GTP was observed when detergent extracts of P10 membrane fractions were analyzed (Figure 21A). Weaker binding of Vam2 to active Vps21 and Ypt53, but not to Ypt52 supports the hypothesis of distinct roles of Vps21, Ypt52 and Ypt53 in endolysosomal transport processes. As shown in Figure 21B, the interaction between Vam2 and Ypt7-GTP clearly depends on Vam6. In this approach, cleared detergent cell lysate was applied to immobilized Rabs, and Vam2 was found to bind strongest to Ypt7-GTP, but not to Vps21-GTP. However, an interaction, though weaker was also observed with the nucleotide-free and GDP form of Ypt7. This could be explained by the heterogeneous composition of the lysate, containing also intact HOPS and thus Vam6, which might mediate the observed binding pattern. Interestingly, no interaction between any of the Ypt7 forms and Vam2 was observed in cells lacking Vam6 (Figure 21B). Thus, only the fully assembled HOPS complex is

functionally active. The results of the Rab pull-down experiments presented here are consistent with previously described results and in case of the Vam6 requirement for Ypt7-Vam2 binding even give new insights into the complex interplay between the vacuolar Rab GTPase Ypt7 and components of the HOPS complex. This method therefore proved to be a reliable technique to unravel the more enigmatic processes underlying membrane tethering at the level of endosomes.

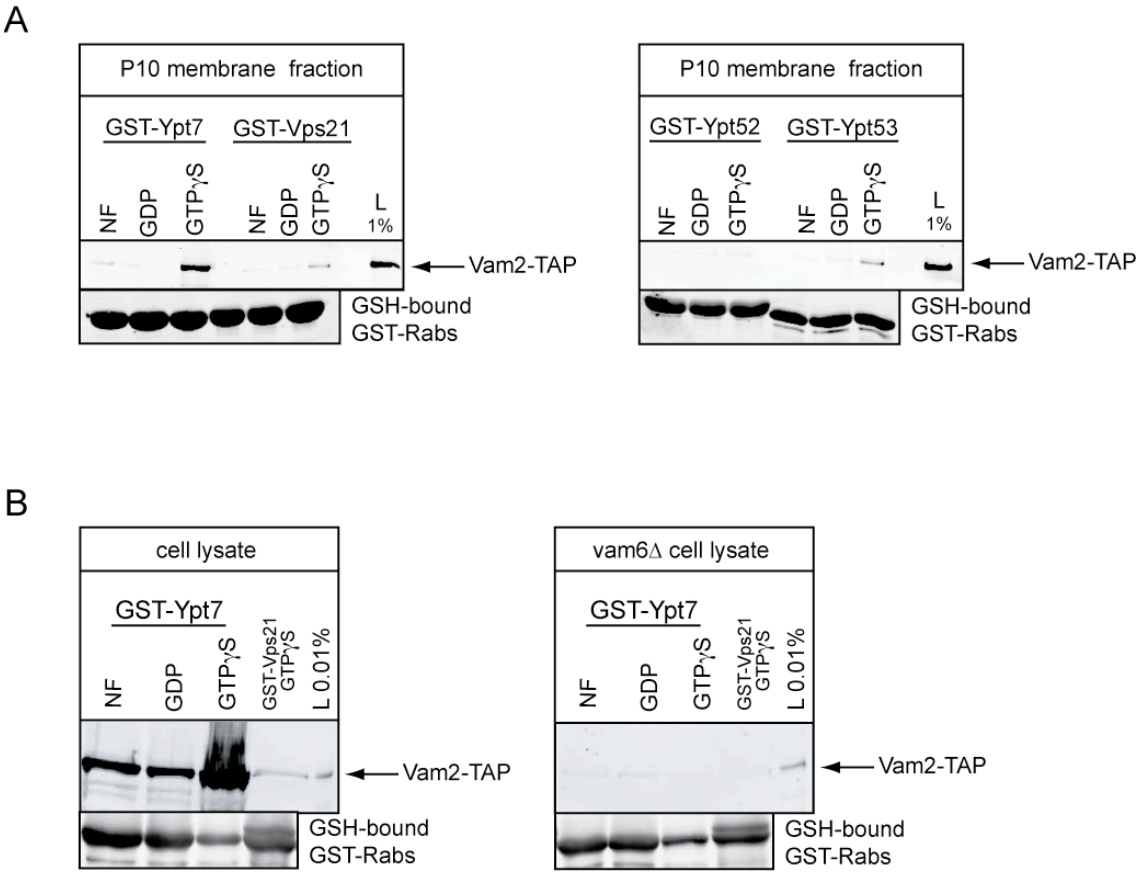

Figure 21 Interaction of the HOPS subunit Vam2 with endolysosomal Rab GTPases
(A) Detergent extracts of P10 membrane fractions of cells expressing Vam2-TAP were applied to immobilized GST-Rab GTPases as described in Figure 20. (B) Detergent extracts of whole cell lysate of wild-type and vam6Δ cells were applied to immobilized GST-Rab GTPases as described in Figure 20.

3.2 The endosomal tethering system

In contrast to the vacuolar tethering system, little is known about membrane tethering that most likely occurs during endocytic and biosynthetic transport at the level of late endosomes. Besides studies of Christoforidis et al.[121] in the mammalian system, showing that the yeast Vac1 homolog EEA1 is involved in docking of endosomes, only little progress has been made in identifying endosomal tethering factors and describing the underlying mechanism of endosomal membrane tethering. An important step for the further understanding of endosomal tethering was the identification of the CORVET complex by Peplowska et al.[191]. This hexameric complex consists of the Class C core, also found in the HOPS complex, and Vps3 and Vps8, the latter ones being homologs of Vam6 and Vam2, respectively. The striking similarity made it appealing to believe that the CORVET complex might also act as tethering complex. Since, Vps3 and Vps8 were described to be required for sorting to the vacuole[193 160 194], CORVET was supposed to fulfill its putative tethering function at the level of endosomes. However, besides the identification of the complex, several important answers were missing: What is the Rab GTPase that acts together with CORVET and how do both functionally mediate tethering?

3.2.1 Endosomal Rab GTPases and CORVET

By definition, tethering complexes act together with Rab GTPases. In order to identify a candidate GTPase that might act together with CORVET, the localization of the CORVET subunits Vps3 and Vps8 was compared to the localization of the endosomal Rab Vps21 and its two homologs Ypt52 and Ypt53. GFP-Vps3 and Vps8 revealed a strong cytosolic distribution with some dot-like structures visible that most likely correspond to endosomes (Figure 22B). Of the three Rab GTPases analyzed, only GFP-

Vps21 showed a similar distribution (Figure 22A). Whereas Vps21 was mainly detected in the cytosol and few puncta, less dot-like structures were observed for GFP-Ypt52 and Ypt53. Furthermore, weak GFP-signals of both Vps21 homologs could be detected on membranes. Because of the cellular distribution and the interaction of Ypt52 and Ypt53 with Vam2 and Vam6, Vps21 was considered to be the most likely candidate as CORVET associated Rab GTPase

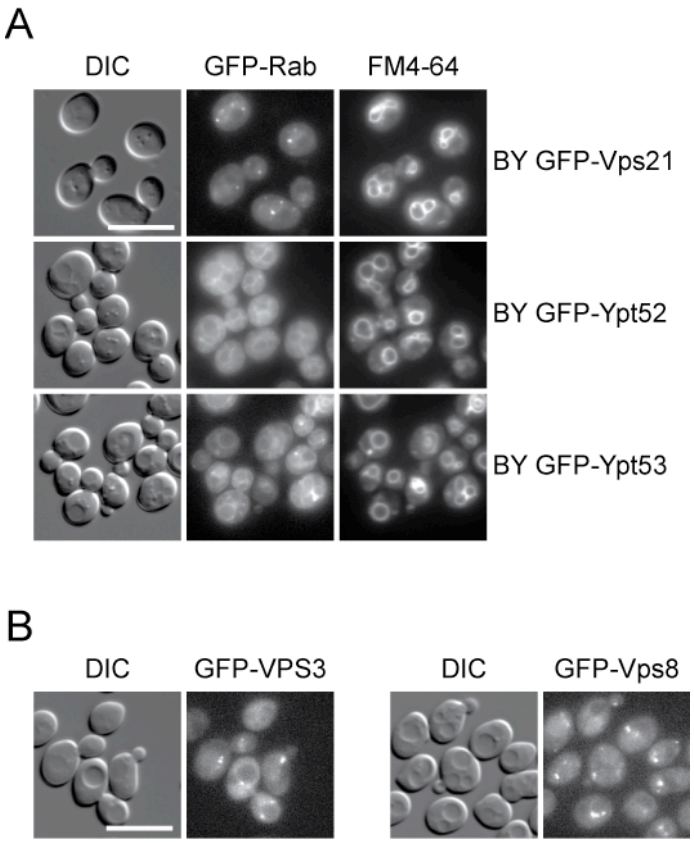

Figure 22 Localization of proteins implicated in endosomal tethering
(A) Localization of GFP-tagged Vps21, Ypt52 and Ypt53. Cells expressing GFP-fusions of the indicated Rab GTPases were stained with FM4-64 and analyzed by fluorescence microscopy as described in Figure 19 (B) Localization of the CORVET subunits Vps3 and Vps8. Cells expressing GFP-Vps3 or GFP-Vps8 were analyzed by fluorescence microscopy. Size bar = 10µm

.

3.2.2 Vps21 interacts with the CORVET complex

To unravel the relationship between the Rab5 homolog Vps21 and the CORVET complex as well as its subunits, different approaches were used. In a first approach the binding properties of the entire complex were investigated. Therefore, the CORVET complex was purified from cells that overexpress TAP-tagged Vps3 by IgG pull-down, followed by gel filtration chromatography. This method, initially used by Peplowska et al.[191] to identify and characterize CORVET, nicely separates the CORVET complex from monomeric subunits as well as impurities (Figure 23A). The purified complex fractions were then used in Rab pull-down experiments. As shown in Figure 23B, the purified CORVET complex binds exclusively to Vps21-GTP. A similar result was observed when detergent extracts of P10 membrane fractions of cells expressing Vps3-TAP were analyzed. Vps3 was recovered with Vps21-GTP, but not Ypt7 (Figure 23C), indicating that membrane associated Vps3 is mainly part of the CORVET complex.

Since Vam6 was described to interact with Ypt7-GDP and promotes nucleotide exchange[132], the Rab binding properties of its homolog Vps3 were investigated. Therefore, cells co-overexpressing GST-tagged Rabs and Vps3 or Vps9 were used for GSH pull-down experiments to identify binding partners of the respective GTPase. Vps9 is a described GEF for Vps21[187] and thus was used as positive control in this assay.

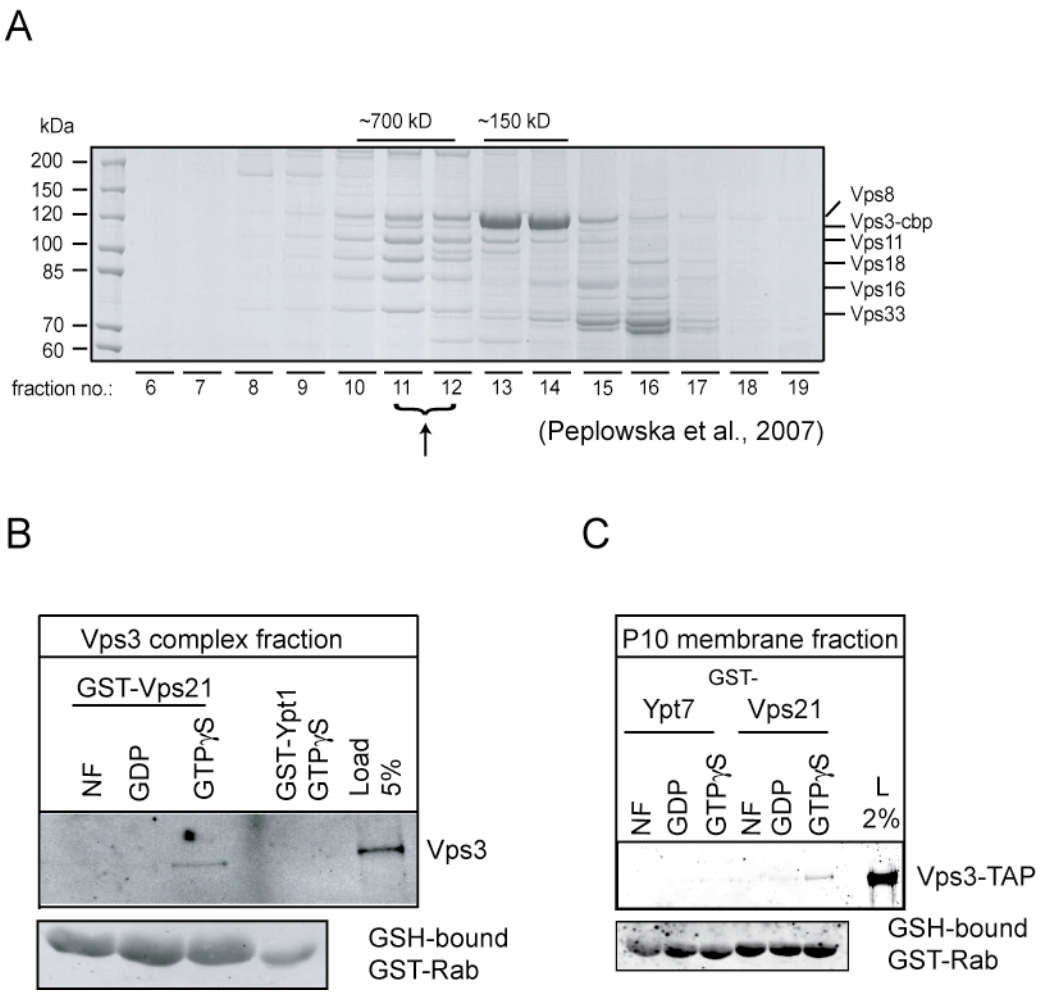

Figure 23 Interaction of the Rab GTPase Vps21 with CORVET
(A) Purification of the CORVET complex. Adapted from Peplowska et al.[191]. Cells carrying Vps3-TAP were lysed and Vps3 was captured on IgG-Sepharose. After TEV cleavage, the eluate was applied to a Superose 6 column, and the eluted proteins were analyzed by SDS-PAGE and Coomassie staining. Indicated bands were identified by mass spectrometry. (B) Interaction of CORVET with Vps21. CORVET was purified from cells overexpressing Vps3-TAP, analogous to A. The complex fraction (11, 12) was applied to immobilized GST-Vps21 and Ypt1, which were preloaded with the indicated nucleotide (NF, nucleotide-free). Further processing of the samples was done as described in Figure 20 (C) Detergent extracts of P10 membrane fractions of cells expressing Vps3-TAP were applied to immobilized GST-Rab GTPases as described in Figure 20.

As shown in Figure 24A, Vps9 and Vps3 both interact with Vps21 (lane 2 and 5). No interaction was observed between Vps3 and Ypt1 (lane 4), a Rab that is involved in ER to Golgi transport. The lower band in lane 3 is most likely a degradation product of

Vps3 that seems to bind efficiently to Vps21-S21N. This indicates that Vps3 binds stronger to the GDP mutant of Vps21, a finding that is supported by the lower amount of GST-Vps21 S21N that was bound to the GSH-matrix (Figure 24A lane 3).

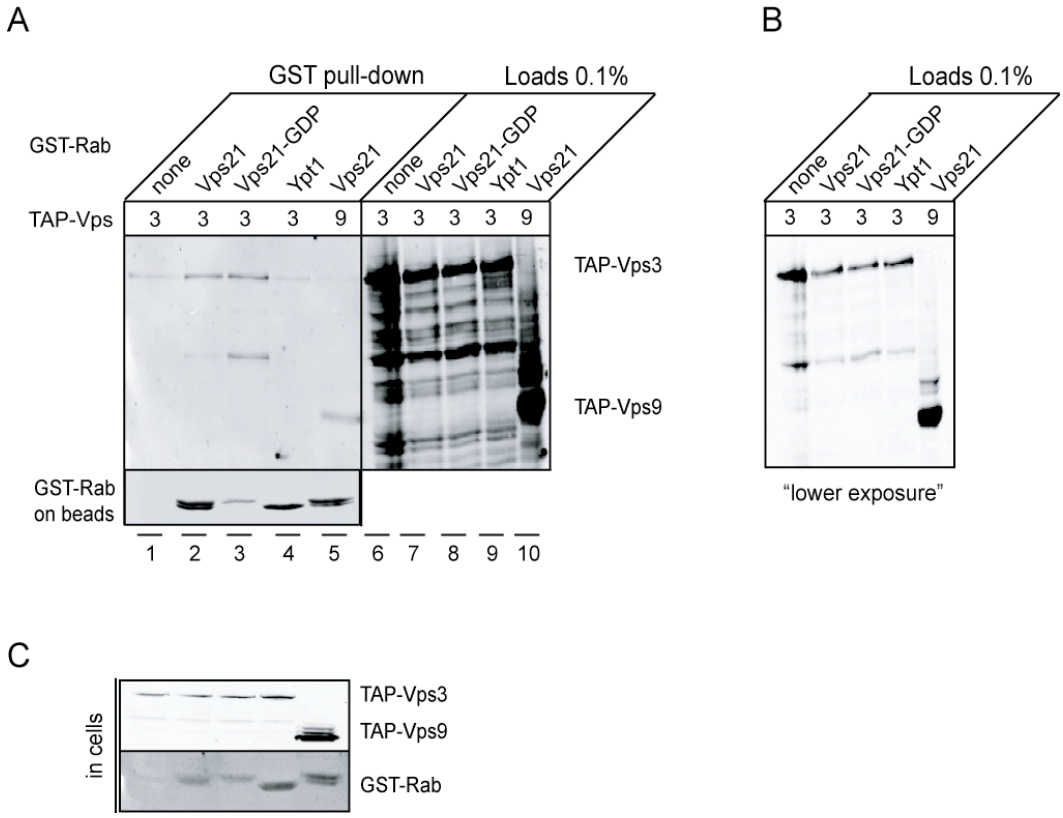

Figure 24 Co-overexpression Rab pull-down
(A) Cells co-overexpressing the indicated Rab GTPase in the wild-type or GDP-locked form (S21N mutant) and TAP-tagged Vps3 (3) or Vps9 (9) were grown in galactose containing medium and processed for a GSH pull down as described in 5.12. (B) Lower exposure of the loads shown in A. (C) Expression levels of overexpressed GST- and TAP-fusion proteins *in vivo*. The indicated strains were grown in galactose containing medium. Equal amounts of protein extracts were separated by SDS-PAGE and Western blots were decorated with anti-GST and Protein A-peroxidase antibodies.

In a second approach, lysate from cells overexpressing Vps3 was applied to GST-Ypt7, Vps21 and Ypt1 (Figure 25A). Vps3 was recovered specifically with Vps21 but not Ypt7 or Ypt1.

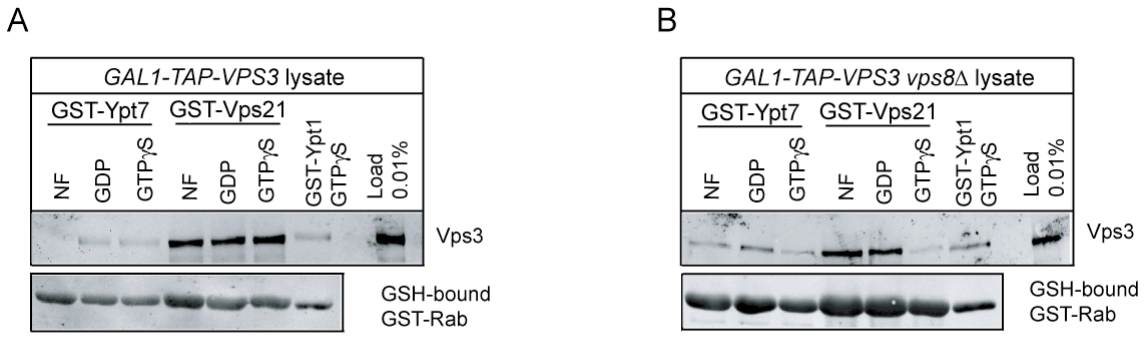

Figure 25 Interaction of the Rab GTPase Vps21 with Vps3
Detergent lysate prepared from 3L of cells overexpressing Vps3 in the presence (A) or absence (B) of Vps8 was applied to immobilized GST-Rabs containing the indicated nucleotide. Analysis was done as in Figure 20.

Surprisingly, no nucleotide-specific binding was observed, suggesting that different Vps3 populations (as monomer and as part of the CORVET complex) were analyzed. Therefore, the assay was repeated using lysate from vps8Δ cells, which lack the CORVET complex. Under these conditions Vps3 preferentially bound to the GDP and nucleotide-free form of Vps21 (Figure 25 B), similar to the result obtained in the co-overexpression experiment (Figure 24). In sum, it could be shown that Vps3 binds to Vps21-GDP whereas the entire CORVET complex interacts with the Vps21-GTP. Thus, beside the striking similarity between HOPS and CORVET, both complexes possess similar Rab binding properties towards the different Rab GTPases Ypt7 and Vps21.

3.2.3 The CORVET subunit Vps8 affects localization of Vps21

The identification of an endosomal Rab GTPase that interacts with the newly identified CORVET complex strengthens the hypothesis of a distinct endosomal tethering system. However, functional data that verify tethering function of CORVET and Vps21 are still missing.

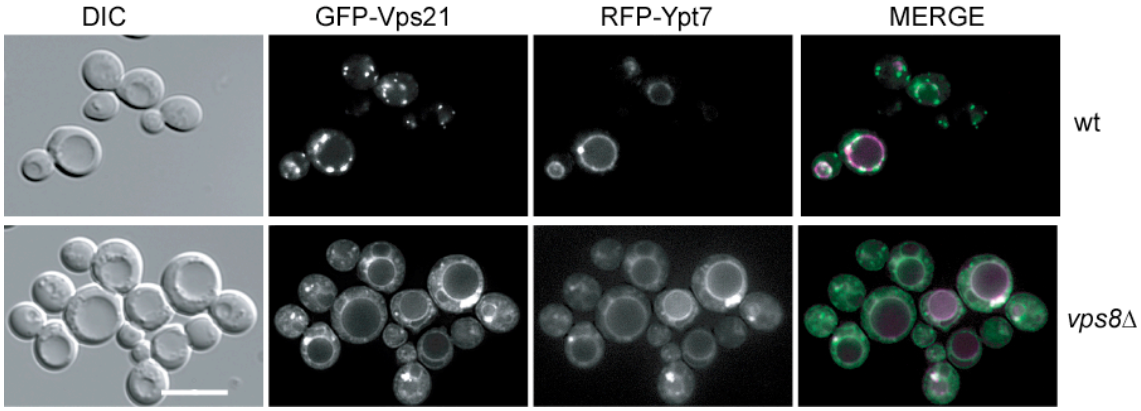

Figure 26 Co-localization of Vps21 and Ypt7
RFP-Ypt7 and GFP-Vps21 were expressed in wild-type and vps8Δ cells and visualized by fluorescence microscopy, as described in Figure 19. Images were processed by deconvolution using the Autoquant software. Size bar = 10µm

A first indication that CORVET and Vps21 functionally interact could be deduced from the observation that the localization of Vps21 is affected by the CORVET subunit Vps8. Vps8 and Vps3 belong to the Class D genes, whose deletion leads to the characteristic phenotype of enlarged vacuoles[195]. These vacuoles show defects in vacuole fragmentation[191 10] though vacuolar markers like Yck3, Vps41, Vam3, Vac8 and Pho8 are properly localized[191]. Interestingly, in contrast to the deletion of the vacuolar Q-SNARE Vam3 in wild-type cells, its deletion in a vps8Δ mutant does not cause vacuole fragmentation[196 191]. It was suggested that the endosomal Q-SNARE Pep12 can take over Vam3 function under these conditions, and that the enlarged vacuole that was observed corresponds to an endosome-vacuole hybrid organelle. In agreement with this, the endosomal Rab GTPase Vps21 and the vacuolar Rab Ypt7 co-localized in a vps8Δ mutant (Figure 26). Whereas the localization of Ypt7 is not affected by the deletion of Vps8, a shift of GFP-Vps21 from endosomal puncta to the vacuole-endosome hybrid rim was observed.

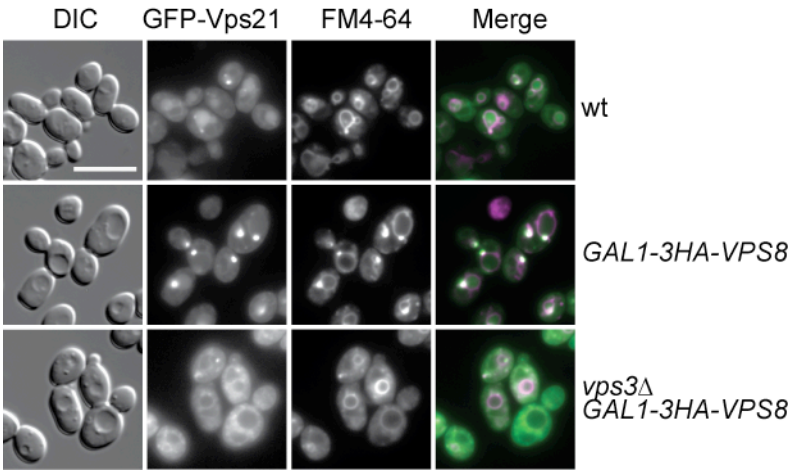

Figure 27 Overexpression of Vps8 leads to clustering of GFP-Vps21
Localization of GFP-Vps21 in different background strains. Wild-type and Vps8-overexpressing cells in the presence or absence of Vps3 were grown in galactose containing medium and analyzed by fluorescence microscopy as described in Figure 19. Size bar = 10µm

Besides the deletion of Vps8, also its overexpression was shown to have severe effects on the localization of Vps21 (Figure 27)[191]. In wild type cells, GFP-Vps21 appeared as dispersed cytosolic staining with few puncta visible, whereas the upregulation of Vps8 led to a striking dot-like accumulation of Vps21. These prominent structures can be labeled with the endocytosed lipophilic dye FM4-64 (Figure 27). Because of the striking effect on Vps21 localization, the observed structure was termed the "Vps21-compartment". As shown in Figure 27, the accumulation of GFP-Vps21 upon Vps8 overexpression required Vps3, indicating that the CORVET subunits Vps8 and Vps3 cooperate in Vps21 localization (Figure 27)[191].

As shown in Figure 28, the co-overexpression of Vps8 and Vps3 resulted in the accumulation of Vps21 (Figure 28). Since the overexpression of Vps3 leads to vacuole fragmentation, caused by the formation of a CORVET-HOPS intermediate complex at the expense of functional HOPS[191], these observed Vps21 clusters appeared less

prominent and often multiple structures were observed per cell. The localization of Vps21 was not affected by the co-overexpression of all CORVET subunits.

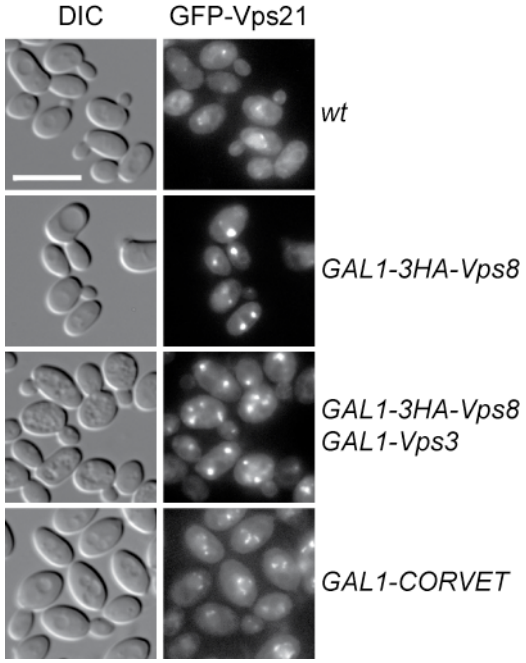

Figure 28 Co-overexpression of Vps8 and Vps3 or CORVET
Localization of GFP-Vps21 in the indicated background strains. Wild-type, Vps8 overexpressing, Vps8 and Vps3 co-overexpressing cells and cells that overexpress all CORVET subunits were analyzed by fluorescence microscopy as described in Figure 19. Size bar = 10µm

The effect of Vps8 overexpression was specific for the Rab GTPase Vps21. Only minor changes in the localization of the Vps21 homolog Ypt53 were observed upon Vps8 overexpression, whereas the localization of GFP-Ypt52 was not affected by the upregulation of Vps8 (Figure 29). Ypt7 was found to co-localize with GFP-Vps21 upon overexpression of Vps8 to some extend. However, its main vacuolar localization was not affected (Figure 29C).

Co-localization studies of overexpressed GFP-Vps8 and an RFP-tagged version of Vps21 confirmed that Vps8 is found at the observed Vps21 cluster (Figure 30).

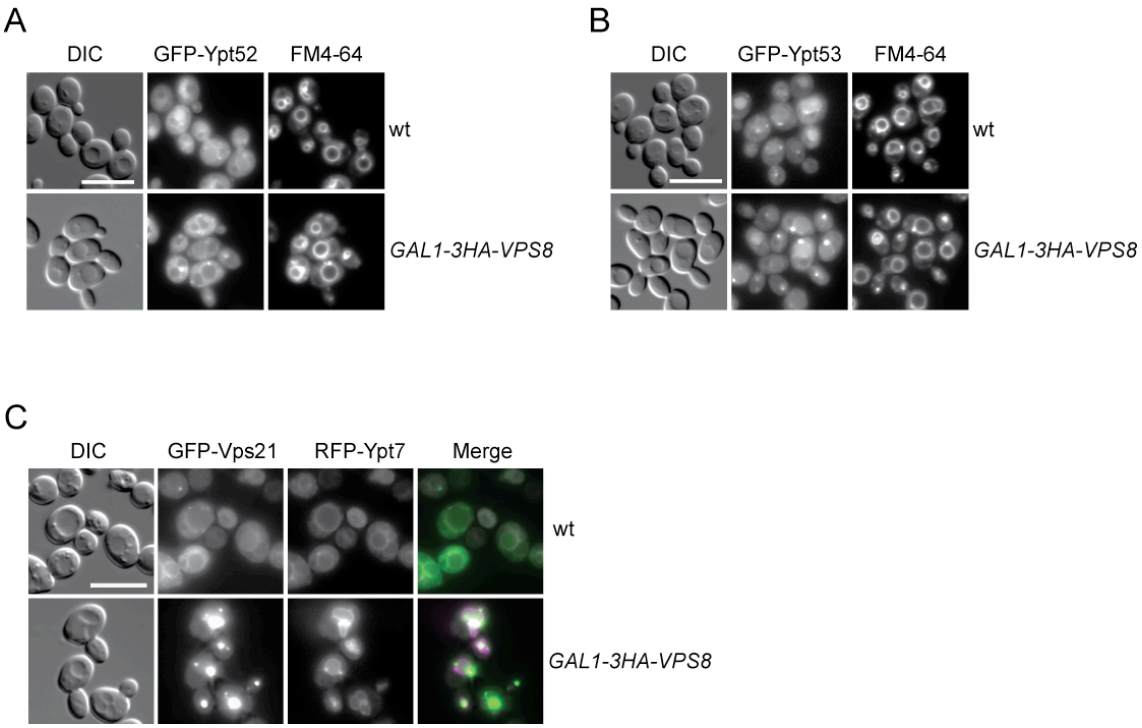

Figure 29 The effect of Vps8 overexpression on Ypt7 and the Vps21 homologs Ypt52 and Ypt53
(A, B) Localization of GFP-tagged Ypt52 (A) and Ypt53 (B) in wild-type and Vps8-overexpressing cells. Fluorescence microscopy of FM4-64 stained cells was done as in Figure 19. (C) Co-localization of Vps21 and Ypt7. RFP-Ypt7 and GFP-Vps21 were co-expressed in wild type and Vps8-overexpressing cells and visualized by fluorescence microscopy. Size bar = 10µm

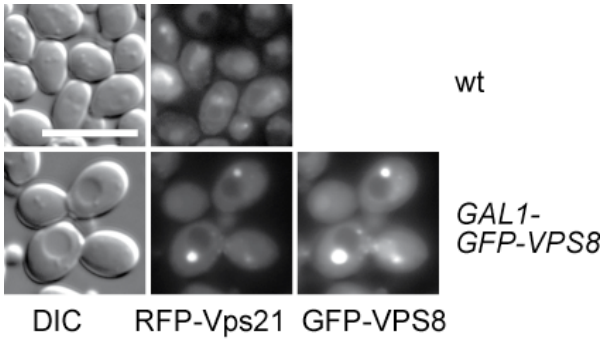

Figure 30 Co-localization of RFP-Vps21 and overexpressed GFP-Vps8
Wild-type cells expressing only RFP-Vps21 (upper panel) and cells co-overexpressing GFP-Vps8 (bottom panel) were analyzed by fluorescence microscopy. Size bar =10µm

Analysis of the expression level of PHO5 promoter regulated GFP-Vps21 revealed that under conditions that induce Vps21-compartment formation (galactose induced overexpression of Vps8), Vps21 is slightly upregulated compared to endogenous levels (Figure 31A). Regulation of Vps21 expression by the ADH1 promoter resulted in PHO5 promoter equivalent cellular levels (Figure 31A). Consistent with this, ADH1 promoter driven GFP-Vps21 accumulated at prominent puncta that co-localize with FM4-64 upon overexpression of Vps8 (Figure 31B). Further experiments that do not require GFP-tagging of Vps21 were therefore conducted using strains that express Vps21 from the ADH1 promoter.

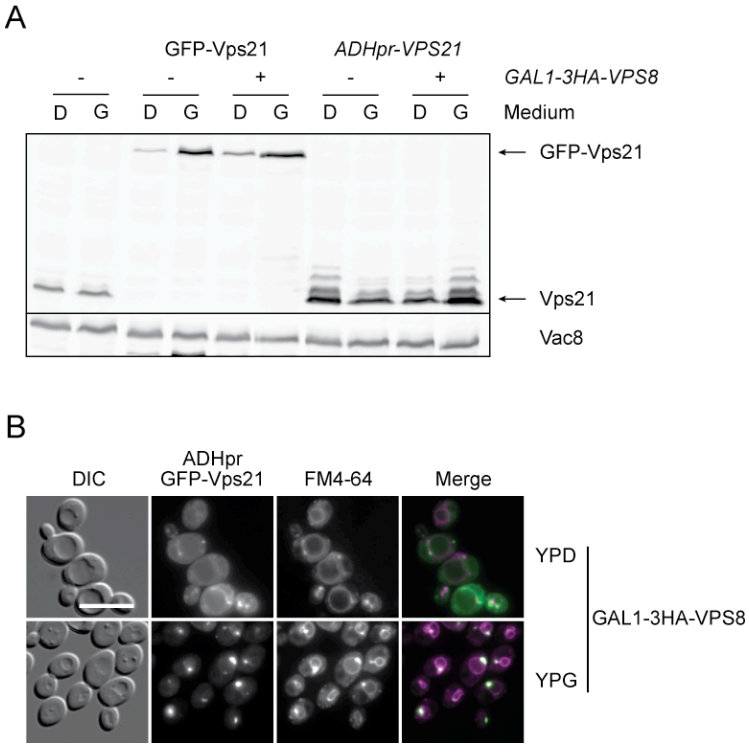

Figure 31 Analysis of Vps21 expression levels
(A) Vps21 expression levels in glucose (D) and galactose (G) containing media in the presence or absence of Vps8 (B) Characterization of GFP-Vps21 regulated by the ADH1 promoter. Cells expressing GFP-Vps21 under the control of the ADH1 promoter and galactose inducible Vps8 were stained with FM4-64 and analyzed by fluorescence microscopy. Size bar = 10µm

3.2.4 The Vps21-compartment resembles a late endosomal structure

To determine the identity of the Vps21-compartment, GFP-Vps21 was co-localized with endosomal and vacuolar protein markers. In wild-type cells, an RFP-tagged version of the late endosomal SNARE Pep12 is mainly found in the cytosol and at few dot-like structures (Figure 32A), whereas RFP-tagged Vam3, a vacuolar SNARE, localizes to the vacuolar membrane (Figure 32B). The overexpression of Vps8 did not affect the localization of RFP-Vam3 but led to the accumulation of RFP-Pep12 at the Vps21-compartment (Figure 32A, B).

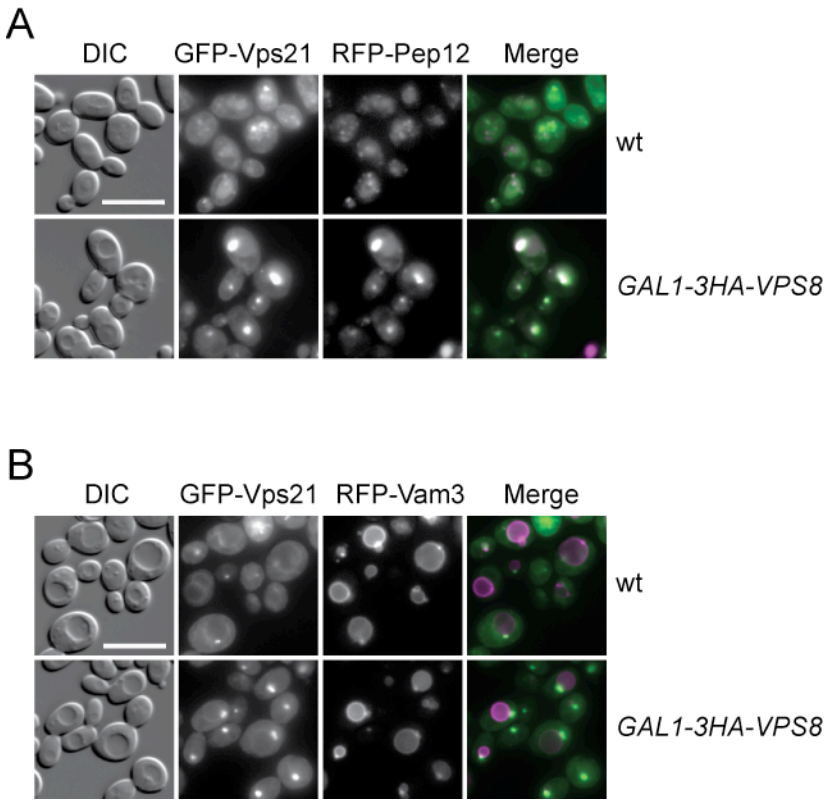

Figure 32 The Vps21-compartment resembles a late endosomal structure
(A) Co-localization of Vps21 and Pep12. RFP-Pep12 and GFP-Vps21 were co-expressed in wild-type and Vps8-overexpressing cells and visualized by fluorescence microscopy. (B) Co-localization of Vps21 and Vam3. RFP-Vam3 and GFP-Vps21 were co-expressed and analyzed as in A. Size bar = 10µm

3.2.5 Formation of the Vps21-compartment does not affect the subcellular distribution of CORVET and Rabs

Biochemical fractionation of cells overexpressing Vps8 revealed no major shift in the distribution of the CORVET subunit Vps3 and the Rab GTPase Ypt7 compared to wild type control cells (Figure 33). Increased amounts of Vps21 in the P100 fraction are not due to Vps8 overexpression since they were also observed when Vps8 expression was repressed by growing cells in glucose (YPD). Importantly, the subcellular distribution of Vps8 was only slightly affected by its overexpression, suggesting that the formation of the Vps21-compartment rather corresponds to changes in the inter-organelle organization than to the rearrangement of individual proteins.

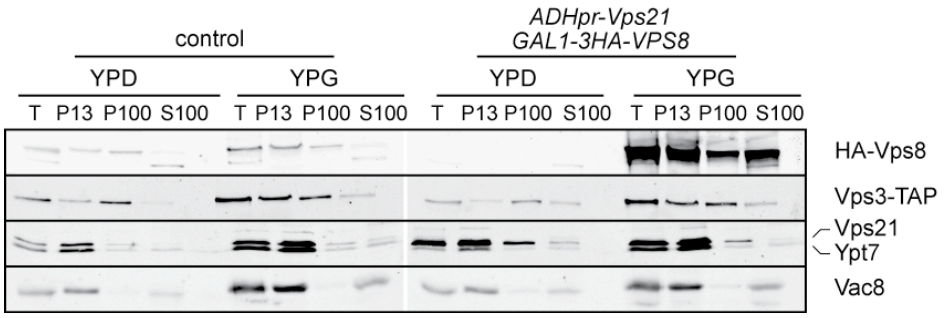

Figure 33 Subcellular distribution of endosomal proteins
Lysed spheroplasts of wild type (control) and Vps8 and Vps21 co-overexpressing cells were subjected to two different centrifugations, resulting in a 13000g pellet (P13), a 100000g pellet (P100) and a final supernatant (S100). Fractions were analyzed by Western blotting using antibodies against the indicated proteins.

To test whether the formation of the Vps21-compartment indeed can be explained by the reorganization of existing, organelles a sucrose gradient centrifugation analysis was conducted. This method can be used to separate organelles from cell extracts. Lysed spheroplasts of wild-type and Vps8 and Vps21 co-overexpressing cells were

applied to a linear sucrose density gradient and separation of organelle was achieved by equilibrium centrifugation.

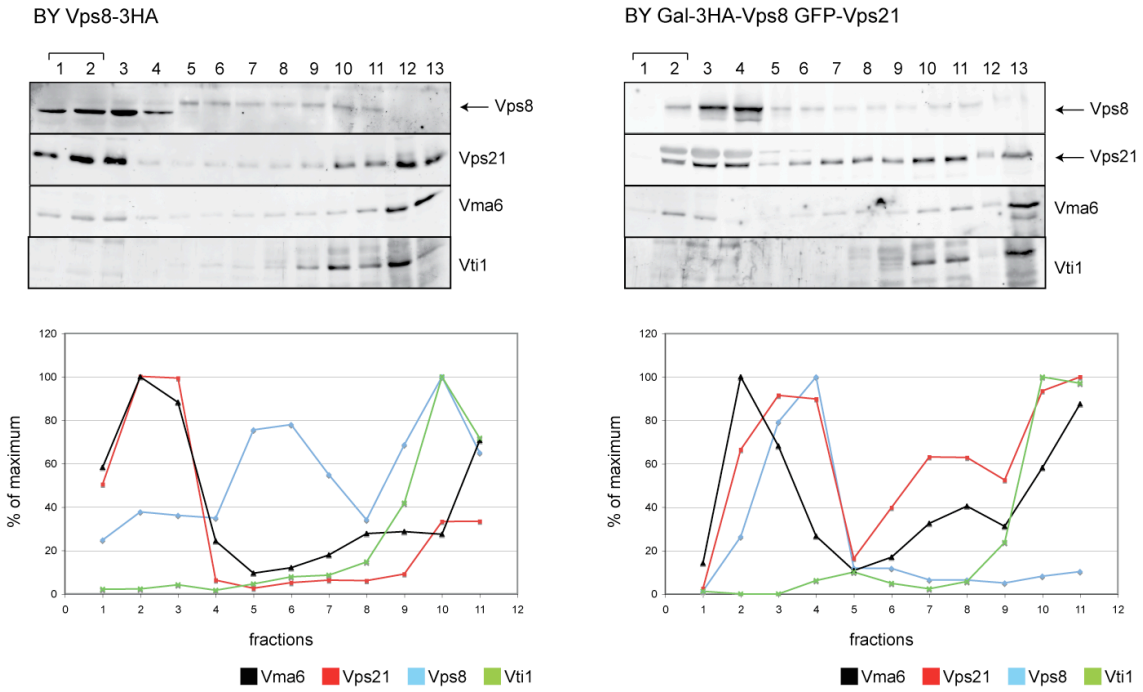

Figure 34 Sucrose gradient centrifugation – The Vps21-compartment as unique structure
Lysed spheroplasts of wild-type cells or cells co-overexpressing Vps8 and Vps21 were applied to a linear 16 to 60% sucrose gradient and centrifuged for 18h at 100000 x g. 1ml fractions were collected from the top, TCA precipitated and analyzed by SDS-PAGE and Western blotting, using anti-HA, -Vps21, -Vma6, and anti-Vti antibodies. Brackets above blot-labels indicate the loaded sample volume. Lower panel shows quantification of signal intensities detected by immuno-blotting. Maximum signal intensities of individual decorations were set to 100%.

As shown in Figure 34, intracellular organelles were successfully separated by sucrose density centrifugation. Vacuoles, detected by the presence of Vma6, a subunit of the V-ATPase, were found in low-density fractions 1 to 3, whereas the SNARE Vti, a marker for vesicles originating from the TGN[197] was detected mainly in fraction 10. Vps8 was found in two peaks. First, it co-sedimented with Vti, being consistent with its role in TGN to vacuole transport. A second peak of Vps8 was found in intermediate fractions 5 and 6. It can only be speculated at this stage that this resembles less dense late

endosomal structures. In contrast, Vps21 clearly co-migrated with the vacuolar marker Vma6. Either Vps21 was recovered with vacuoles because it resides on late endosomal structures/MVBs that were tethered to vacuoles, or its presence in fractions 1-3 can be explained by similar properties of the early sorting endosome compared to the vacuole. When cells, co-overexpressing Vps8 and Vps21 were analyzed, a clear shift of Vps8 and Vps21 was observed. Whereas the sedimentation of Vma6 and Vti1 was not affected, the peaks of Vps8 and Vps21 collapsed into one fraction (Fraction 4, Figure 34). This indicates that the Vps21-compartment, generated by upregulation of Vps8, resembles a distinct, unique intracellular structure.

3.2.6 Deletion of Class D genes lead to the formation of Vps21-compartment-like structures

In order to place the endosomal Vps21-compartment in a more defined trafficking step of the endosomal route to the vacuole, the localization of GFP-Vps21 in wild type cells was compared to that in Class D vps mutants[37]. Most of the Class D Vps proteins, including the Vps21 GEF Vps9, the Sec1-like protein Vps45 and the SNARE Pep12 are implicated in vesicle fusion at the late endosome. Their deletion leads to an enlarged vacuole but also to the accumulation of small, 40 nm vesicles throughout the cytoplasm that are unable to fuse with late endosomes[198 199 200]. In agreement with this, endocytic and biosynthetic cargo protein sorting is blocked. When the localization of GFP-Vps21 was analyzed in vps9Δ, vps45Δ and pep12Δ mutants, an accumulation of Vps21 (Figure 35A), similar though weaker compared to the strong accumulation of GFP-Vps21 upon overexpression of Vps8 (Figure 27, Figure 35B) was observed. Vps21 clustering was slightly enhanced when Vps8 was overexpressed in the same backgrounds (Figure 35B).

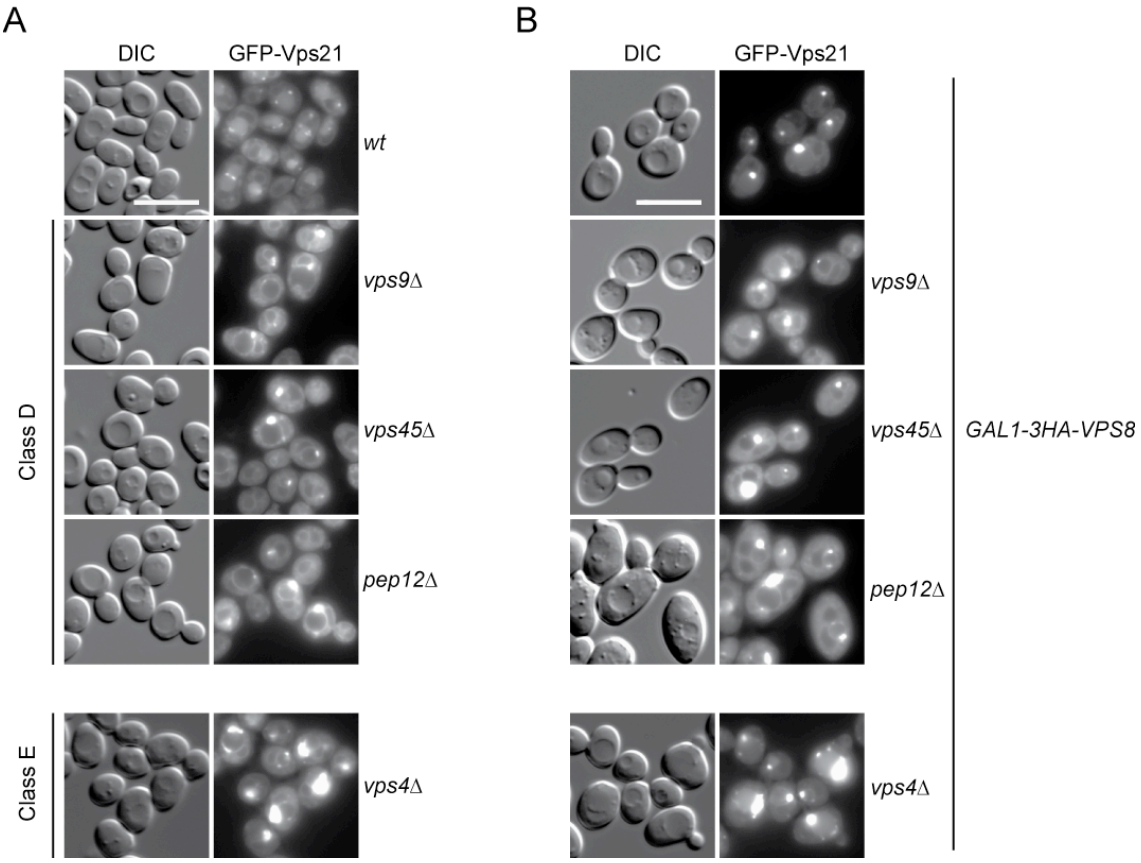

Figure 35 Characterization of the Vps21-compartment
Localization of GFP-Vps21 in the indicated Class D and E vps deletion strains in absence (A) or presence (B) of overexpressed Vps8. Cells were analyzed by fluorescence microscopy as described in Figure 19. Size bar = 10µm

The similar effect on Vps21 localization upon Class D gene deletion or Vps8 overexpression led to the hypothesis that the Vps21-compartment is formed by the accumulation of vesicular structures. Interestingly, an accumulation of GFP-Vps21 was also observed in the Class E vps4Δ mutant (Figure 35A). Deletion of these genes leads to the formation of an aberrant Class E organelle that resembles an MVB-like structure that cannot fuse with the vacuole. As a conclusion, GFP-Vps21 localizes to the late endosomal/MVB related Class E organelle. The observation that the additional overexpression of Vps8 still allows Vps21 accumulation indicates that the Vps21 compartment might be placed upstream of MVBs.

3.2.7 The Vps21-compartment corresponds to clustered late endosomal structures

To address the question whether the Vps21-compartment is formed by the accumulation of vesicular structures, wild type and Vps8-overexpression cells in the presence of upregulated Vps21 were analyzed by electron microscopy (EM, Figure 37 A-H). Vps8 was placed under control of the strong TEF-promoter in the SEY6210 strain, which was used for the EM analyses. Although the expression levels of Vps8 driven by the TEF promoter were lower compared to those when Vps8 is under the control of the GAL1 promoter (Figure 36 A), GFP-Vps21 still primarily accumulated in a single bright dot adjacent to the vacuole (Figure 36 B). TEF-promoter driven GFP-Vps8 accumulated at prominent puncta when Vps21 was under control of the strong ADH1 promoter (Figure 36C).

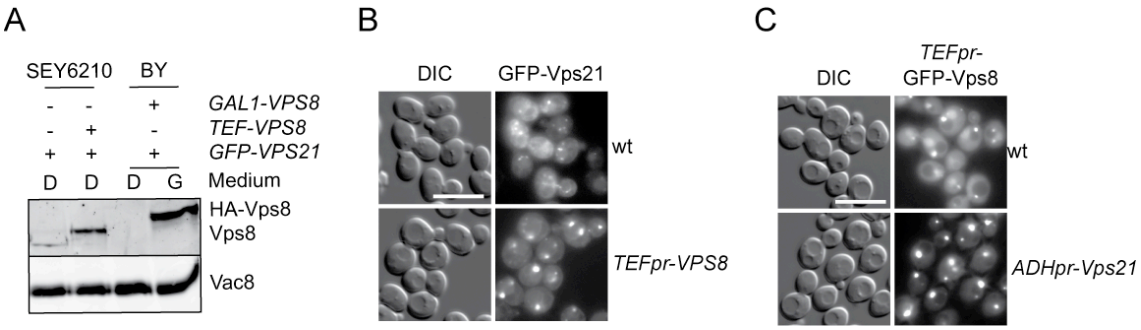

Figure 36 Characterization of strains used for EM and immuno-EM analysis
(A) Protein expression levels. P13 membrane fractions obtained from cells grown in glucose or galactose-containing media were analyzed by separating equal amounts of protein by SDS-PAGE and by decorating Western blots with antibodies against Vps8 and Vac8 as loading control. (B) Formation of the Vps21-compartment in the SEY6210 strain background upon Vps8 overproduction. Localization of GFP-Vps21 in wild type and TEF-promoter driven Vps8 expressing cells. (C) Localization of TEF promoter driven GFP-Vps8 in SEY6210 wild type cells and the SEY6210 strain expressing ADH promoter regulated Vps21. Fluorescence microscopy analysis was done as in Figure 19. Size bar = 10µm.

Cells expressing GFP-Vps21 alone (Figure 37A) were morphologically identical to the untransformed wild type strain (personal communication Fulvio Reggiori) when analyzed by electron microscopy. In contrast, the overproduction of Vps8 led to two evident morphological phenotypes. First, it was much easier to detect vesicular structures in the cytoplasm (Figure 37B, arrowhead). Those were dark vesicles with a diameter of approximately 80-100 nm (Figure 37B). Second, the 80-100nm vesicles were also detected clustered together adjacently to the vacuole (Figure 37 C-E). Consequently, these clusters of vesicles, with a diameter of approximately 400-500 nm, very likely represent the perivacuolar Vps21-compartment imaged by fluorescence microscopy (e.g. Figure 27). The close proximity of the vesicles to each other suggests that these structures could correspond to tethered late endosomes.

To determine the distribution of GFP-Vps8 within these structures, the same cells were analyzed by immuno-EM using anti-GFP antibodies (Figure 37F,G). This clearly showed that Vps8 is found at the interfaces between clustered endosomes with internal membranes, which are reminiscent of MVBs. Similar observations were made for Vps21 when tagged with GFP instead of Vps8 (Figure 37H). These MVB-like structures are heterogeneous in form and size, though smaller compared to wild type cells (personal communication Fulvio Reggiori), and were always found in close proximity to the vacuole; they very likely represent the clusters of vesicles observed by conventional EM.

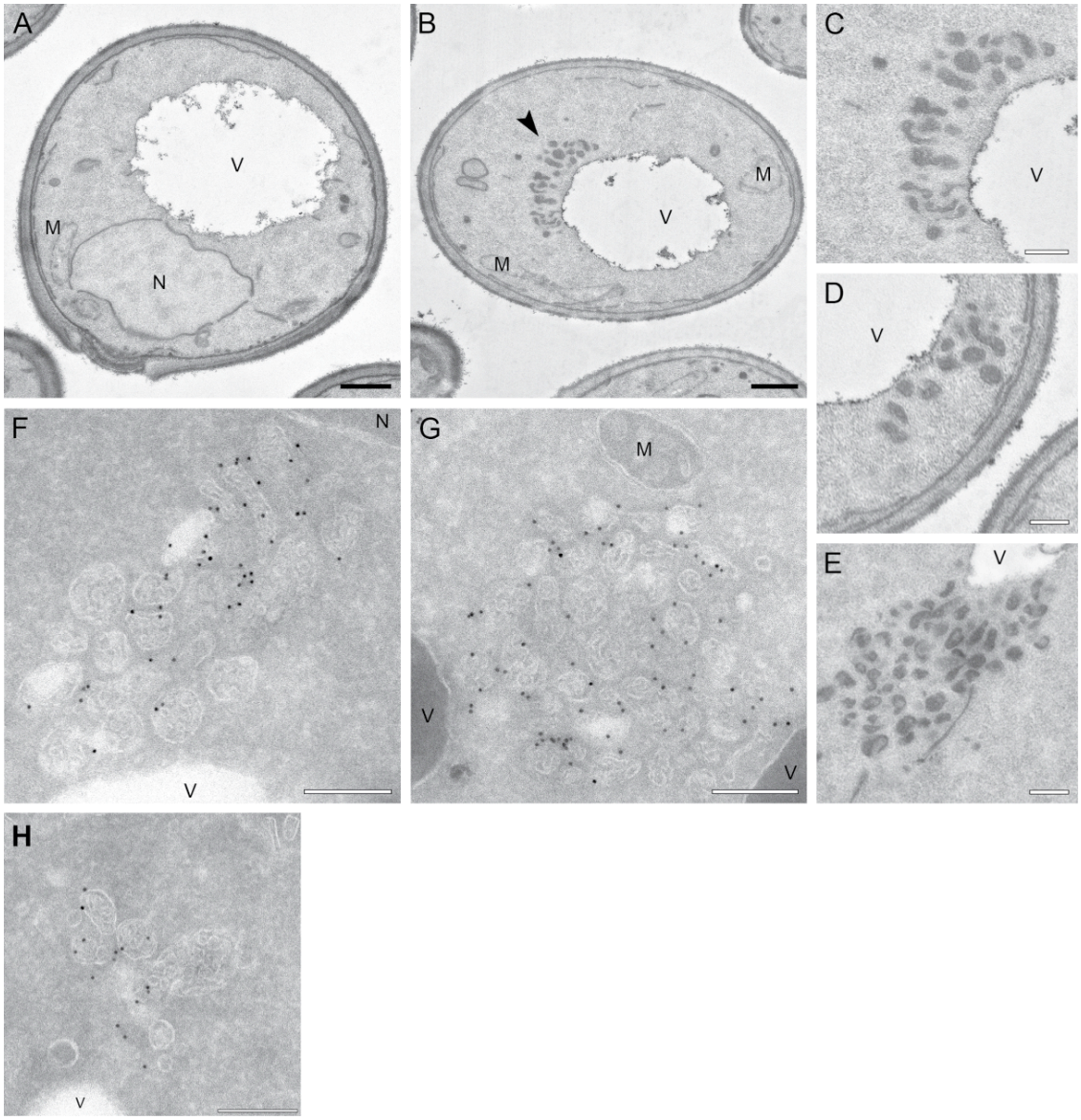

Figure 37 Ultrastructural analysis reveals clustering of late endosomes
(A-H) The strains SEY6210 PHO5pr-GFP-Vps21 (Panel A), SEY6210 PHO5pr-GFP-Vps21 TEFpr-Vps8 (Panels B-E), SEY6210 TEFpr-GFP-Vps8 ADHpr-Vps21 (Panels F, G) and SEY6210 PHO5pr-GFP-Vps21 TEFpr-Vps8 (H) were grown to exponential phase and embedded in Spurr´s resin (A-E) or prepared for IEM (Panels F-H) as described in material and methods. Cryosections (Panel F-H) were first incubated with goat anti-GFP antibodies (Rockland, Gilbertsville, PA) and then with 15-nm gold particles conjugated to protein A. Arrowheads in Panel B indicate the abnormal structures observed in those cells. Panels C to E highlight the clusters of vesicles observed in cells overexpressing Vps8. Clusters of small MVBs were observed in proximity to the vacuole limiting membrane. V, vacuole; M, mitochondrion; PM. Plasma membrane; CW, cell wall; ER, endoplasmic reticulum, Black bar, 500 nm; white bar 200 nm. EM was performed by F. Reggiori.

Taken together the data presented so far, the overexpression of Vps8 leads to a strong accumulation of GFP-Vps21, Vps8 itself and the late endosomal marker Pep12 into prominent dots (Figure 27, 30, 32), which, as shown by EM and immuno-EM, correspond to clusters of vesicular structures. Based on the close proximity of these clustered vesicles to the vacuole and the observation of internal membranes within these vesicles, it would stand to reason that Vps8 is involved in tethering of functional late endosomes.

3.2.8 Vps8 expression levels correlate with size of vesicle clusters

Based on the assumption that Vps8 is involved in endosomal tethering events or itself mediates tethering, the size of the vesicle cluster was expected to correlate with the expression levels of Vps8. To analyze the interdependency of Vps8 and Vps21 localization to vesicle clusters, Vps8 expression levels were altered. As shown in Figure 38, the dot-like accumulation of GFP-Vps21 was lost upon reduction of expression levels of Vps8 (Figure 38B, C). Depletion of Vps8 to wild type levels after approximately 300 min resulted in wild-type localization of GFP-Vps21 (compare Figure 38C 300' to 38A).

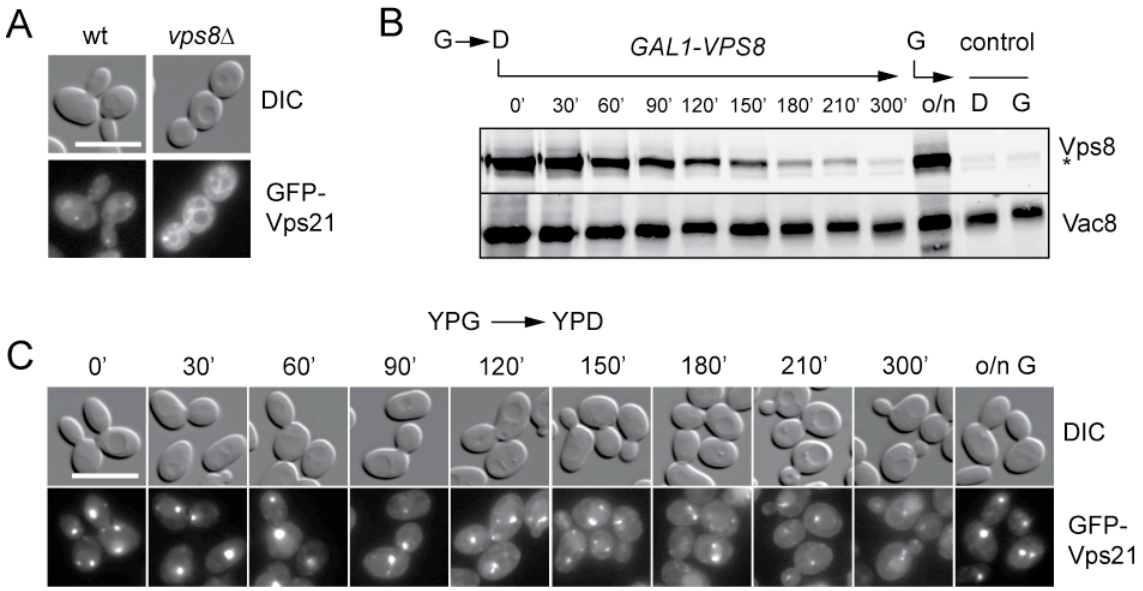

Figure 38 Vps8 expression correlates with the size of the Vps21 compartment
(A) Localization of GFP-Vps21 in wild type and vps8Δ cells. (B) Vps8 expression levels. Cells expressing GFP-Vps21 under control of the ADH1 promoter and overexpressing 3HA-Vps8 were grown in galactose and the shifted to glucose containing medium. At the indicated time points, total cell extracts were prepared and analyzed by SDS-PAGE and western blotting using antibodies against the HA-tag or Vac8. Control cells contain 3HA-tagged Vps8 under control of the endogenous promoter. (C) Localization of GFP-Vps21 upon Vps8 depletion. The samples were taken and imaged at the same time points as in (B). Fluorescence microscopy analysis in A, C was done as described in Figure 19. Size bar = 10 µm

3.2.9 The Vps21-compartment is a functional intermediate in endosomal transport

The biosynthetic and the endocytic pathway intersect at the level of the late endosome. At this stage, a multivesicular body is formed by the invagination of the limiting late endosomal membrane. Cargo proteins, packed into these intralumenal vesicles are delivered to the vacuolar lumen by fusion of the outer MVB membrane with the vacuole (Figure 39A). According to this model, Vps8 driven tethering of late endosomal structures should not affect sorting of biosynthetic and endocytic cargo. To test this, the

sorting of the biosynthetic cargo carboxypeptidase S (Cps1) and the endocytic cargo Ste3 was analyzed by fluorescence microscopy.

In wild-type cells, GFP-Cps1 is sorted into the lumen of the vacuole (Figure 39B)[201]. In contrast, GFP-Cps1 is partially mislocalized to the vacuolar rim in a vps8Δ mutant (Figure 39B). Similarly, some RFP-Cps1 was confined to the vacuole rim in cells, where the Gal1-driven Vps8 expression was repressed by glucose (Figure 39C).

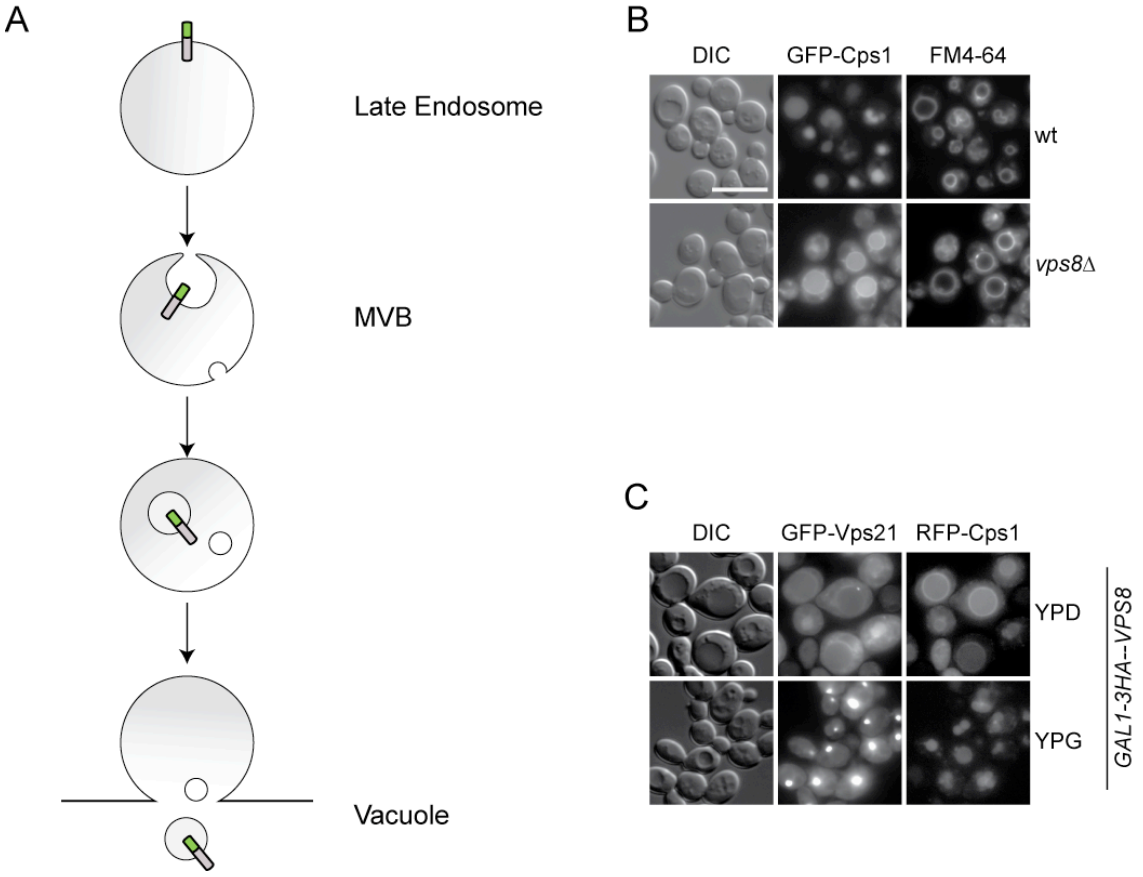

Figure 39 Biosynthetic cargo sorting is not affected by Vps21-compartment formation
(A) Scheme of biosynthetic cargo sorting. GFP-Cps1is transported from the TGN via endosomes to the late endosome. After sorting into intralumenal vesicles and fusion of the resulting MVB with the vacuole, GFP-Cps1 reaches the vacuolar lumen. (B) GFP-tagged Cps1 was expressed in wild type or vps8Δ strains and cells were stained with FM4-64 before being analyzed by fluorescence microscopy as described in Figure 19. (C) Co-localization of RFP-tagged Cps1 and GFP-Vps21 in cells overexpressing Vps8. Fluorescence analysis was performed as in Panel B. Size bar 10µm.

As expected, in these cells GFP-Vps21 was detected on the vacuolar rim and as cytosolic background (Figure 26, 39C). Consistent with the model of Vps8 being involved in endosomal tethering, formation of vesicle clusters, visualised by accumulation of GFP-Vps21, did not affect sorting of RFP-Cps1 (Figure 39C). Similar results were obtained, when GFP-Cps1 sorting was analyzed in the SEY6210 strain, used for EM analysis (Figure 40). Whereas GFP-Cps1 is sorted properly to the vacuolar lumen in wild-type cells, deletion of the vacuolar SNARE Vam3 resulted in vacuole fragmentation and in a dispersed distribution of GFP-Cps1. Intriguingly, beside being sorted to the vacuole in SEY6210 cells that co-overexpress Vps8 and Vps21, a bright dot-like accumulation of GFP-Cps1 adjacent to the vacuole was observed. This result demonstrates that biosynthetic cargo transport is not affected by, and occurs via the Vps21-compartment.

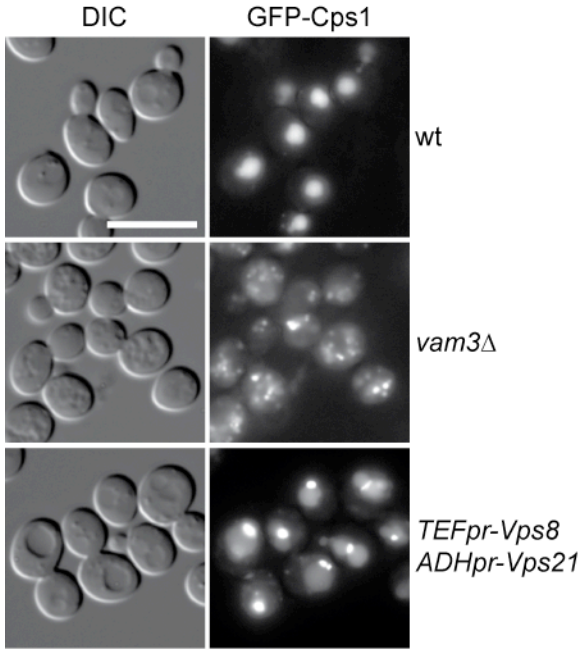

Figure 40 Biosynthetic cargo sorting via the Vps21-compartment
GFP-tagged Cps1 was expressed in SEY6210 wild-type, vam3Δ or Vps8 and Vps21 co-overexpressing (TEFpr-Vps8 ADH1pr-Vps21) strains and cells were stained with FM4-64 before being analyzed by fluorescence microscopy as described in Figure 19. Size bar = 10µm

In a next step, sorting of the endocytic cargo Ste3 was analyzed by fluorescence microscopy (Figure 41). Whereas Ste3-GFP is sorted into the lumen of the vacuole in wild type cells, deletion of the CORVET subunits Vps3 or Vps8 led to its mislocalization. Similar to the results obtained for GFP-Cps1, inhibition of the Gal1 driven expression of Vps8 by glucose resulted in sorting defects, whereas the formation of the Vps21-compartment did not affect sorting of Ste3-GFP (Figure 41).

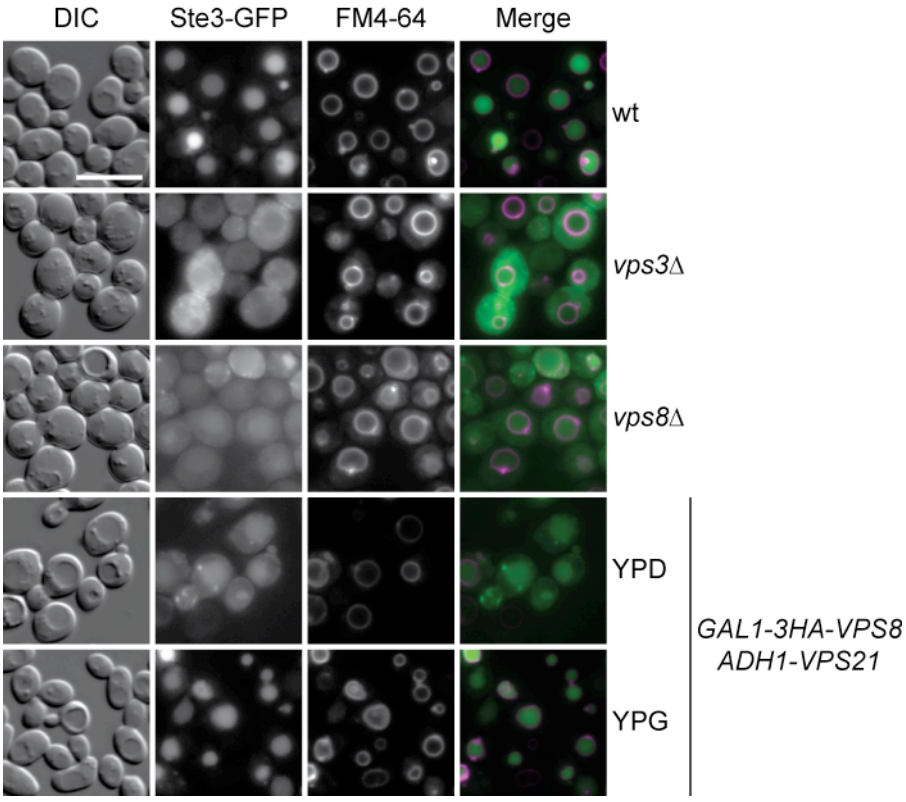

Figure 41 Sorting of endocytic cargo upon Vps8 overproduction
Localization of Ste3-GFP was analyzed in wild type, vps3Δ, vps8Δ and Vps21 co-overexpressing (Gal1-3HA-Vps8 ADH1pr-Vps21) cells by fluorescence microscopy after vacuole staining with FM4-64. Size bar = 10µm

In contrast to GFP-Cps1, which was shown to be sorted via the Vps21-compartment, Ste3-GFP was not found in these puncta. However, to confirm that endocytic cargo is indeed transported via the vesicle clusters, trafficking of the lipophilic dye FM4-64

from the plasma membrane to the vacuole was followed over time (Figure 42). In wild-type cells, FM4-64 is transported from the plasma membrane via endosomes to the vacuole (Figure 42A). This is reflected by the co-localization of GFP-Vps21 and FM4-64 at early time points. When Vps8 is overproduced, transport of FM4-64 occurs via the Vps21-clusters to the vacuole. The transport rate is slower, but the dye still arrives at the vacuolar rim (Figure 42B).

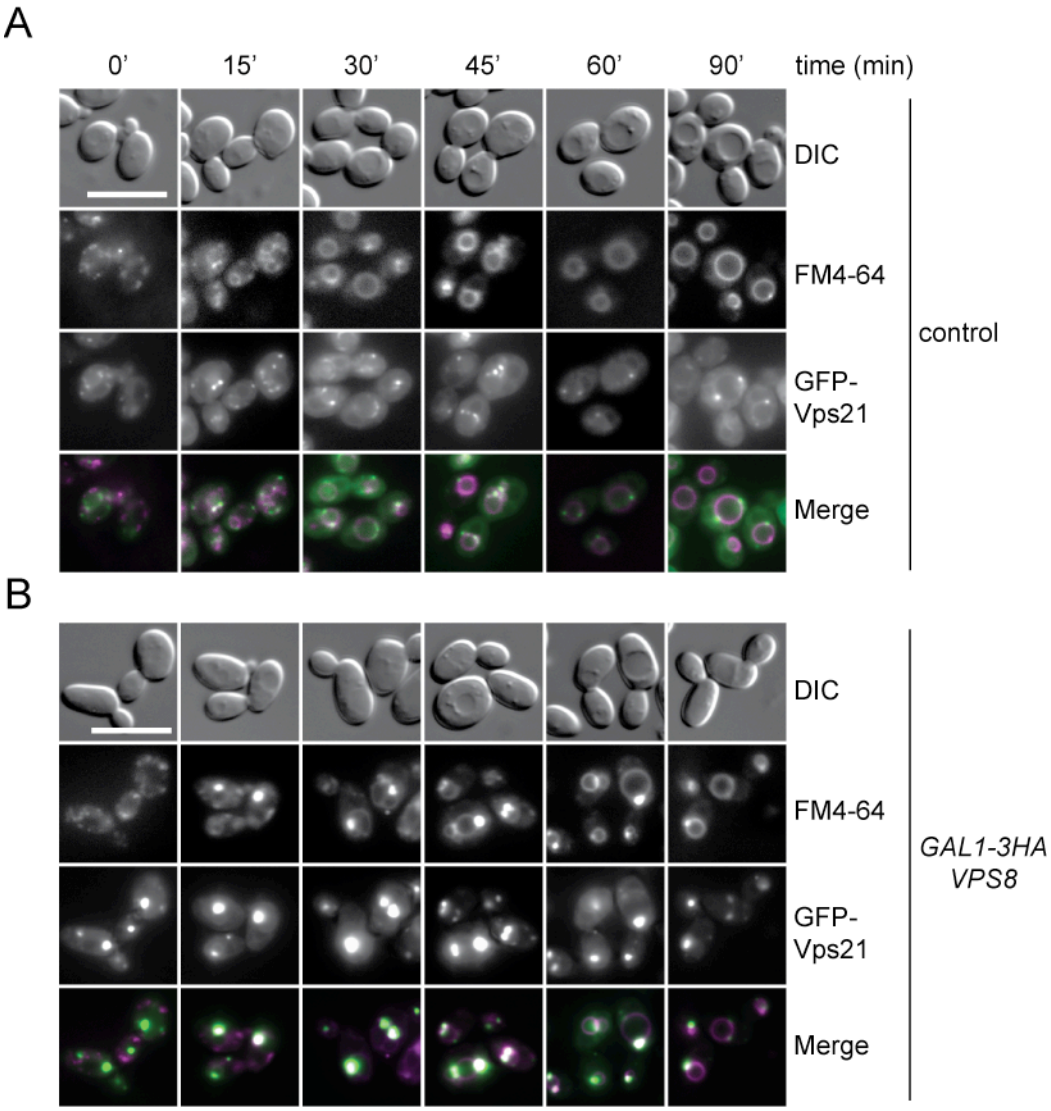

Figure 42 Time course of FM4-64 sorting
Cells expressing GFP-Vps21 (A) and additionally overexpress Vps8 (B) were incubated for 2min at 30°C with FM4-64, chased for the indicated time and analyzed by fluorescence microscopy. Size bar = 10µm

The delay in transport of FM4-64 to the vacuole and the presence of GFP-Cps1 at the Vps21-compartment indicates that further processing of the tethered structures, which would lead to fusion with the vacuole, is less efficient compared to wild-type. Further proof for this assumption comes from carboxypeptidase Y (CPY) secretion analysis shown in Figure 43. A block of endosomal transport from the TGN to the vacuole redirects this vacuolar hydrolase to the plasma membrane and the extracellular space. Whereas no secretion of CPY was observed in wild-type cells, the deletion of Vps21 or Vps8 led resulted in the secretion of CPY (Figure 43)[202 160].

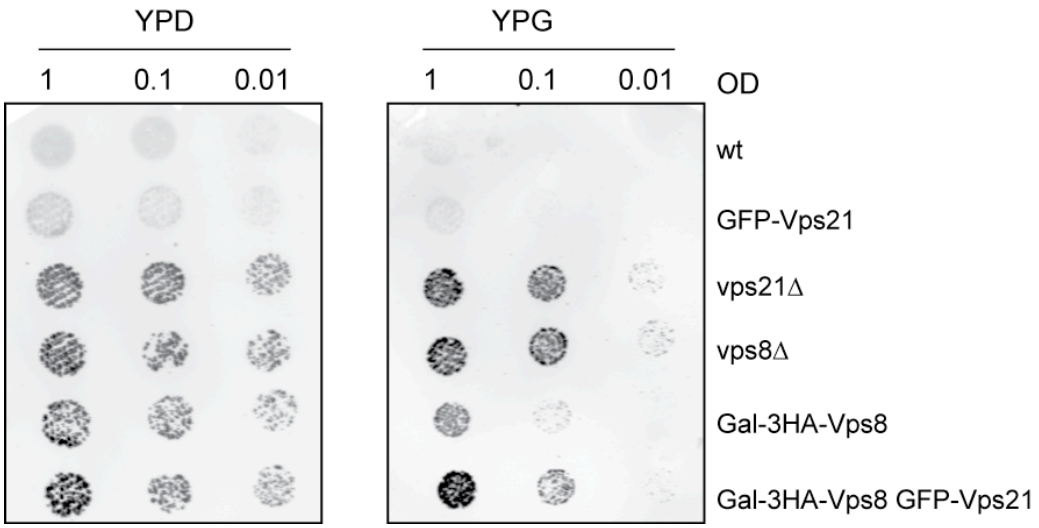

Figure 43 CPY secretion assay
Serial dilutions of the indicated strains were spotted on glucose or galactose containing media plates. After overnight incubation at 30°C, plates were replica plated onto nitrocellulose filters which were placed on fresh YPD or PYG plates, respectively. Filters were subjected to standard western blotting immuno-detection after a second overnight incubation step at 30°C. A CPY antibody was used to detect secreted CPY.

Similarly, the overexpression of Vps8 clearly led to secretion of CPY. Taken together, the overexpression of Vps8 leads to enhanced clustering of late endosomal vesicles that allow sorting of biosynthetic as well as endocytic cargo proteins. However, the Vps21

compartment seems to represent a bottleneck, which delays cargo transport, or, in the case of CPY, redirects cargo proteins.

3.2.10 Vps8 and Vps21 interact directly to coordinate early steps of late endosome accumulation

The data presented so far indicate that Vps8 and Vps21 cooperate to achieve clustering of late endosomal vesicles. It would stand to reason that clustering results from a direct interaction between Vps8 and Vps21. First indications supporting this hypothesis were deduced from the observation that the accumulation of GFP-Vps8 at the Vps21-compartment requires Vps21 (Figure 44).

Overexpressed, GFP-tagged Vps8 could be detected at some distinct puncta in wild-type cells. A portion of this GFP-fusion protein was detected in the cytosol and, as shown by co-labelling with DAPI, accumulated in the nucleus. The deletion of Vps21 abolished Vps8 localization to puncta at the expense of a stronger nuclear accumulation. When Vps21 levels were raised by expressing it from the stronger ADH1 promoter, Vps8 was confined to a single strong fluorescent dot, which corresponds to the clustered late endosomal structures observed before (Figure 35F,G). Interestingly, Vps8 localization was not affected by the deletion of the CORVET subunit Vps3, which was shown to be required for Vps21 accumulation. GFP-tagged Vps8 was equally overexpressed in the strains analyzed (Figure 44B).

To test whether Vps8 is a direct effector of Vps21, the Vps8 interaction with wild-type, constitutive inactive (S21N) and active (Q66L) forms of Vps21 was analyzed using the yeast two-hybrid assay.

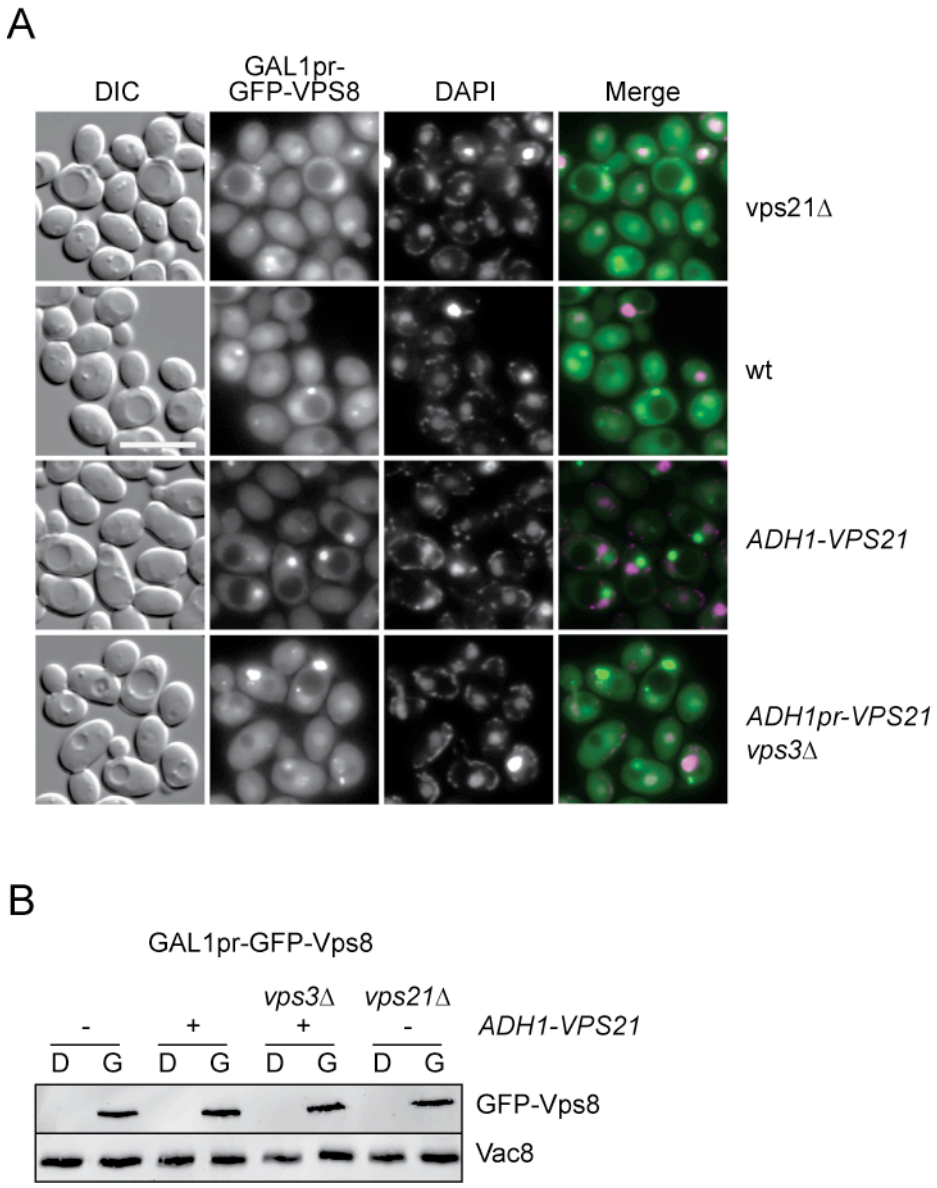

Figure 44 Recruitment of Vps8 to sites of tethering requires Vps21
Fluorescence analysis of cells overexpressing GFP-tagged Vps8. Vps21 was either deleted (vps21Δ), present at endogenous levels (wt), or under the control of the ADH1-promoter in presence or absence of Vps3. Cells were stained with DAPI and analyzed by fluorescence microscopy as described in Figure 19. (B) Vps8 expression levels. Cells overexpressing GFP-tagged Vps8 in the indicated background background strains were grown in galactose and glucose-containing media. Equal amounts of protein extracts were separated by SDS-PAGE and Western blots were decorated with anti-GFP and anti-Vac8 antibodies.

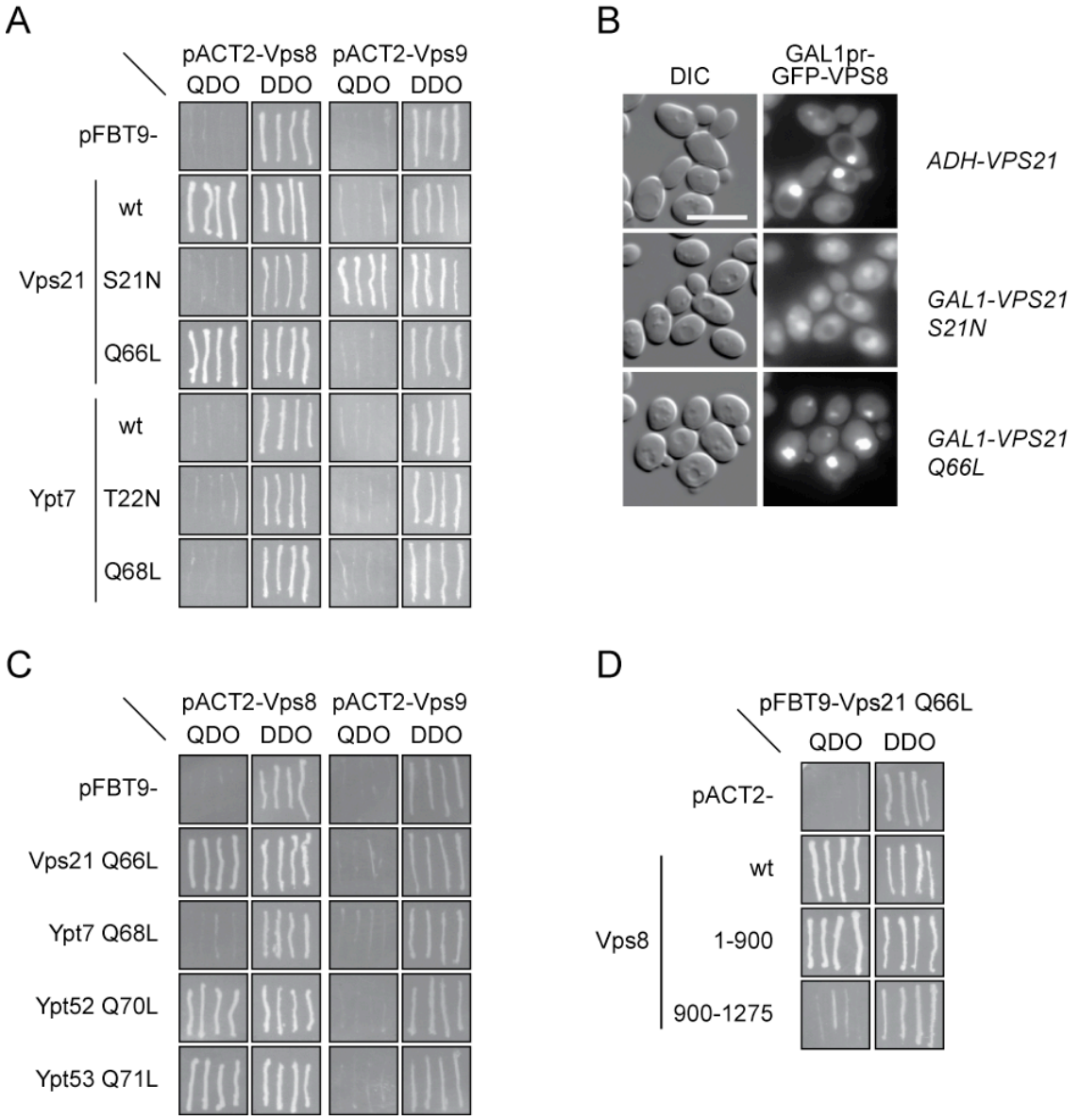

Figure 45 A direct interaction with Vps21 recruits Vps8 to tethered late endosomal compartments

(A) Interaction of Vps21 and Vps8 by yeast two-hybrid analysis. Plasmids pACT2-Vps8 or pACT2-Vps9 were co-transformed with pFBT9 vectors carrying different forms of VPS21 (wt, S21N, Q66L) or YPT7 (wt, T22N, Q68L). All transformants were re-streaked onto QDO and DDO plates. An interaction allows transformants to grow on QDO medium. (B) Fluorescence microscopy analysis of vps21Δ cells co-overexpressing GFP-tagged Vps8 and Vps21 S21N or Q66L. Size bar = 10µm. (C) Interaction of the Vps21 homologs Ypt52/53 and Vps8 by yeast two-hybrid analysis. (D) Interaction of Vps21 and Vps8 fragments. Plasmids pFBT9-Vps21 was co-transformed with pACT2 vectors carrying different fragments of Vps8 (wt, 1-900aa, 900-1275aa) as described in A).

As shown in Figure 45A, Vps8 interacts with Vps21 wild-type and the GTP-locked Q66L mutant. Binding of Vps8 to the active mutant of Vps21 is mediated by the first 900aa of Vps8 (Figure 45D). Vps8 also interacts with the GTP-locked mutants of the Vps21 homologs Ypt52 and Ypt53 (Figure 45C). In agreement with earlier studies (Hama et al., 1999), the Vps21-GEF Vps9 interacts exclusively with the GDP-locked S21N mutant of Vps21 (Figure 45A). No binding between Vps8, Vps9 and any of the Ypt7 forms was detected confirming that the CORVET complex acts with a set of Rab proteins different from those interacting with the HOPS complex. Consistent with the yeast two-hybrid results, an accumulation of GFP-Vps8 was only observed when the active form of Vps21 was co-overexpressed. The co-overexpression of inactive Vps21 did not lead to Vps8 clustering (Figure 45B). Together with the results from the Rab pull-down experiments presented in Figure 25, it can be concluded that Vps8 directly binds to Vps21-GTP and most likely corresponds to the effector subunit of the CORVET complex.

3.2.11 Differential requirements of CORVET subunits in Vps21 clustering

Considering that Vps8 is a subunit of the hexameric CORVET complex, I asked whether a functional CORVET complex is a prerequisite for GFP-Vps21 accumulation that accompanies clustering of late endosomal structures. Therefore, the localization of GFP-Vps21 was analyzed in strains overexpressing Vps8, but lacking the remaining CORVET subunits Vps11, Vps16, Vps18 or Vps33 that form the class C core. GFP-Vps21 clearly accumulated in a single punctate structure in vps11Δ and vps18Δ, but not in vps16Δ cells (Figure 46A). Importantly, the expression level of GFP-Vps21 was unaltered in the absence of Vps16 (Figure 46A). In vps33Δ cells, however, multiple

GFP-Vps21 puncta were visible. Thus, the data presented here suggest that the dot-like accumulation of GFP-Vps21 mainly requires Vps3 and the Class C core subunit Vps16.

To complement these findings, the localization of selected HOPS and CORVET subunits in cells simultaneously overexpressing Vps8 and Vps21 was analyzed. As shown in Figure 46B, the subcellular distribution of GFP-tagged Vam2, Vam6, Vps3, Vps11, Vps16 and Vps18 was unaffected by the Vps8 and Vps21 overproduction, indicating that the clustering activity can be ascribed primarily to the interaction of Vps8 and Vps21. This is supported by the relative expression levels of the individual CORVET subunits. Wild-type cells contain comparable levels of all CORVET subunits, whereas Vps8 is about 10-fold more abundant after overexpression (Figure 46C). As a conclusion, tethering is mediated by the cooperation of Vps21 and Vps8, the latter one acting independently from the remaining CORVET complex.

The result of Vps16 being the only CORVET subunit besides Vps3 that is involved in clustering of GFP-Vps21 and thus most likely also in endosomal tethering could be further complemented by sucrose gradient centrifugation analysis. As shown in Figure 47A (see also Figure 34), the overexpression of Vps8 led to the co-sedimentation of Vps8 and Vps21 in fraction 4, resembling the presence of both at the Vps21-compartment. Whereas no affect on this distribution was observed upon deletion of Vps11 (Figure 47B), the deletion of Vps16 led to the displacement of Vps21 from this structure (Figure 47C). Vps21 was evenly distributed in all fractions, with higher amounts only detected in high-density fractions. Interestingly, the sedimentation properties (Figure 47C) and the subcellular distribution of overexpressed Vps8 (Figure 48) were not affected in cells lacking Vps16.

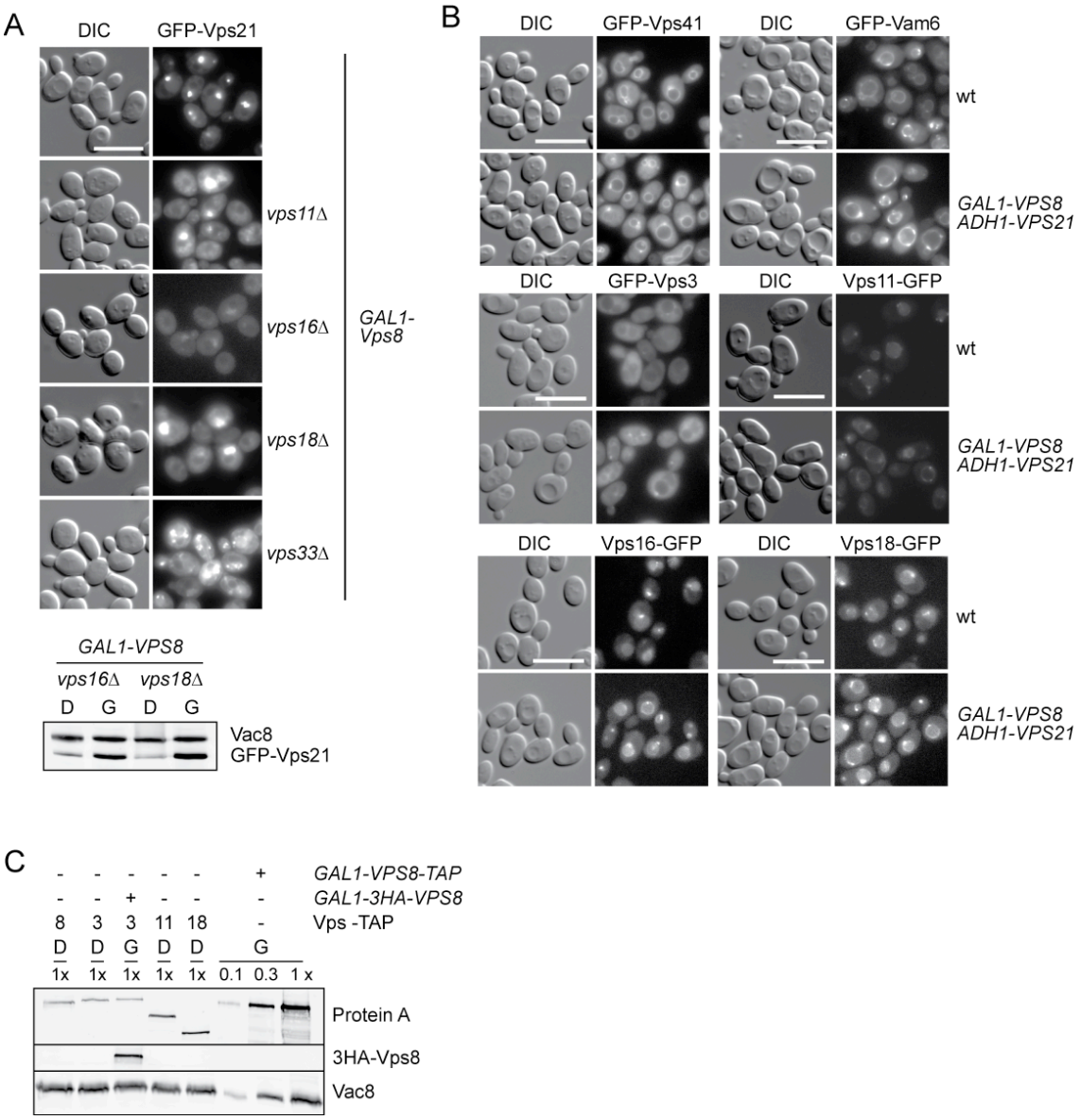

Figure 46 Role of the Class C proteins in Vps21 localization to endosomal clusters
(A) Localization of GFP-tagged Vps21 in the indicated strains. Cells were analyzed by fluorescence microscopy as described in Figure 19. Exposure times were identical for each strain. Size bar = 10 µm. Bottom; Control of expression levels. Total cell lysates were prepared from the indicated strains. Proteins were analyzed by SDS-PAGE and Western blotting, using anti-GFP and anti-Vac8 antibodies. (B) Localization of GFP-tagged Vps41 and Vam6 (top), Vps3 and Vps11 (middle), Vps16 and Vps18 (bottom) upon Vps8 overproduction. Analysis was done as in Figure 19. (C) Relative expression levels of CORVET subunits. Cells expressing the indicated TAP-tagged proteins were grown in glucose (D) and galactose (G). Total protein extracts were analyzed by SDS-PAGE, followed by Western blotting. Extracts from Gal1-Vps8-TAP were loaded in the indicated concentrations on the gel.

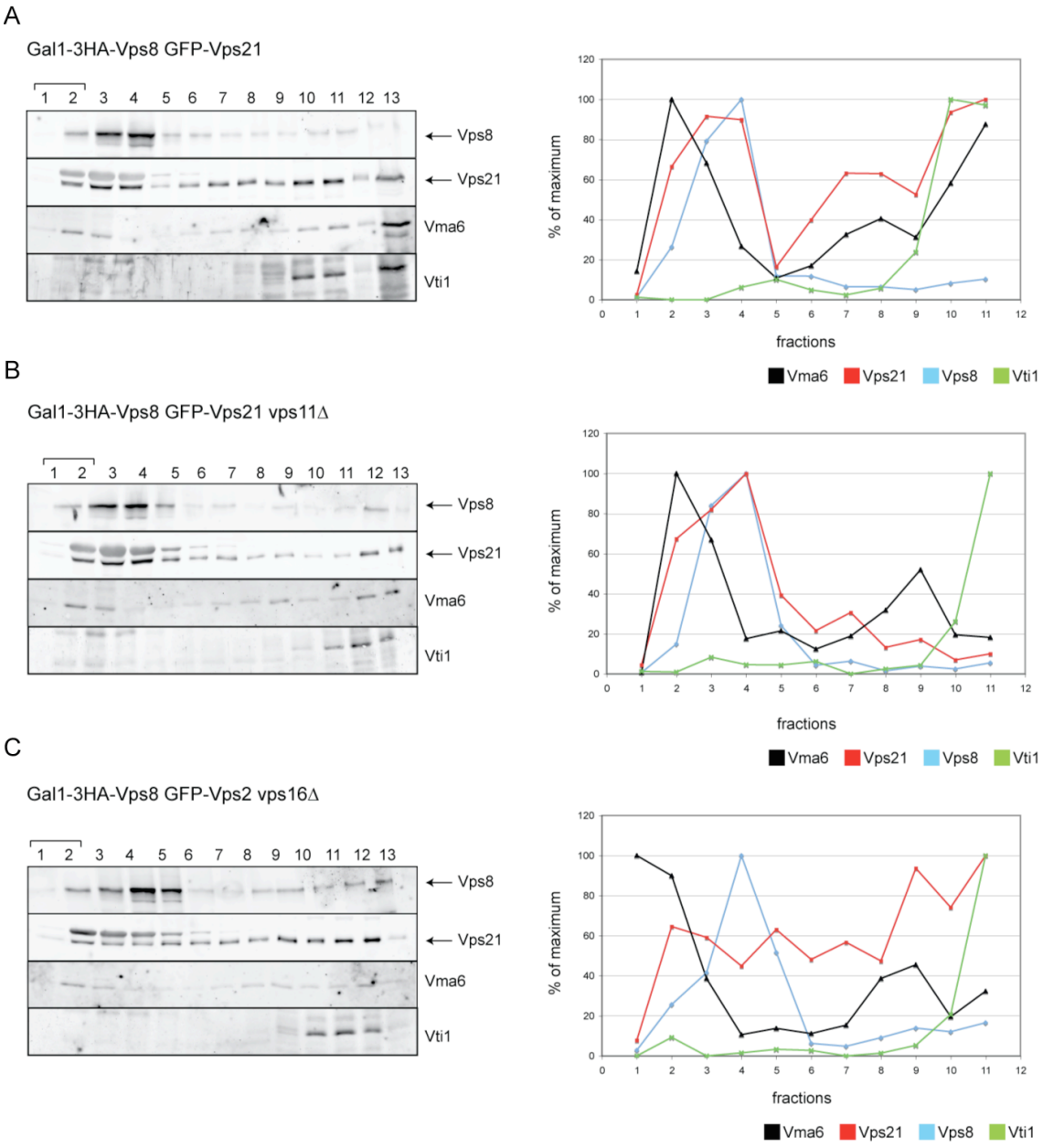

Figure 47 Sucrose gradient centrifugation - Differential requirements of CORVET subunits in tethering

Lysed spheroplasts of cells co-overexpressing Vps8 and Vps21 in the presence (A) or absence of Vps11 (B) and Vps16 (C) were applied to a linear 16 to 60% sucrose gradient and further processed as described in Figure 34

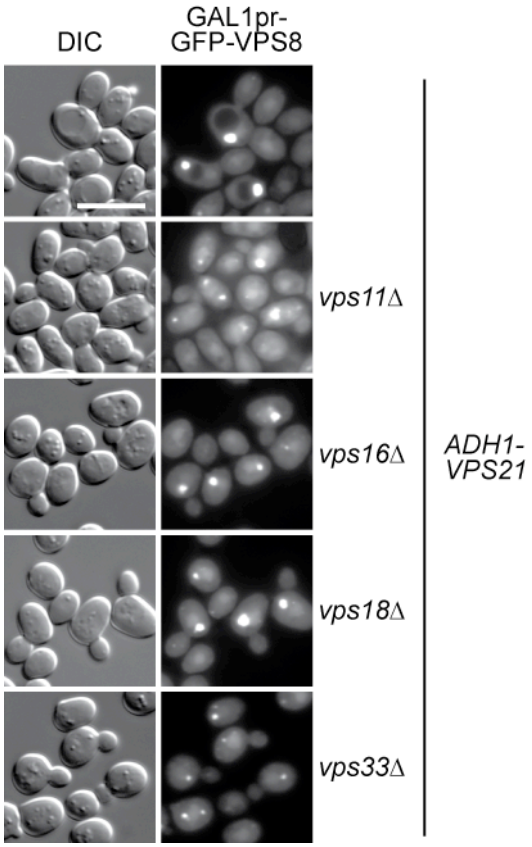

Figure 48 Localization of Vps8 upon deletion of Class C proteins
Localization of overexpressed GFP-tagged Vps8 in the indicated background strains. Fluorescence microscopy analysis was done as described in Figure 19

3.2.12 The N-terminus of Vps8 is required for Vps21 clustering

Vps8 consists of an N-terminal domain with predicted b-sheets, followed by an a-helical C-terminal part. The β-sheet part contains several WD40-regions that may form a β-propeller structure, similar to several proteins operating in the endomembrane system[203]. To determine which part of Vps8 is responsible or the late endosomal clustering, we sequentially truncated Vps8 from the N-terminus in a region preceding the potential β-propeller, and followed the localization of GFP-Vps21 (Figure 49). For this, potential domain boundaries marked by proline residues were selected and accordingly, the first 47 (Δ47) and 90 (Δ90) amino acids of Vps8 were deleted (Figure 49A). All analyzed Vps8 truncations were equally well expressed (Figure 49B). The deletion of the first 47 amino acids did not affect the ability of Vps8 in mediating Vps21

accumulation (Figure 49C). Intriguingly, the further deletion of 43 amino acids strongly diminished the accumulation of GFP-Vps21 (Figure 49B). Analysis of the Vps8 fragments in a yeast two-hybrid assay showed that the Δ90 mutant lost the ability to interact with active Vps21, whereas the Δ47 mutant still was able to bind this GTPase (Figure 49C). This suggests that Vps8 binding to Vps21 depends on its N-terminus.

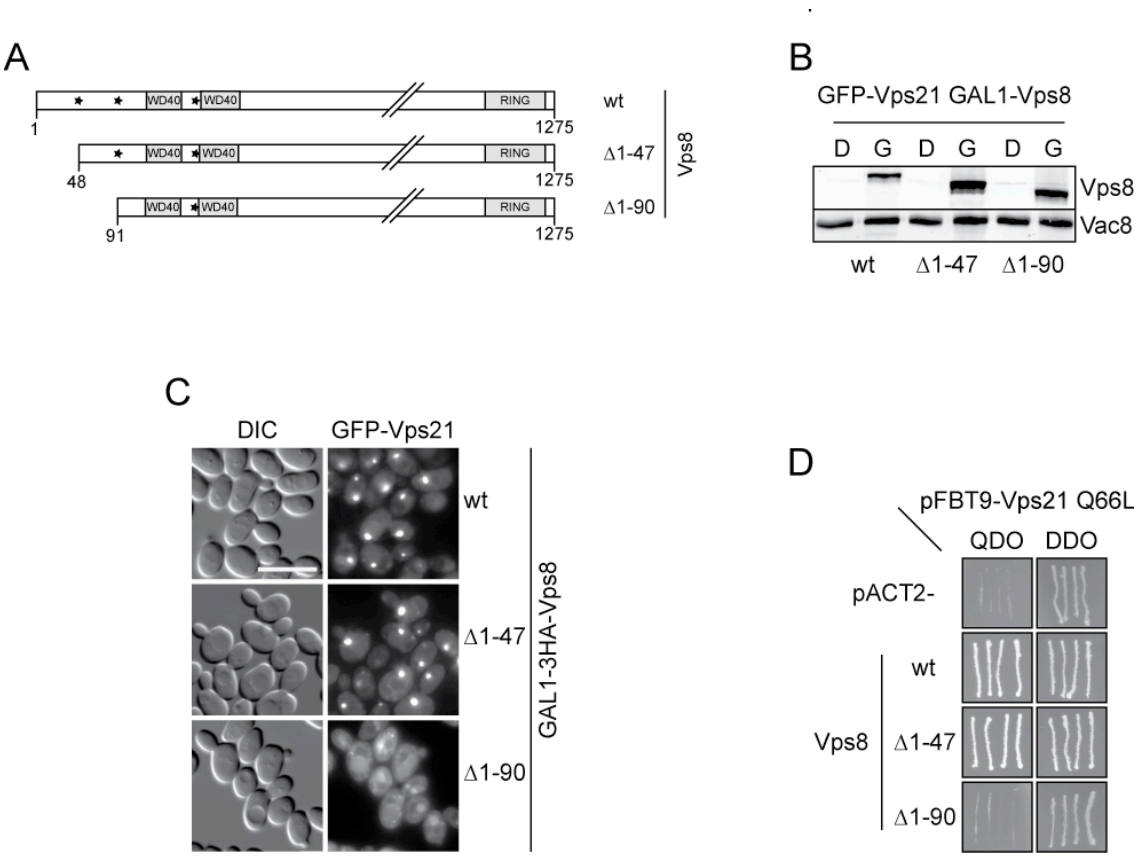

Figure 49 The N-terminus of Vps8 mediates binding to Vps21 and is required for tethering

A) Scheme of the generated Vps8 truncations. Asterisks indicate proline residues that were considered as marks of domain boundaries. WD40 indicates b-propeller regions, RING the C-terminal RING domain (B) Vps8 expression levels. The indicated strains were grown in glucose or galactose containing medium. Equal amounts of protein extracts were separated by SDS-PAGE and Western blots were decorated with anti-HA and anti-Vac8 antibodies. (C) Localization of GFP-tagged Vps21 in cells overexpressing full length or N-terminal truncations of Vps8. Cells were analyzed by fluorescence microscopy as described in Figure 19. Size bar = 10µm. (D) Interaction of truncated Vps8 with Vps21 Q66L. Plasmid pFBT9-Vps8 and the respective truncation mutants were co-transformed with pACT2-Vps21 Q66L. Transformants were re-streaked onto QDO and DDO plates.

The deletion of the first 90 amino acids of Vps8 did not affect the subcellular distribution when analyzed by differential centrifugation (Figure 50B). Accordingly, some overexpressed GFP-tagged Vps8 accumulated in dot-like structures (Figure 50A), though these structures did not correspond to the clusters of vesicles that were observed in electron micrographs of cells that overexpress full length Vps8 (Figure 49C).

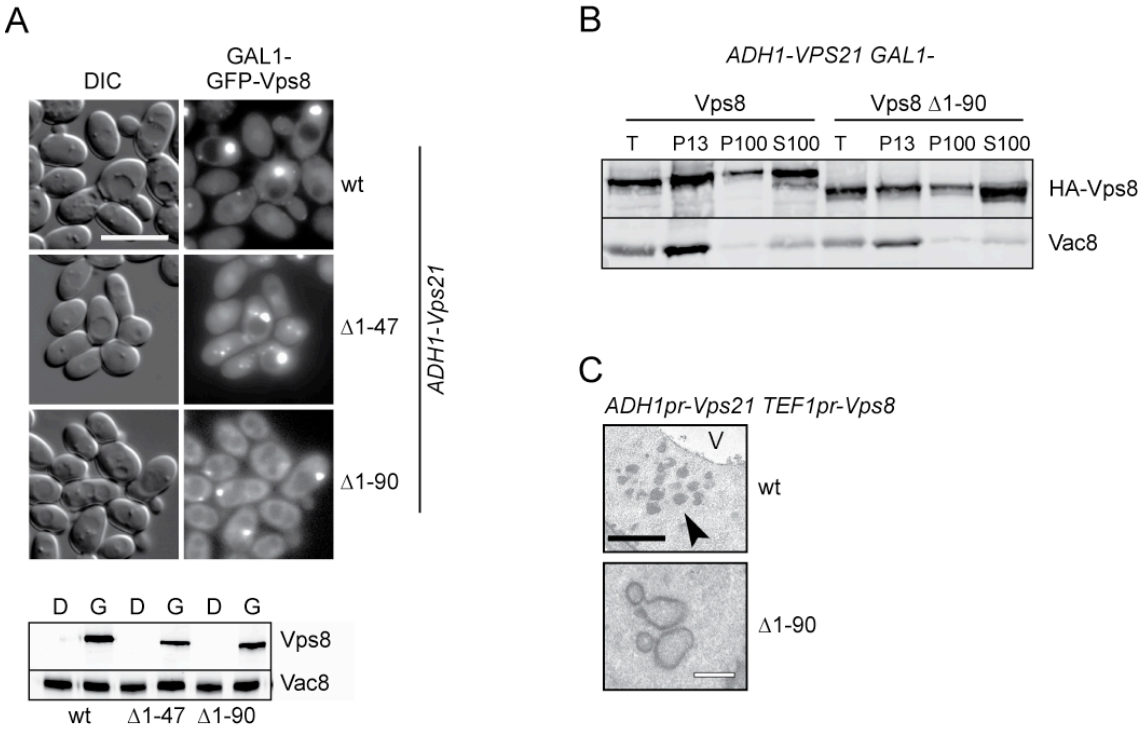

Figure 50 Analysis of N-terminal Vps8 truncation
(A) Localization of N-terminal Vps8 truncations. Cells co-overexpressing Vps21 and full length Vps8 or truncations lacking the first 47 or 90 amino acids were analyzed by fluorescence microscopy as described in Figure 19. Size bar = 10µm. Bottom; Control of expression levels. Analysis was done as described in Figure 44B. (B) Subcellular distribution of N-terminal Vps8 truncation. Lysed spheroplasts of cells co-overexpressing Vps21 and full length or N-terminally truncated Vps8 were subjected to two different centrifugations, resulting in a 13000g pellet (P13), a 100000g pellet (P100) and a final supernatant (S100). Fractions were analyzed by Western blotting using anti-HA and anti-Vac8 antibodies. (C) Ultrastructural analysis of the indicated SEY6210 strains. V, vacuole; Black bar, 500 nm; white bar 200 nm. EM analysis was performed by F. Reggiori.

4 Discussion

The data presented in this study contribute to the detailed understanding of endosomal membrane tethering. Main components of this system were identified and their complex interplay has been addressed. This section aims to critically discuss these results and place them in the cellular context.

4.1 The vacuolar tethering system – gaining insights by verifying methods

Tethering complexes, by definition, interact and cooperate with Rab GTPases to mediate membrane tethering. In yeast, the vacuolar HOPS tethering complex was shown to interact with the active form of the Rab7 homolog Ypt7[132]. These results were confirmed by Rab pull-down experiments (Figure 20, 21), which had to be established in this study in order to investigate the endosomal tethering system. Furthermore, it could be shown that binding of Ypt7-GTP to Vam2 depends on Vam6 (Figure 21). Within the cell, the GEF activity of Vam6 towards Ypt7 leads to a pool of active Ypt7 on the vacuolar surface, which is then recognized by effector proteins such as the HOPS complex. Contrary, Ypt7 would stay in its GDP-bound, cytosolic state when Vam6 is missing and the interaction between Rab and HOPS/Vam2 is abolished. However, the result presented does not incorporate Vam6 GEF activity, since active, GTP bound Ypt7 is provided as bait in the pull-down experiment. As a conclusion, besides its GEF activity, Vam6 is required for the structural integrity of HOPS, which is a prerequisite for its recognition by Ypt7-GTP.

4.2 CORVET and the Rab5 homolog Vps21 mediate endosomal tethering

The identification of the CORVET[191] complex led to the question whether it is involved in membrane tethering processes. Both CORVET subunits, Vps3 and Vps8, were shown to be involved in transport processes to the vacuole. Since Vps8 was described to functionally interact with Vps21[160] and because of the similar cellular distribution of Vps3, Vps8 and Vps21 (Figure 22), the Rab5 homolog Vps21 was considered as a likely binding partner of CORVET. Indeed, a direct interaction between the CORVET complex and the active from of Vps21 (Figure 23), analogous to the HOPS Ypt7-GTP interaction at the vacuole (Figure 20,21)[132] could be shown (Figure 23B,C)[191]. Furthermore, Vps3 preferentially binds to the GDP form of Vps21 (Figure 24, 25), equivalent to its homolog Vam6, which binds to Ypt7-GDP at the vacuole. These data indicate that CORVET is an effector of the Rab5 homolog Vps21 and suggest that Vps3 may act as a GEF for Vps21.

First indications that CORVET and Vps21 also functionally interact were deduced from the observation that Vps21 strongly accumulates in late endosomal structures upon overexpression of the CORVET subunit Vps8 (Figure 27)[191]. The effect of Vps8 overexpression was specific for the Rab GTPase Vps21 (Figure 29). Because of the strong effect on Vps21 localization, the Vps8 overexpression phenotype was used as a tool to unravel the interplay between this Rab GTPase and CORVET underlying endosomal tethering.

An enrichment of Vps21 was also detected in cells lacking the Vps21 GEF Vps9, the Sec1 homolog Vps45 or the endosomal SNARE Pep12 (Figure 35). These proteins belong to the Class D group of Vps proteins and are required for the endosomal

transport pathway to the vacuole. Previous EM analyses have shown that the deletion of the corresponding genes leads to the accumulation of 40 nm vesicles throughout the cytoplasm[198 199 200]. Since Class D proteins are involved in the fusion process with late endosomes, their deletion leads to a block of fusion and to the observed accumulation of vesicles, which is accompanied by the accumulation of Vps21. Interestingly, the Vps21-compartment that was described in this study, differs from the Vps21-positive structure in these previous studies. EM and immuno-EM analysis of the Vps21-compartment revealed an accumulation of larger vesicles (80-100nm) with internal membranes that are organized in large clusters adjacent to the vacuole (Figure 37). These accumulated vesicular structures, reminiscent of MVBs, are smaller than wild-type MVBs (personal communication Fulvio Reggiori). However, such a massive accumulation of late endosomal structures has not been observed before and differs from the dispersed vesicles accumulated in the Class D mutants. The results presented here indicate that the clustering of vesicles can be ascribed to late endosome tethering induced by overexpression of Vps8. Consistent with a direct role of Vps8 in late endosome tethering, the size of the vesicle clusters was shown to correlate with Vps8 expression levels (Figure 38).

The tethered late endosomal structures are functional and allow biosynthetic and endocytic cargo sorting to the vacuole (Figure 39, 41). However, transport is delayed, leading to the retention of some cargo at the clusters or to redirection and secretion of cargo in the case of CPY (Figure 40, 42 and 43). It might be well possible that factors, required for further processing of the tethered vesicles are limiting under Vps8 overexpression conditions (discussed below).

4.3 Vps8 is the direct Vps21 effector subunit of the CORVET complex

The described tethering of late endosomal vesicles depends mainly on Vps8. Consistent with its crucial role in Vps21 clustering, accompanying vesicle tethering, it directly interacts with the active form of Vps21 (Figure 45A). This is in agreement with previous experiments showing that CORVET loses its ability to interact with Vps21-GTP in cells lacking Vps8 (Figure 25). Binding of Vps8 to Vps21-GTP is required for its recruitment to late endosomal structures (Figure 43, 44), and thus for tethering (Figure 49).

The data presented here indicate that the CORVET complex consists of subunits with distinct functions. In addition to Vps8, Vps3 and Vps16 are the only CORVET subunits that are required for clustering of Vps21 at late endosomes (Figure 27, 45). Since neither Vps3 nor Vps16 accumulate together with Vps8 and Vps21 under overexpression conditions (Figure 46B), this suggests that these proteins might be involved in transient processes like Rab recruitment or displacement, respectively. A putative GEF function of Vps3 is supported by its homology to the described Ypt7 GEF Vam6[191], its preferential binding to the nucleotide-free and GDP-form of Vps21 (Figure 25) and the fact that Vps21 accumulation was still observed in the absence of the previously described GEF Vps9 (Figure 35). The effect of Vps16 on the clustering of Vps21 has to be assessed in the context of Vps8 localization. Whereas GFP-Vps21 did not accumulate in the absence of Vps16, Vps8 was still found concentrated at prominent structures (Figure 45, 47). Since Vps21 is required for Vps8 clustering, tethering must have taken place. This suggests that inactivation and removal of Vps21 from the

clustered structures occurs at higher rates in vps16Δ cells. Vps16 thus could be a negative regulator of a Vps21 GAP.

Contrary to the deletion of Vps3 and Vps16, clustering of late endosomes was still observed in the absence of Vps11, Vps18 and Vps33. This result suggests that these CORVET subunits might be dispensable for tethering, but could play a role in the further processing of the tethered structures, such as promoting fusion by controlling SNARE protein assembly. A similar function was assigned to the homologous HOPS complex, which promotes fusion, interacts with SNAREs and proofreads SNARE assemblies[204 105]. Consistent with this, the simultaneous overexpression of all CORVET subunits does not lead to an accumulation of Vps21 (Figure 28), indicating that under those conditions, enhanced tethering is followed by efficient downstream processing, leading to fusion with the vacuole. It stands to reason that the observed accumulation of cargo at the tethered late endosomes and secretion of CPY (Figure 40, 42 and 43) would not occur when Vps8 and the remaining CORVET subunits were co-overexpressed.

4.4 The mechanism of late endosomal tethering

Based on the data presented in this study, tethering in the endolysosomal system can be explained by the following model. At early endosomes, Vps21 is activated by its GEF Vps9[187] leading to further recruitment of effectors like Vac1/EEA1[205]. Since EEA1 was shown to be required for early endosome docking, it would be interesting to investigate whether this displays a unique early endosome tethering system, distinct from late endosome tethering events described here. At late endosomes, Vps21-GTP, activated by Vps9 at early endosomes or re-activated by its putative GEF Vps3, recruits the CORVET subunit Vps8. Previous studies have shown that Vps8 is required for fusion of vesicles with the late endosome[160 194]. Tethering events described here therefore very

likely correspond to fusion of Golgi-derived and endocytic vesicles with late endosomes. Under overexpression conditions, tethering via Vps8 and Vps21 occurs independently of the assembled CORVET complex, though the mechanism by which opposing membranes are held together remains unknown. However, the basis for the tethering function of Vps8 is the binding to Vps21-GTP via its N-terminus (Figure 44, 49). Dimerization of Vps8 could then be required to connect Vps21-bound

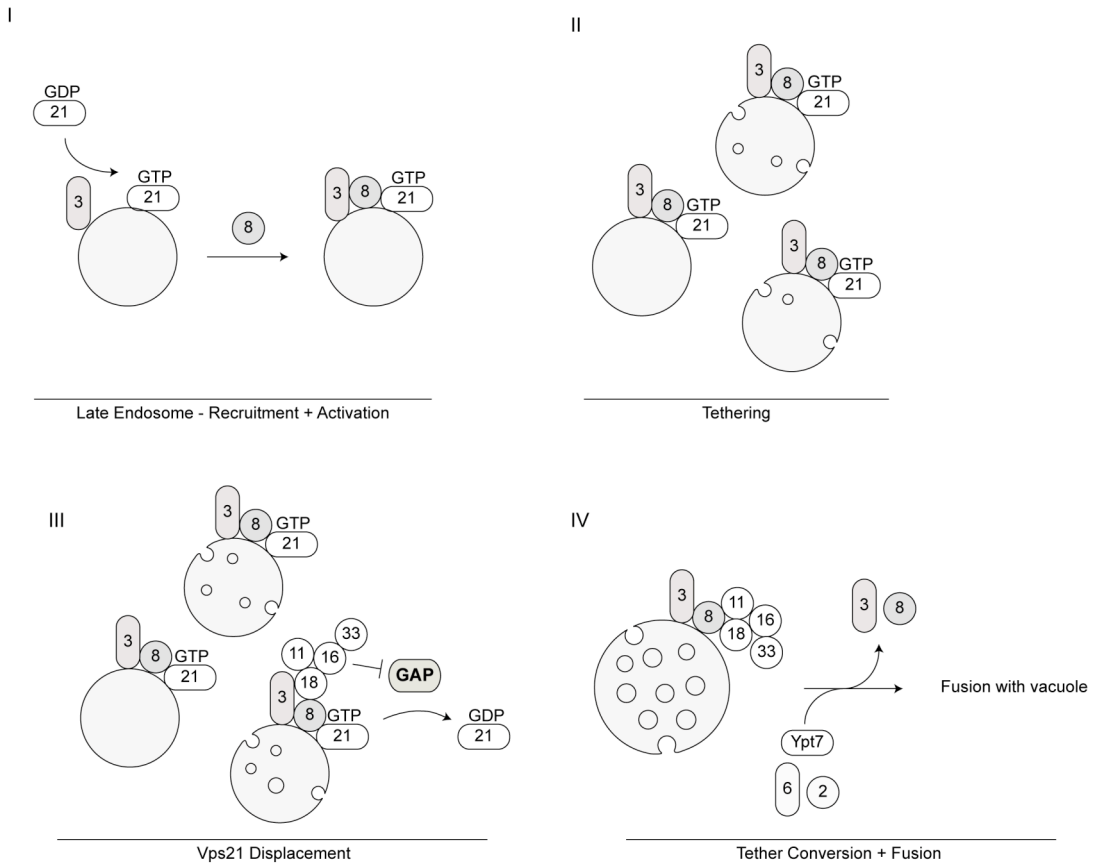

Figure 51 Model of LE tethering and tether conversion
Sequential stages of late endosomal tethering and fusion processes. I) Vps21 is activated by Vps3, leading to a pool of GTP bound Vps21 on the endosomal surface. Active Vps21 recruits its effector Vps8. II) Vps21 and Vps8 mediate tethering of late endosomes. The precise mechanism by which opposing membranes are held together is not known so far. III) Further processing of tethered structures requires release of Vps21. Vps16 is supposed to negatively regulate the Vps21 GAP. Assembly of the CORVET complex allows fusion of tethered late endosomal vesicles. IV) Exchange of Vps3 and Vps8 for Vam6 and Vam2 drives fusion of the MVB with the vacuole.

Vps8 on opposing membranes during tethering, which is supported by preliminary results showing that Vps8 self-interacts in a yeast two-hybrid assay (personal communication Karolina Peplowska). In an alternative model, the gap between opposing membranes could be spanned by a single Vps8 molecule. Bound to one membrane via Vps21, Vps8 could bind to the opposing membrane indirectly by its C-terminal RING domain. Many RING domain containing proteins were described to function as E3 ligases. Binding of the Vps8 RING domain to an E2 conjugating enzyme on the opposing vesicular membrane would then tether both vesicles. Furthermore, this would couple late endosomal tethering to ubiquitin dependent sorting of cargo into intralumenal vesicles and MVB formation.

Under overexpression conditions, the complex of Vps21 and Vps8 might not be turned over efficiently, resulting in the massive accumulation of MVB-like structures. It is therefore very likely that Vps21 and Vps8 release has to proceed to permit fusion of the MVB with the vacuole. A pivotal role in this process could be assigned to Vps16, which might negatively regulate a Vps21 GAP. However, the precise mechanism by which Vps16 regulates Vps21 and how this is connected to CORVET assembly is still not understood. Nevertheless, CORVET assembly could allow for fusion of the tethered structures, thereby generating a fully matured MVB, which, after conversion of CORVET into HOPS by an exchange of Vps8 and Vps3 for Vam6 and Vam2, fuses with the vacuole. Whereas no accumulation of Vam6 and Vam2 was observed upon overexpression of Vps8, the localization of the vacuolar Rab GTPase Ypt7 was shown to overlap with Vps21 at the tethered vesicles (Figure 29C). This strongly supports the idea that Rab conversion, as described by Rink et al.[158], occurs at late endosomal structures and indicates that this precedes conversion of tethering factors.

The results presented in this study, nicely complement and support observations made on other tethering systems. In the yeast secretory pathway, overexpression of the exocyst subunit Sec15, an effector of the exocytic GTPase Sec4, leads to the formation of a cluster of secretory vesicles and a patch of Sec15 close to the plasma membrane that co-localizes with Sec4[206]. It was shown that Sec4 and its GEF Sec2, similar to Vps21 and its putative GEF Vps3 in this study, are required for Sec15 dependent clustering. It would be interesting to investigate whether Sec15 and its binding partner Sec10 are also required for initial tethering of secretory vesicles, whereas the remaining exocyst subunits assemble to promote fusion with the plasma membrane.

The intriguing similarity between the results obtained for the endosomal and the exocytic tethering system might indicate that tethering at different compartments of the endomembrane system follows basic principles. However, in both studies, an overexpression phenotype was exploited to unravel the complex interplay between Rab GTPases and tethering factors. Future studies therefore have to reconstitute the initial tethering processes in order to dissect tethering processes in more detail.

4.5 Conclusion

The results presented in this study describe the direct interplay between Rab GTPases and tethering factors underlying endosomal membrane tethering. The Rab5 homolog Vps21 was shown to directly interact with its effector Vps8, thereby initiating endosomal tethering. Whereas tethering is confined to Vps8 and Vps21, the entire CORVET complex might act at later stages to mediate the transition from tethering to fusion by binding other effectors or assembling SNAREs. Despite the substantial progress in understanding endosomal tethering, many additional questions have to be addressed in future studies. Especially the function of Vps3 and Vps16 needs to be

investigated in more detail in order to reveal the precise order of events in late endosomal maturation.

5 Material and Methods

5.1 Chemicals and reagents

All reagents were purchased from Sigma unless differently indicated. Restriction enzymes as well as reagents for molecular cloning were purchased from NEB and Fermentas.

5.2 Yeast strains and plasmids

Strains used are listed in table S1. Deletion and tagging of genes was done by homologous recombination of PCR fragments. Vam2, Vam6, Vps3, Vps21, Ypt7 and Cps1 were genomically tagged at the N-terminus using an *URA3-PHO5pr-GFP-Myc* cassette, amplified from plasmid pGL (gift from S.Munro, MRC, Cambridge, UK). *VPS8* was placed under the control of the *GAL1*-promoter using PCR fragments containing flanking regions of the *VPS8* gene, amplified from pFA6a-*HIS3MX6-GAL1pr-3xHA*, pFA6a-*TRP1-PGAL1-3HA* or pFA6a-*HIS3MX6-PGAL1-GFP* as template[207]. *ADH1*- and *TEF*-promoters with or without *GFP* inserts were inserted in front of *VPS21* and *VPS8* by amplifying PCR products from pYM-N7, pYM-N9 or pYM-N19 that contain flanking regions of the respective genes[208]. Vps3, Vam6 and Vam2 was C-terminally tagged with the TAP-tag using a *TAP-URA3* cassette amplified from plasmid pBS1539[209]. The plasmid carrying GFP-tagged Ste3 was kindly provided by J. Gerst (Weizman Institute of Science, Rehovot Israel). To generate RFP-tagged versions of Pep12, Vam3, Vps21, Ypt7 and Cps1, genes were amplified from genomic DNA, digested with *Bam*HI / *Sac*I and inserted into *Bam*HI / *Sac*I site of the pV2

plasmid that carries DsRed from pRSET-B DsRed dimer (provided by S. Munro, MRC Cambridge, UK). Yeast two hybrid (Y2H) analyses were conducted using the pACT2 (CLONTECH Laboratories, Inc.) and pFBT9 (a modified pGBT9 vector from CLONTECH Laboratories, Inc.) vectors (provided by Francis Barr, University of Liverpool, UK). Genes of interest were amplified from genomic DNA and after digestion with *Bam*HI and *Xho*I ligated into pACT2, or into a *Bam*HI -*Sal*I site of pFBT9. Mutant versions of *VPS21*, *YPT7*, *YPT52,* and *YPT53* were generated by first cloning wild-type genes into pGEX4T3 vector followed by site directed mutagenesis using the quick-change mutagenesis kit (Stratagene). Mutated Rab versions were amplified from these vectors and cloned into pACT2 and pFBT9 as described above. All inserts and mutations were confirmed by sequencing.

5.3 Yeast cell lysis

After overnight growth in rich medium containing 2% glucose (YPD) or 2% galactose (YPG), cell cultures were diluted to OD_{600}=0.5 and incubated for 2 hours in 30°C. Cells (50 OD_{600} units) were collected, washed once with dithiotretiol (DTT) buffer (10 mM DTT, 0.1 M Tris/HCl, pH 9.4), resuspended in 1ml of DTT buffer and incubated for 10 minutes in 30°C. They were then centrifuged (2 min, 4620*g*), resuspended in 300µl of spheroplasting buffer (0.16 x YPD, 50 µM KPi buffer pH 7.4, 0.6 M sorbitol), and incubated for 20 min at 30°C in the presence of lyticase. Cells were centrifuged for 3 min at 1530*g*, the pellet was resuspended in 1 ml of lysis buffer (0.2 M sorbitol, 150 mM KCl, 20 mM HEPES/KOH pH 6.8, 1 mM DTT, 1 mM PMSF, 1xPIC) supplemented with 6µl of 0.4 mg/ml DEAE dextran, and incubated for 5 minutes on ice. Samples were briefly heat shocked (2 min, 30°C), and cell debris was removed by centrifugation at 300*g* for 3 min. The cell lysate was used in further experiments.

5.4 Biochemical fractionation of yeast cells

Fractionation was done as described[10]. Briefly, yeast cell lysate was prepared and centrifuged for 15 min at 13000*g* at 4°C. The supernatant was centrifuged for 1 h at 100,000*g* resulting in a P100 pellet and a S100 supernatant fraction. The S100 fraction was trichloroacetic acid (TCA)-precipitated, acetone washed and, as the P13 and P100 pellet fractions, resuspended in SDS sample buffer. Proteins were analyzed by SDS-PAGE and Western blotting.

5.5 Sucrose density gradient centrifugation

Lysed spheroplasts of the indicated strains were prepared (see 8.3) and the lysate was adjusted to 1.3 mg/ml (wild-type) or 0.6 mg/ml (Vps8 and Vps21 co-overexpressing cells) in 20mM HEPES/KOH (pH 7.4), 100 mM NaCl, 1xPIC, 1mM PMSF, 16% sucrose. Samples (2ml) were applied to a linear 16 to 60% sucrose gradient and centrifuged for 18h at 100,000g. 1ml fractions were collected from the top, TCA precipitated and analyzed by SDS-PAGE and Western blotting, using anti-HA, -Vps21, -Vma6, and anti-Vti antibodies. Signal intensities, detected by immuno-blotting were quantified by the Odyssey Infrared Imaging System 2.1 (Licor Biosciences). Maximum signal intensities of individual decorations were set to 100%.

5.6 Total protein extraction from yeast

To quantify protein content of yeast cells, protein extracts of the indicated strains were generated by alkaline lysis. One OD_{600} unit of yeast cells was lysed in 0.25 M NaOH, 140 mM β-ME, 3 mM PMSF. After 10 min incubation on ice, samples were subjected

to TCA precipitation followed by acetone wash. SDS-sample buffer was added and equal amounts of proteins were analyzed by SDS-PAGE and western blotting.

5.7 CPY spotting assay

After overnight growth in glucose or galactose containing medium, cells were serial diluted to 1, 0.1 and 0.01 OD_{600} and 5µl of each dilution were spotted on YPD and YPG medium plates. Plates were incubated overnight at 30°C and replica plated onto nitrocellulose filters which were placed on fresh YPD or YPG plates. After incubation at 30°C over night, filters were removed, thoroughly washed and further processed like normal Western Blots. Secreted CPY was detected by decorating filters with anti-CPY antibody.

5.8 Yeast two-hybrid analysis

Analysis was carried out as described by Shorter et al.[210]. Combinations of pACT2- and pFBT9-Y2H vectors, encoding the DNA sequence of the indicated proteins, were transformed into yeast strain PJ69-4A and plated onto synthetic media lacking leucine and tryptophane (double drop out, DDO). Transformants were transferred first onto medium lacking leucine, tryptophane, histidine and adenine (quadruple drop-out, QDO) and afterwards on DDO medium containing 2% glucose. For each Y2H-vector combination, four clones were analyzed. An interaction between tested proteins results in the capability to grow on QDO medium.

5.9 Fluorescence microscopy

Staining of cells with the lipophilic dye FM4-64 was done by following a pulse-chase procedure. 1OD of cells was collected by centrifugation and resuspended in 50µl of medium containing FM4-64 (2µl of a 2mg/ml stock). After 30min incubation at 30°C (pulse), cells were washed with water, resuspended and incubated in medium for 45 min. Cells were washed once in PBS before imaging. For fluorescence microscopy of cells carrying GFP- and RFP-tagged proteins, cells were grown to logarithmic phase in YPD or selective medium, collected by centrifugation and washed once with 1 ml of PBS buffer and imaged. To follow Ste3-GFP sorting, cycloheximide (3,125 µg/ml) was added to cells. After 45 min incubation, cells were washed twice and analyzed by fluorescence microscopy. To monitor DNA-staining and GFP-fluorescence simultaneously, DAPI (4', 6-diamidino-2-phenylindole) was added to PBS washed cell to a final concentration of 2 µg/ml. Cells were incubated for 5 minutes at 30°C, washed twice with PBS buffer before collecting the fluorescence signals. Images were acquired using a Leica DM5500 microscope and a SPOT Pursuit-XS camera using filters for GFP, FM4-64, RFP and DAPI. The pictures were processed using Adobe Photoshop 7.

5.10 EM analyses

Ultrastructural analyses of strains generated in this study were kindly done by Muriel Mari, Janice Griffith and Fulvio Reggiori (University Medical Centre Utrecht). In brief, strains were grown to exponential phase before being processed for electron microscopy. Permanganate fixation, dehydration and embedding in the Spurr´s resin, and immunogold labelling of cryosections were carried out as described[211]. Sections were viewed in Jeol 1200 transmission electron microscope (Jeol, Tokyo, Japan) and images were recorded on Kodak 4489 sheet films.

5.11 GSH Rab Pull-Down

GST fusion proteins (400 µg per sample) were incubated with 500µl 20 mM HEPES/NaOH (pH 7.4), 20 mM EDTA and 10 mM GDP, GTPγS or no nucleotide for 15 min at 30°C. The GDP and GTPγS samples were adjusted to 25 mM $MgCl_2$, and loaded onto 50µl of washed GSH-beads. The nucleotide free sample was added to the beads without $MgCl_2$ treatment. After incubation for 1h at 4°C, the GSH-bound nucleotide free form was washed once with 20mM HEPES/NaOH (pH 7.4), 20 mM EDTA before resuspending in 200µl 20 mM HEPES/NaOH (pH 7.4) 100 mM NaCl, 1 mM $MgCl_2$). GDP and GTPγS loaded Rabs were resuspended in 200µl 20mM HEPES/NaOH (pH 7.4) 100 mM NaCl, 1 mM $MgCl_2$ and 10 mM GDP or GTPγS, respectively. Preloaded Rab GTPases were used in pull-down experiments. Purified CORVET was prepared from the GAL1-TAP-Vps3 overexpression strain, as described in Peplowska et al. (2007). Alternatively, lysates from the indicated strains were prepared from the indicated strains by glass bead lysis from 3L of cells in 20 mM HEPES/NaOH (pH 7.4), 100 mM NaCl 1 mM TX100, centrifuged (1hr, 100,000g, 4°C), concentrated to 2 ml using an Amicon Ultra Centrifugal Filter Device (MWCO 10,000) and added to the prebound Rab GTPases (Figure 25). Similarly, detergent extracts of whole cell lysates (Figure 21B) or membrane fractions, generated following mild lysis (see 8.3) were applied to immobilized Rabs. Beads were incubated for 1h at 4°C on a rotating wheel, washed three times with decreasing TX100 concentrations, and eluted by incubating beads with 20 mM HEPES/NaOH (pH 7.4), 200 mM NaCl, 20 mM EDTA, 0.1% TX100 for 20 min at room temperature. Eluates were TCA precipitated and analyzed by SDS-PAGE and western blotting.

5.12 Co-overexpression GSH Rab Pull-Down

Cells were grown overnight in the presence of galactose to overproduce GST-Rab protein (Vps21, Ypt7 or Ypt1) together with TAP-tagged Vps3 or Vps9. 200 ODs of cells were collected, washed once with 1 ml of buffer A (20 mM Tris/HCl pH 7.4, 150 mM NaCl, 5 mM $MgCl_2$) and lysed with glass beads in the presence of 300 ml of buffer A containing 1xPIC and 1 mM PMSF. Lysis was repeated twice and each time 300 ml of lysate were collected. The lysate (25 mg) was supplemented with 0.5% TX100, centrifuged (30 min, 100,000*g*, 4°C), and then loaded onto 50µl equilibrated glutathione (GSH) beads. An aliquot of the lysate (0.1%) was removed as a loading control. Beads were incubated at 4°C for 1.5h and then washed extensively (2 x 15 min with buffer A + 0.1% TX100 and 2 x 15 min with buffer A + 0.025% TX100). Proteins were eluted by incubating the beads for 20 min at room temperature in 600µl elution buffer (20 mM Tris/HCl pH 7.4, 1.5 M NaCl, 20 mM EDTA), TCA precipitated, and analyzed by using 7.5% SDS-PAGE and western blotting

5.13 Strains used in this study

Table 1 Strains used in this study

Strain	Genotype	Reference
CUY93	MATa *trp1Δ63 ura3Δ0*	Brachman et al., 1998
CUY100	BY4727 MATalpha *his3*Δ200 *leu2*Δ0 *lys2*Δ0 *met15*Δ0 *trp1*Δ63 *ura3*Δ0	EUROSCARF library
CUY105	BY4732 MATa *his3*Δ200 *leu2*Δ0 *met15*Δ0 *trp*1Δ63 *ura3*Δ0	EUROSCARF library
CUY106	BY4733 MATalpha *his3*Δ200 *leu2*Δ0 *met15*Δ0 *trp1*Δ63 *ura3*Δ0	EUROSCARF library
CUY350	CUY867; *VPS21::URA3-Pho5pr-GFP*	This study
CUY380	CUY2008; *Ypt53::URA3-Pho5pr-GFP*	This study
CUY381	CUY2008; *Ypt52::URA3-Pho5pr-GFP*	This study
CUY473	MATa *his3*Δ *leu2*Δ *met15*Δ *ura3*Δ *vps8*Δ::kanMX	EUROSCARF library
CUY482	MATa *his3*Δ *leu2*Δ *met15*Δ *ura3*Δ *vps21*Δ::kanMX	EUROSCARF library

CUY516	*MATa his3Δ leu2Δ met15Δ ura3Δ vam6Δ::*kanMX	EUROSCARF library
CUY520	MATa *his3Δ leu2Δ met15Δ ura3Δ vps33Δ*::kanMX	EUROSCARF library
CUY521	MATa *his3Δ leu2Δ met15Δ ura3Δ vps16Δ*::kanMX	EUROSCARF library
CUY523	MATa *his3Δ leu2Δ met15Δ ura3Δ vps18Δ*::kanMX	EUROSCARF library
CUY594	MATa *his3Δ leu2Δ met15Δ ura3Δ pep12Δ*::kanMX	EUROSCARF library
CUY820	*MATa his3Δ1 leu2Δ0 met15Δ0 ura3Δ0 YPT7::HIS5-PHO5pr-Myc-GFP*	LaGrassa and Ungermann, 2005[8]
CUY827	CUY2008; *VPS21*::natNT2-ADHpr	This study
CUY867	MATa *his3Δ1 leu2Δ0 met15Δ0 ura3Δ0 vps4Δ::*kanMX	EUROSCARF library
CUY902	MATa *his3Δ leu2Δ met15Δ ura3Δ vps45Δ*::kanMX	EUROSCARF library
CUY1014	MATa *his3Δ leu2Δ met15Δ ura3Δ vps3Δ*::kanMX	EUROSCARF library
CUY1030	*MATa his3Δ leu2Δ met15Δ ura3Δ VAM2::HIS5-PHO5pr*-GFP	Takeda et al., 2008
CUY1792	*MATa his3Δ1 leu2Δ0 met15Δ0 ura3Δ0 VPS8::*TAP-kanMX	Peplowska et al., 2007[155]
CUY1795	*MATa his3Δ1 leu2Δ0 met15Δ0 ura3Δ0 VPS3::*TAP-*URA3*	Peplowska et al., 2007[155]
CUY1800	MATa his3Δ1 leu2Δ0 met15Δ0 ura3Δ0 *VAM2::TAP-URA3*	Peplowska et al., 2007[155]
CUY1819	CUY473; *VPS21::URA3-PHO5pr*-GFP	This study
CUY1824	MATalpha *his3Δ200 leu2Δ0 met15Δ0 trp1Δ63 ura3Δ0 VAM6::*TAP-kanMX	This study
CUY1874	CUY1792; *VPS8::HIS3-GAL1pr*	This study
CUY1895	MATalpha *his3Δ200 leu2Δ0 met15Δ0 trp1Δ63 ura3Δ0 VPS3::TRP1-Gal1pr*-TAP	Peplowska et al., 2007[155]
CUY1906	MATa *his3Δ leu2Δ met15Δ ura3Δ vps11Δ::URA3*	EUROSCARF library
CUY1936	MATalpha *his3Δ200 leu2Δ0 met15Δ0 trp1Δ63 ura3Δ0 VPS3::TRP1-Gal1pr*-TAP *VPS21::*kanMX-*GAL1pr*-GST	Peplowska et al., 2007[155]
CUY1948	MATalpha *his3Δ200 leu2Δ0 met15Δ0 trp1Δ63 ura3Δ0 VPS3::TRP1-Gal1pr-TAP YPT1::*kanMx-*Ga1lpr*-GST	Peplowska et al., 2007[155]
CUY1949	MATalpha *his3Δ200 leu2Δ0 met15Δ0 trp1Δ63 ura3Δ0 VPS3::TRP1-Gal1pr*-TAP *VPS21::*kanMX-*GAL1pr*-GST	Peplowska et al., 2007[155]
CUY1951	MATa *trp1Δ63 ura3Δ0 vps8Δ::*kanMx	Peplowska et al., 2007[155]
CUY1958	CUY93; *trp1Δ63 ura3Δ0 YPT52::URA3-Pho5pr*-GFP	This study
CUY1960	MATa *trp1Δ63 ura3Δ0 vps8Δ::*kanMx *VPS21::URA3-Pho5pr*-GFP *pV2-RFP-Ypt7 (TRP1)*	Peplowska et al., 2007[155]
CUY1969	MATalpha *his3Δ200 leu2Δ0 met15Δ0 trp1Δ63 ura3Δ0 VPS9::TRP1-Gal1pr*-TAP *Vps21::*kanMX-*Gal1pr*-GST	Peplowska et al., 2007[155]
CUY1972	MATa *trp1Δ63 ura3Δ0 VPS21::URA3-Pho5pr-GFP pV2-RFP-Ypt7 (TRP1)*	Peplowska et al., 2007[155]
CUY1990	CUY93; trp1Δ63 ura3Δ0 YPT53::*URA3-Pho5*-GFP	This study
CUY2008	CUY106; *VPS8*::*TRP1-GAL1pr*-3HA	This study

CUY2123	MATa *his3*Δ1 *leu2*Δ0 *met15*Δ0 *ura3*Δ0 *vps9*Δ::kanMX	EUROSCARF library
CUY2253	MATalpha *his3*Δ200 *leu2*Δ0 *met15*Δ0 *trp1*Δ63 *ura3*Δ0 *VPS8*::*TRP1-GAL1*pr-3HA *VPS21*::*URA3-PHO5pr*-GFP	Peplowska et al., 2007[155]
CUY2267	CUY2123; *VPS21*::*URA3-PHO5pr*-GFP	This study
CUY2268	CUY902; *VPS21*::*URA3-PHO5pr*-GFP	This study
CUY2569	CUY100; *VPS18*::TAP-*URA3*	This study
CUY2270	CUY594; *VPS21*::*URA3-PHO5pr*-GFP	This study
CUY2278	MATa *his3*Δ *leu2*Δ *met15*Δ *ura3*Δ *vps3*Δ::kanMX *VPS21*::*URA3-PHO5pr*-GFP *VPS8*::*HIS3-GAL1pr*-3HA	Peplowska et al., 2007[155]
CUY2359	MATa *trp1*Δ*63 ura3*Δ*0 vps8*::kanMx *VPS3::TRP1-Gal1pr*-TAP	Peplowska et al., 2007[155]
CUY2590	CUY100; *URA3::pRS316-Ste3-GFP*	This study
CUY2593	CUY100; *CPS1*::*URA3-PHO5pr*-GFP	This study
CUY2650	CUY1014; *CPS1*::*URA3-PHO5pr*-GFP	This study
CUY2653	CUY473; *CPS1*::*URA3-PHO5pr*-GFP	This study
CUY2682	CUY2268; *VPS8*::*HIS3-GAL1pr*-3HA	This study
CUY2693	CUY350; *VPS8::HIS3-GAL1pr*-3HA	This study
CUY2694	SEY6210 MATalpha *leu2-3*,112 *ura3-52 his3*-Δ200 *trp*-Δ901 *lys*2-801 suc2-Δ9 GAL	Robinson et al.[212]
CUY2695	CUY2694; *VPS21*::*URA3-PHO5pr*-GFP	This study
CUY2696	CUY106; *VPS21*::*URA3-PHO5pr*-GFP	This study
CUY2704	CUY1014; *URA3*::*pRS316-Ste3*-GFP	This study
CUY2705	CUY473; *URA3*::*pRS316-Ste3*-GFP	This study
CUY2716	CUY2696; *VPS8*::*HIS3-GAL1pr*-3HA	This study
CUY2719	CUY2008; *VPS21*::natNT2-*ADHpr*-GFP	This study
CUY2762	CUY2716; *pV2-PHO5pr-RFP-Cps1* (TRP1)	This study
CUY2767	CUY2696; *pV2-PHO5pr-RFP-Pep12* (TRP1)	This study
CUY2768	CUY2716; *pV2-PHO5pr-RFP-Pep12* (TRP1)	This study
CUY2770	CUY827; *URA3::pRS316-Ste3*-GFP	This study
CUY2771	CUY827; *VAM6*::*URA3-PHO5pr*-GFP	This study
CUY2772	CUY827; *Vps3*::*URA3-PHO5pr*-GFP	This study
CUY2773	CUY827; *VAM2*::*HIS3-PHO5pr*-GFP	This study
CUY2842	CUY106; *VPS21*::natNT2-*ADH1pr*	This study
CUY2843	CUY2842; *VPS8*::*HIS3-GAL1pr*-GFP	This study
CUY2844	CUY2267; *VPS8*::*HIS3-GAL1pr*-3HA	This study
CUY2845	CUY2695; *VPS8*::natNT2-*TEFpr*	This study

CUY2871	CUY2270; *VPS8*::*HIS3-GAL1pr*-3HA	This study
CUY2896	CUY106; *VPS8*::*HIS3-GAL1pr*-GFP	This study
CUY2900	CUY106; *VPS11*::TAP-*URA3*	This study
CUY2921	CUY1014; *VPS8::HIS-Gal1pr*-GFP	This study
CUY2922	CUY482; *VPS8*::*HIS3-GAL1pr*-GFP	This study
CUY2935	CUY106; *VPS11*::GFP-hphNT1	This study
CUY2949	CUY2920; *VPS3*::TAP-*URA3*	This study
CUY2950	CUY827; *VPS3*::TAP-*URA3*	This study
CUY2964	CUY2921; *VPS21::natNT2-ADHpr*	This study
CUY3025	CUY105; *VPS18*::GFP-hpNT1	This study
CUY3026	CUY105; *VPS16*::GFP-hpNT1	This study
CUY3051	CUY2716; *pV2-Pho5pr-RFP-Ypt7 (TRP1)*	This study
CUY3101	CUY2696; *VPS8Δ1-90*::*HIS3-GAL1pr*-3HA	This study
CUY3217	CUY827; *VPS11*::GFP-hphNT1	This study
CUY3218	CUY2842; *VPS8Δ1-90::HIS-Gal1pr*-GFP	This study
CUY3243	CUY106; *VAM3*::*URA3-PHO5pr*-GFP	This study
CUY3244	CUY106; *VPS3*::*URA3-PHO5pr*-GFP	This study
CUY3276	CUY106; *his3Δ200 leu2Δ0 met15Δ0 trp1Δ63 ura3Δ0 VPS8::GFP-TRP1*	This study
CUY3277	CUY827; *VPS18*::GFP-hpNT1	This study
CUY3279	CUY521; *VPS8*::*HIS3-GAL1pr*-3HA	This study
CUY3281	CUY1906; *VPS8::HIS3-Galpr*-GFP	This study
CUY3282	CUY521; *VPS8::HIS3-Gal1pr*-GFP	This study
CUY3283	CUY523: *VPS8::HIS3-Gal*-GFP	This study
CUY3289	CUY523; *VPS8*::*HIS3-GAL1pr*-3HA	This study
CUY3299	CUY520; *VPS8::HIS3-Gal1pr-GFP*	This study
CUY3309	CUY3281; *VPS21::natNT2-ADHpr*	This study
CUY3310	CUY3282; *VPS21::natNT2-ADHpr*	This study
CUY3311	CUY3283; *VPS21*::natNT2-*ADH1pr*	This study
CUY3312	CUY3279; *VPS21*::*URA3-PHO5pr*-GFP	This study
CUY3315	CUY3289; *VPS21*::*URA3-PHO5pr*-GFP	This study
CUY3324	CUY2922; *GAL1pr*::*pRS406-GAL1pr-Vps21 Q66L*	This study
CUY3337	CUY2694; *VPS21::*kanMX-*ADHpr*	This study
CUY3338	CUY2694; *VPS8*::natNT2-TEF*pr-GFP*	This study
CUY3339	CUY520; *VPS8*::*HIS3-GAL1pr*-3HA	This study

CUY3340	CUY3299; *VPS21::natNT2-ADHpr*	This study
CUY3356	CUY2696; *VPS8Δ1-47::HIS3-GAL1pr*-3HA	This study
CUY3357	CUY2842; *VPS8Δ1-47::HIS3-GAL1pr*-GFP	This study
CUY3358	CUY3339; *VPS21*::*URA3-PHO5pr*-GFP	This study
CUY3359	CUY3338; *VPS21*::kanMX-*ADH1pr*	This study
CUY3381	CUY106; *pV2-PHO5pr-RFP-Vps21* (TRP1)	This study
CUY3382	CUY2896; *pV2-PHO5pr-RFP-Vps21* (TRP1)	This study
CUY3391	CUY2253; *vps11Δ::HIS3*	This study
CUY3393	CUY2922; *GAL1pr::pRS406-GAL1pr-Vps21 S21N*	This study
CUY3403	CUY2253; *his3Δ200 leu2Δ0 met15Δ0 trp1Δ63 ura3Δ0 VPS8::TRP1-Gal1pr-3HA VPS21::URA3-Pho5pr-GFP VPS3:*:kanMX-*GAL1pr*	This study
CUY3404	CUY827; *VPS16*::GFP-kanMX	This study
CUY3422	CUY2696; *pV2-Pho5pr-RFP-Vam3* (TRP1)	This study
CUY3423	CUY2716; *pV2-Pho5pr-RFP-Vam3* (TRP1)	This study
CUY3593	CUY3337; *VPS8::natNT2-TEFpr*	This study
CUY3615	CUY2845; *vam3Δ::HIS3*	This study
CUY3616	CUY3593; *CPS1::URA3-PHO5pr*-GFP	This study

6 Table of Figures

7 References

[1] Holthuis, J. C., van Meer, G., and Huitema, K., Lipid microdomains, lipid translocation and the organization of intracellular membrane transport (Review). *Mol Membr Biol* **20** (3), 231 (2003).

[2] van Meer, G., Voelker, D. R., and Feigenson, G. W., Membrane lipids: where they are and how they behave. *Nat Rev Mol Cell Biol* **9** (2), 112 (2008).

[3] Malhotra, J. D. and Kaufman, R. J., The endoplasmic reticulum and the unfolded protein response. *Semin Cell Dev Biol* **18** (6), 716 (2007).

[4] Meusser, B., Hirsch, C., Jarosch, E., and Sommer, T., ERAD: the long road to destruction. *Nat Cell Biol* **7** (8), 766 (2005).

[5] Puthenveedu, M. A. and Linstedt, A. D., Subcompartmentalizing the Golgi apparatus. *Curr Opin Cell Biol* **17** (4), 369 (2005).

[6] Gleeson, P. A., Targeting of proteins to the Golgi apparatus. *Histochem Cell Biol* **109** (5-6), 517 (1998).

[7] Pelham, H. R., Traffic through the Golgi apparatus. *J Cell Biol* **155** (7), 1099 (2001).

[8] Thumm, M., Structure and function of the yeast vacuole and its role in autophagy. *Microsc Res Tech* **51** (6), 563 (2000).

[9] Takegawa, K. et al., Vesicle-mediated protein transport pathways to the vacuole in Schizosaccharomyces pombe. *Cell Struct Funct* **28** (5), 399 (2003).

[10] LaGrassa, T. J. and Ungermann, C., The vacuolar kinase Yck3 maintains organelle fragmentation by regulating the HOPS tethering complex. *J Cell Biol* **168** (3), 401 (2005).

[11] Weisman, L. S., Yeast vacuole inheritance and dynamics. *Annu Rev Genet* **37**, 435 (2003).

[12] Ostrowicz, C. W., Meiringer, C. T., and Ungermann, C., Yeast vacuole fusion: A model system for eukaryotic endomembrane dynamics. *Autophagy* **4** (1), 5 (2007).

[13] Holthuis, J. C. and Levine, T. P., Lipid traffic: floppy drives and a superhighway. *Nat Rev Mol Cell Biol* **6** (3), 209 (2005).

[14] Haucke, V. and Di Paolo, G., Lipids and lipid modifications in the regulation of membrane traffic. *Curr Opin Cell Biol* **19** (4), 426 (2007).

[15] Maxfield, F. R., Plasma membrane microdomains. *Curr Opin Cell Biol* **14** (4), 483 (2002).

[16] Seigneuret, M. and Devaux, P. F., ATP-dependent asymmetric distribution of spin-labeled phospholipids in the erythrocyte membrane: relation to shape changes. *Proc Natl Acad Sci USA* **81** (12), 3751 (1984).

[17] Simonsen, A., Wurmser, A. E., Emr, S. D., and Stenmark, H., The role of phosphoinositides in membrane transport. *Curr Opin Cell Biol* **13** (4), 485 (2001).

[18] Roth, M. G., Phosphoinositides in constitutive membrane traffic. *Physiol Rev* **84** (3), 699 (2004).

[19] Lemmon, M. A., Phosphoinositide recognition domains. *Traffic* **4** (4), 201 (2003).

[20] Stenmark, H., Aasland, R., and Driscoll, P. C., The phosphatidylinositol 3-phosphate-binding FYVE finger. *FEBS Lett* **513** (1), 77 (2002).

[21] Chen, H. et al., Epsin is an EH-domain-binding protein implicated in clathrin-mediated endocytosis. *Nature* **394** (6695), 793 (1998).

[22] Ford, M. G. et al., Curvature of clathrin-coated pits driven by epsin. *Nature* **419** (6905), 361 (2002).

[23] Fruman, D. A., Meyers, R. E., and Cantley, L. C., Phosphoinositide kinases. *Annu Rev Biochem* **67**, 481 (1998).

[24] Stack, J. H., Herman, P. K., Schu, P. V., and Emr, S. D., A membrane-associated complex containing the Vps15 protein kinase and the Vps34 PI 3-kinase is essential for protein sorting to the yeast lysosome-like vacuole. *EMBO J* **12** (5), 2195 (1993).

[25] Gary, J. D. et al., Fab1p is essential for PtdIns(3)P 5-kinase activity and the maintenance of vacuolar size and membrane homeostasis. *J Cell Biol* **143** (1), 65 (1998).

[26] Lee, M. C. et al., Bi-directional protein transport between the ER and Golgi. *Annu Rev Cell Dev Biol* **20**, 87 (2004).

[27] Saraste, J. and Svensson, K., Distribution of the intermediate elements operating in ER to Golgi transport. *J Cell Sci* **100 (Pt 3)**, 415 (1991).

[28] Chao, D. S. et al., SNARE membrane trafficking dynamics in vivo. *J Cell Biol* **144** (5), 869 (1999).

[29] Lavoie, C. et al., Roles for alpha(2)p24 and COPI in endoplasmic reticulum cargo exit site formation. *J Cell Biol* **146** (2), 285 (1999).

[30] Watson, P. et al., Sec16 defines endoplasmic reticulum exit sites and is required for secretory cargo export in mammalian cells. *Traffic* **7** (12), 1678 (2006).

[31] Morgan, A., Exocytosis. *Essays Biochem* **30**, 77 (1995).

[32] Teter, S. A. and Klionsky, D. J., Transport of proteins to the yeast vacuole: autophagy, cytoplasm-to-vacuole targeting, and role of the vacuole in degradation. *Semin Cell Dev Biol* **11** (3), 173 (2000).

[33] Marcusson, E. G. et al., The sorting receptor for yeast vacuolar carboxypeptidase Y is encoded by the VPS10 gene. *Cell* **77** (4), 579 (1994).

[34] Whyte, J. R. and Munro, S., A yeast homolog of the mammalian mannose 6-phosphate receptors contributes to the sorting of vacuolar hydrolases. *Curr Biol* **11** (13), 1074 (2001).

[35] Seaman, M. N., Marcusson, E. G., Cereghino, J. L., and Emr, S. D., Endosome to Golgi retrieval of the vacuolar protein sorting receptor, Vps10p, requires the function of the VPS29, VPS30, and VPS35 gene products. *J Cell Biol* **137** (1), 79 (1997).

[36] Stepp, J. D., Huang, K., and Lemmon, S. K., The yeast adaptor protein complex, AP-3, is essential for the efficient delivery of alkaline phosphatase by the alternate pathway to the vacuole. *J Cell Biol* **139** (7), 1761 (1997).

[37] Raymond, C. K., Howald-Stevenson, I., Vater, C. A., and Stevens, T. H., Morphological classification of the yeast vacuolar protein sorting mutants: evidence for a prevacuolar compartment in class E vps mutants. *Mol Biol Cell* **3** (12), 1389 (1992).

[38] Cowles, C. R., Odorizzi, G., Payne, G. S., and Emr, S. D., The AP-3 adaptor complex is essential for cargo-selective transport to the yeast vacuole. *Cell* **91** (1), 109 (1997).

[39] Darsow, T., Burd, C. G., and Emr, S. D., Acidic di-leucine motif essential for AP-3-dependent sorting and restriction of the functional specificity of the Vam3p vacuolar t-SNARE. *J Cell Biol* **142** (4), 913 (1998).

[40] Sun, B. et al., The yeast casein kinase Yck3p is palmitoylated, then sorted to the vacuolar membrane with AP-3-dependent recognition of a YXXPhi adaptin sorting signal. *Mol Biol Cell* **15** (3), 1397 (2004).

[41] Riezman, H., Woodman, P. G., van Meer, G., and Marsh, M., Molecular mechanisms of endocytosis. *Cell* **91** (6), 731 (1997).

[42] Abeliovich, H., Darsow, T., and Emr, S. D., Cytoplasm to vacuole trafficking of aminopeptidase I requires a t-SNARE-Sec1p complex composed of Tlg2p and Vps45p. *EMBO J* **18** (21), 6005 (1999).

[43] Wang, C. W. and Klionsky, D. J., The molecular mechanism of autophagy. *Mol Med* **9** (3-4), 65 (2003).

[44] Wieland, F. T., Gleason, M. L., Serafini, T. A., and Rothman, J. E., The rate of bulk flow from the endoplasmic reticulum to the cell surface. *Cell* **50** (2), 289 (1987).

[45] Malkus, P., Jiang, F., and Schekman, R., Concentrative sorting of secretory cargo proteins into COPII-coated vesicles. *J Cell Biol* **159** (6), 915 (2002).

[46] Belden, W. J. and Barlowe, C., Role of Erv29p in collecting soluble secretory proteins into ER-derived transport vesicles. *Science* **294** (5546), 1528 (2001).

[47] Bonifacino, J. S., Marks, M. S., Ohno, H., and Kirchhausen, T., Mechanisms of signal-mediated protein sorting in the endocytic and secretory pathways. *Proc Assoc Am Physicians* **108** (4), 285 (1996).

[48] Bonifacino, J. S. and Traub, L. M., Signals for sorting of transmembrane proteins to endosomes and lysosomes. *Annu Rev Biochem* **72**, 395 (2003).

[49] Kirchhausen, T., Clathrin. *Annu Rev Biochem* **69**, 699 (2000).

[50] Robinson, M. S., Adaptable adaptors for coated vesicles. *Trends Cell Biol* **14** (4), 167 (2004).

[51] Boll, W. et al., The mu2 subunit of the clathrin adaptor AP-2 binds to FDNPVY and YppØ sorting signals at distinct sites. *Traffic* **3** (8), 590 (2002).

[52] Ohno, H. et al., Interaction of tyrosine-based sorting signals with clathrin-associated proteins. *Science* **269** (5232), 1872 (1995).

[53] Ohno, H., Fournier, M. C., Poy, G., and Bonifacino, J. S., Structural determinants of interaction of tyrosine-based sorting signals with the adaptor medium chains. *J Biol Chem* **271** (46), 29009 (1996).

[54] Hirst, J., Bright, N. A., Rous, B., and Robinson, M. S., Characterization of a fourth adaptor-related protein complex. *Mol Biol Cell* **10** (8), 2787 (1999).

[55] Jackson, T., Transport vesicles: coats of many colours. *Curr Biol* **8** (17), R609 (1998).

[56] Janvier, K. et al., Recognition of dileucine-based sorting signals from HIV-1 Nef and LIMP-II by the AP-1 gamma-sigma1 and AP-3 delta-sigma3 hemicomplexes. *J Cell Biol* **163** (6), 1281 (2003).

[57] Chen, H. J. et al., Mutational analysis of the cation-independent mannose 6-phosphate/insulin-like growth factor II receptor. A consensus casein kinase II site followed by 2 leucines near the carboxyl terminus is important for intracellular targeting of lysosomal enzymes. *J Biol Chem* **268** (30), 22338 (1993).

[58] Dell'Angelica, E. C. et al., GGAs: a family of ADP ribosylation factor-binding proteins related to adaptors and associated with the Golgi complex. *J Cell Biol* **149** (1), 81 (2000).

[59] Hirst, J. and Robinson, M. S., Clathrin and adaptors. *Biochim Biophys Acta* **1404** (1-2), 173 (1998).

[60] Paleotti, O. et al., The small G-protein Arf6GTP recruits the AP-2 adaptor complex to membranes. *J Biol Chem* **280** (22), 21661 (2005).

[61] Donaldson, J. G., Honda, A., and Weigert, R., Multiple activities for Arf1 at the Golgi complex. *Biochim Biophys Acta* **1744** (3), 364 (2005).

[62] Jost, M. et al., Phosphatidylinositol-4,5-bisphosphate is required for endocytic coated vesicle formation. *Curr Biol* **8** (25), 1399 (1998).

[63] Heuser, J. E. and Anderson, R. G., Hypertonic media inhibit receptor-mediated endocytosis by blocking clathrin-coated pit formation. *J Cell Biol* **108** (2), 389 (1989).

[64] Legendre-Guillemin, V. et al., ENTH/ANTH proteins and clathrin-mediated membrane budding. *J Cell Sci* **117** (Pt 1), 9 (2004).

[65] Horvath, C. A. et al., Epsin: inducing membrane curvature. *Int J Biochem Cell Biol* **39** (10), 1765 (2007).

[66] De Camilli, P. et al., The ENTH domain. *FEBS Lett* **513** (1), 11 (2002).

[67] Gallop, J. L. and McMahon, H. T., BAR domains and membrane curvature: bringing your curves to the BAR. *Biochem Soc Symp* (72), 223 (2005).

[68] Tsujita, K. et al., Coordination between the actin cytoskeleton and membrane deformation by a novel membrane tubulation domain of PCH proteins is involved in endocytosis. *J Cell Biol* **172** (2), 269 (2006).

[69] Itoh, T. et al., Dynamin and the actin cytoskeleton cooperatively regulate plasma membrane invagination by BAR and F-BAR proteins. *Dev Cell* **9** (6), 791 (2005).

[70] Ungewickell, E. J. and Hinrichsen, L., Endocytosis: clathrin-mediated membrane budding. *Curr Opin Cell Biol* **19** (4), 417 (2007).

[71] Watson, P. and Stephens, D. J., ER-to-Golgi transport: form and formation of vesicular and tubular carriers. *Biochim Biophys Acta* **1744** (3), 304 (2005).

[72] Tang, B. L., Wang, Y., Ong, Y. S., and Hong, W., COPII and exit from the endoplasmic reticulum. *Biochim Biophys Acta* **1744** (3), 293 (2005).

[73] Sato, K. and Nakano, A., Mechanisms of COPII vesicle formation and protein sorting. *FEBS Lett* **581** (11), 2076 (2007).

[74] Nickel, W. and Wieland, F. T., Biogenesis of COPI-coated transport vesicles. *FEBS Lett* **413** (3), 395 (1997).

[75] Béthune, J., Wieland, F., and Moelleken, J., COPI-mediated transport. *J Membr Biol* **211** (2), 65 (2006).

[76] Spang, A., ARF1 regulatory factors and COPI vesicle formation. *Curr Opin Cell Biol* **14** (4), 423 (2002).

[77] Yoshihisa, T., Barlowe, C., and Schekman, R., Requirement for a GTPase-activating protein in vesicle budding from the endoplasmic reticulum. *Science* **259** (5100), 1466 (1993).

[78] Mesmin, B. et al., Two lipid-packing sensor motifs contribute to the sensitivity of ArfGAP1 to membrane curvature. *Biochemistry* **46** (7), 1779 (2007).

[79] Bigay, J. et al., ArfGAP1 responds to membrane curvature through the folding of a lipid packing sensor motif. *EMBO J* **24** (13), 2244 (2005).

[80] Hammer, J. A. and Wu, X. S., Rabs grab motors: defining the connections between Rab GTPases and motor proteins. *Curr Opin Cell Biol* **14** (1), 69 (2002).

[81] Matanis, T. et al., Bicaudal-D regulates COPI-independent Golgi-ER transport by recruiting the dynein-dynactin motor complex. *Nat Cell Biol* **4** (12), 986 (2002).

[82] Schott, D., Ho, J., Pruyne, D., and Bretscher, A., The COOH-terminal domain of Myo2p, a yeast myosin V, has a direct role in secretory vesicle targeting. *J Cell Biol* **147** (4), 791 (1999).

[83] Short, B. et al., The Rab6 GTPase regulates recruitment of the dynactin complex to Golgi membranes. *Curr Biol* **12** (20), 1792 (2002).

[84] Söllner, T. et al., SNAP receptors implicated in vesicle targeting and fusion. *Nature* **362** (6418), 318 (1993).

[85] Broadie, K. et al., Syntaxin and synaptobrevin function downstream of vesicle docking in Drosophila. *Neuron* **15** (3), 663 (1995).

[86] Jahn, R. and Scheller, R. H., SNAREs--engines for membrane fusion. *Nat Rev Mol Cell Biol* **7** (9), 631 (2006).

[87] Dietrich, L. E., Boeddinghaus, C., LaGrassa, T. J., and Ungermann, C., Control of eukaryotic membrane fusion by N-terminal domains of SNARE proteins. *Biochim Biophys Acta* **1641** (2-3), 111 (2003).

[88] Dietrich, L. E. and Ungermann, C., On the mechanism of protein palmitoylation. *EMBO Rep* **5** (11), 1053 (2004).

[89] Cheever, M. L. et al., Phox domain interaction with PtdIns(3)P targets the Vam7 t-SNARE to vacuole membranes. *Nat Cell Biol* **3** (7), 613 (2001).

[90] Lee, S. A. et al., Molecular mechanism of membrane docking by the Vam7p PX domain. *J Biol Chem* **281** (48), 37091 (2006).

[91] Chen, Y. A. and Scheller, R. H., SNARE-mediated membrane fusion. *Nat Rev Mol Cell Biol* **2** (2), 98 (2001).

[92] Mayer, A., Wickner, W. T., and Haas, A., Sec18p (NSF)-driven release of Sec17p (alpha-SNAP) can precede docking and fusion of yeast vacuoles. *Cell* **85** (1), 83 (1996).

[93] Söllner, T. et al., A protein assembly-disassembly pathway in vitro that may correspond to sequential steps of synaptic vesicle docking, activation, and fusion. *Cell* **75** (3), 409 (1993).

[94] Ungermann, C., Nichols, B. J., Pelham, H. R., and Wickner, W. T., A vacuolar v-t-SNARE complex, the predominant form in vivo and on isolated vacuoles, is disassembled and activated for docking and fusion. *J Cell Biol* **140** (1), 61 (1998).

[95] Nicholson, K. L. et al., Regulation of SNARE complex assembly by an N-terminal domain of the t-SNARE Sso1p. *Nat Struct Biol* **5** (9), 793 (1998).

[96] Dulubova, I. et al., A conformational switch in syntaxin during exocytosis: role of munc18. *EMBO J* **18** (16), 4372 (1999).

[97] Yamaguchi, T. et al., Sly1 binds to Golgi and ER syntaxins via a conserved N-terminal peptide motif. *Dev Cell* **2** (3), 295 (2002).

[98] Dulubova, I. et al., Vam3p structure reveals conserved and divergent properties of syntaxins. *Nat Struct Biol* **8** (3), 258 (2001).

[99] Dulubova, I. et al., How Tlg2p/syntaxin 16 'snares' Vps45. *EMBO J* **21** (14), 3620 (2002).

[100] Yang, B., Steegmaier, M., Gonzalez, L. C., and Scheller, R. H., nSec1 binds a closed conformation of syntaxin1A. *J Cell Biol* **148** (2), 247 (2000).

[101] Bryant, N. J. and James, D. E., Vps45p stabilizes the syntaxin homologue Tlg2p and positively regulates SNARE complex formation. *EMBO J* **20** (13), 3380 (2001).

[102] Peng, R. and Gallwitz, D., Sly1 protein bound to Golgi syntaxin Sed5p allows assembly and contributes to specificity of SNARE fusion complexes. *J Cell Biol* **157** (4), 645 (2002).

[103] Carr, C. M. et al., Sec1p binds to SNARE complexes and concentrates at sites of secretion. *J Cell Biol* **146** (2), 333 (1999).

[104] Sato, T. K., Rehling, P., Peterson, M. R., and Emr, S. D., Class C Vps protein complex regulates vacuolar SNARE pairing and is required for vesicle docking/fusion. *Mol Cell* **6** (3), 661 (2000).

[105] Starai, V. J., Hickey, C. M., and Wickner, W., HOPS Proofreads the *trans*-SNARE Complex for Yeast Vacuole Fusion. *Mol Biol Cell* **19** (6), 2500 (2008).

[106] Zerial, M. and McBride, H., Rab proteins as membrane organizers. *Nat Rev Mol Cell Biol* **2** (2), 107 (2001).

[107] Pereira-Leal, J. B., Hume, A. N., and Seabra, M. C., Prenylation of Rab GTPases: molecular mechanisms and involvement in genetic disease. *FEBS Lett* **498** (2-3), 197 (2001).

[108] Farnsworth, C. C. et al., Rab geranylgeranyl transferase catalyzes the geranylgeranylation of adjacent cysteines in the small GTPases Rab1A, Rab3A, and Rab5A. *Proc Natl Acad Sci USA* **91** (25), 11963 (1994).

[109] Takai, Y., Sasaki, T., and Matozaki, T., Small GTP-binding proteins. *Physiol Rev* **81** (1), 153 (2001).

[110] Zhu, G. et al., Structural basis of Rab5-Rabaptin5 interaction in endocytosis. *Nat Struct Mol Biol* **11** (10), 975 (2004).

[111] Pfeffer, S. R., Dirac-Svejstrup, A. B., and Soldati, T., Rab GDP dissociation inhibitor: putting rab GTPases in the right place. *J Biol Chem* **270** (29), 17057 (1995).

[112] Takai, Y. et al., Regulators of small GTPases. *Ciba Found Symp* **176**, 128 (1993).

[113] Wu, S. K., Zeng, K., Wilson, I. A., and Balch, W. E., Structural insights into the function of the Rab GDI superfamily. *Trends Biochem Sci* **21** (12), 472 (1996).

[114] Pfeffer, S. and Aivazian, D., Targeting Rab GTPases to distinct membrane compartments. *Nat Rev Mol Cell Biol* **5** (11), 886 (2004).

[115] Bos, J. L., Rehmann, H., and Wittinghofer, A., GEFs and GAPs: critical elements in the control of small G proteins. *Cell* **129** (5), 865 (2007).

[116] Dumas, J. J., Zhu, Z., Connolly, J. L., and Lambright, D. G., Structural basis of activation and GTP hydrolysis in Rab proteins. *Structure* **7** (4), 413 (1999).

[117] Behnia, R. and Munro, S., Organelle identity and the signposts for membrane traffic. *Nature* **438** (7068), 597 (2005).

[118] Gillingham, A. K. and Munro, S., Long coiled-coil proteins and membrane traffic. *Biochim Biophys Acta* **1641** (2-3), 71 (2003).

[119] Waters, M. G., Clary, D. O., and Rothman, J. E., A novel 115-kD peripheral membrane protein is required for intercisternal transport in the Golgi stack. *J Cell Biol* **118** (5), 1015 (1992).

[120] Mu, F. T. et al., EEA1, an early endosome-associated protein. EEA1 is a conserved alpha-helical peripheral membrane protein flanked by cysteine "fingers" and contains a calmodulin-binding IQ motif. *J Biol Chem* **270** (22), 13503 (1995).

[121] Christoforidis, S., McBride, H. M., Burgoyne, R. D., and Zerial, M., The Rab5 effector EEA1 is a core component of endosome docking. *Nature* **397** (6720), 621 (1999).

[122] Markgraf, D. F., Peplowska, K., and Ungermann, C., Rab cascades and tethering factors in the endomembrane system. *FEBS Lett* **581** (11), 2125 (2007).

[123] Lupashin, V. and Sztul, E., Golgi tethering factors. *Biochim Biophys Acta* **1744** (3), 325 (2005).

[124] Drin, G. et al., Asymmetric tethering of flat and curved lipid membranes by a golgin. *Science* **320** (5876), 670 (2008).

[125] Bigay, J., Gounon, P., Robineau, S., and Antonny, B., Lipid packing sensed by ArfGAP1 couples COPI coat disassembly to membrane bilayer curvature. *Nature* **426** (6966), 563 (2003).

[126] Whyte, J. R. and Munro, S., Vesicle tethering complexes in membrane traffic. *J Cell Sci* **115** (Pt 13), 2627 (2002).

[127] Ungar, D., Oka, T., Krieger, M., and Hughson, F. M., Retrograde transport on the COG railway. *Trends Cell Biol* **16** (2), 113 (2006).

[128] Conibear, E. and Stevens, T. H., Vps52p, Vps53p, and Vps54p form a novel multisubunit complex required for protein sorting at the yeast late Golgi. *Mol Biol Cell* **11** (1), 305 (2000).

[129] Hsu, S. C., TerBush, D., Abraham, M., and Guo, W., The exocyst complex in polarized exocytosis. *Int Rev Cytol* **233**, 243 (2004).

[130] TerBush, D. R., Maurice, T., Roth, D., and Novick, P., The Exocyst is a multiprotein complex required for exocytosis in Saccharomyces cerevisiae. *EMBO J* **15** (23), 6483 (1996).

[131] Seals, D. F. et al., A Ypt/Rab effector complex containing the Sec1 homolog Vps33p is required for homotypic vacuole fusion. *Proc Natl Acad Sci USA* **97** (17), 9402 (2000).

[132] Wurmser, A. E., Sato, T. K., and Emr, S. D., New component of the vacuolar class C-Vps complex couples nucleotide exchange on the Ypt7 GTPase to SNARE-dependent docking and fusion. *J Cell Biol* **151** (3), 551 (2000).

[133] Munson, M. and Novick, P., The exocyst defrocked, a framework of rods revealed. *Nat Struct Mol Biol* **13** (7), 577 (2006).

[134] Kraynack, B. A. et al., Dsl1p, Tip20p, and the novel Dsl3(Sec39) protein are required for the stability of the Q/t-SNARE complex at the endoplasmic reticulum in yeast. *Mol Biol Cell* **16** (9), 3963 (2005).

[135] Sacher, M. et al., TRAPP, a highly conserved novel complex on the *cis*-Golgi that mediates vesicle docking and fusion. *EMBO J* **17** (9), 2494 (1998).

[136] Jones, S., Newman, C., Liu, F., and Segev, N., The TRAPP complex is a nucleotide exchanger for Ypt1 and Ypt31/32. *Mol Biol Cell* **11** (12), 4403 (2000).

[137] Cao, X., Ballew, N., and Barlowe, C., Initial docking of ER-derived vesicles requires Uso1p and Ypt1p but is independent of SNARE proteins. *EMBO J* **17** (8), 2156 (1998).

[138] Suvorova, E. S., Duden, R., and Lupashin, V. V., The Sec34/Sec35p complex, a Ypt1p effector required for retrograde intra-Golgi trafficking, interacts with Golgi SNAREs and COPI vesicle coat proteins. *J Cell Biol* **157** (4), 631 (2002).

[139] Kim, Y. G. et al., The architecture of the multisubunit TRAPP I complex suggests a model for vesicle tethering. *Cell* **127** (4), 817 (2006).

[140] Allan, B. B., Moyer, B. D., and Balch, W. E., Rab1 recruitment of p115 into a *cis*-SNARE complex: programming budding COPII vesicles for fusion. *Science* **289** (5478), 444 (2000).

[141] Shorter, J. et al., Sequential tethering of Golgins and catalysis of SNAREpin assembly by the vesicle-tethering protein p115. *J Cell Biol* **157** (1), 45 (2002).

[142] Short, B., Haas, A., and Barr, F. A., Golgins and GTPases, giving identity and structure to the Golgi apparatus. *Biochim Biophys Acta* **1744** (3), 383 (2005).

[143] VanRheenen, S. M. et al., Sec35p, a novel peripheral membrane protein, is required for ER to Golgi vesicle docking. *J Cell Biol* **141** (5), 1107 (1998).

[144] VanRheenen, S. M. et al., Sec34p, a protein required for vesicle tethering to the yeast Golgi apparatus, is in a complex with Sec35p. *J Cell Biol* **147** (4), 729 (1999).

[145] Sacher, M. et al., TRAPP I implicated in the specificity of tethering in ER-to-Golgi transport. *Mol Cell* **7** (2), 433 (2001).

[146] Morozova, N. et al., TRAPPII subunits are required for the specificity switch of a Ypt-Rab GEF. *Nat Cell Biol* **8** (11), 1263 (2006).

[147] Ortiz, D., Medkova, M., Walch-Solimena, C., and Novick, P., Ypt32 recruits the Sec4p guanine nucleotide exchange factor, Sec2p, to secretory vesicles; evidence for a Rab cascade in yeast. *J Cell Biol* **157** (6), 1005 (2002).

[148] Medkova, M., France, Y. E., Coleman, J., and Novick, P., The rab exchange factor Sec2p reversibly associates with the exocyst. *Mol Biol Cell* **17** (6), 2757 (2006).

[149] Novick, P. et al., Interactions between Rabs, tethers, SNAREs and their regulators in exocytosis. *Biochem Soc Trans* **34** (Pt 5), 683 (2006).

[150] de Renzis, S., Sönnichsen, B., and Zerial, M., Divalent Rab effectors regulate the sub-compartmental organization and sorting of early endosomes. *Nat Cell Biol* **4** (2), 124 (2002).

[151] Li, G., Rab5 GTPase and endocytosis. *Biocell* **20** (3), 325 (1996).

[152] Mohrmann, K. and van der Sluijs, P., Regulation of membrane transport through the endocytic pathway by rabGTPases. *Mol Membr Biol* **16** (1), 81 (1999).

[153] Pfeffer, S., Membrane domains in the secretory and endocytic pathways. *Cell* **112** (4), 507 (2003).

[154] Lippé, R. et al., Functional synergy between Rab5 effector Rabaptin-5 and exchange factor Rabex-5 when physically associated in a complex. *Mol Biol Cell* **12** (7), 2219 (2001).

[155] Shin, H. W. et al., An enzymatic cascade of Rab5 effectors regulates phosphoinositide turnover in the endocytic pathway. *J Cell Biol* **170** (4), 607 (2005).

[156] Barbieri, M. A. et al., Role of rab5 in EGF receptor-mediated signal transduction. *Eur J Cell Biol* **83** (6), 305 (2004).

[157] Ceresa, B. P., Regulation of EGFR endocytic trafficking by rab proteins. *Histol Histopathol* **21** (9), 987 (2006).

[158] Rink, J., Ghigo, E., Kalaidzidis, Y., and Zerial, M., Rab conversion as a mechanism of progression from early to late endosomes. *Cell* **122** (5), 735 (2005).

[159] Subramanian, S., Woolford, C. A., and Jones, E. W., The Sec1/Munc18 protein, Vps33p, functions at the endosome and the vacuole of Saccharomyces cerevisiae. *Mol Biol Cell* **15** (6), 2593 (2004).

[160] Horazdovsky, B. F. et al., A novel RING finger protein, Vps8p, functionally interacts with the small GTPase, Vps21p, to facilitate soluble vacuolar protein localization. *J Biol Chem* **271** (52), 33607 (1996).

[161] Piper, R. C. and Luzio, J. P., Ubiquitin-dependent sorting of integral membrane proteins for degradation in lysosomes. *Curr Opin Cell Biol* **19** (4), 459 (2007).

[162] Urbé, S., Ubiquitin and endocytic protein sorting. *Essays Biochem* **41**, 81 (2005).

[163] Ding, W. X. and Yin, X. M., Sorting, recognition and activation of the misfolded protein degradation pathways through macroautophagy and the proteasome. *Autophagy* **4** (2), 141 (2008).

[164] Hicke, L., Ubiquitin-dependent internalization and down-regulation of plasma membrane proteins. *FASEB J* **11** (14), 1215 (1997).

[165] Katzmann, D. J., Odorizzi, G., and Emr, S. D., Receptor downregulation and multivesicular-body sorting. *Nat Rev Mol Cell Biol* **3** (12), 893 (2002).

[166] Hicke, L. and Dunn, R., Regulation of membrane protein transport by ubiquitin and ubiquitin-binding proteins. *Annu Rev Cell Dev Biol* **19**, 141 (2003).

[167] Di Fiore, P. P., Polo, S., and Hofmann, K., When ubiquitin meets ubiquitin receptors: a signalling connection. *Nat Rev Mol Cell Biol* **4** (6), 491 (2003).

[168] Enmon, J. L., de Beer, T., and Overduin, M., Solution structure of Eps15's third EH domain reveals coincident Phe-Trp and Asn-Pro-Phe binding sites. *Biochemistry* **39** (15), 4309 (2000).

[169] Pelham, H. R., Membrane traffic: GGAs sort ubiquitin. *Curr Biol* **14** (9), R357 (2004).

[170] Russell, M. R., Nickerson, D. P., and Odorizzi, G., Molecular mechanisms of late endosome morphology, identity and sorting. *Curr Opin Cell Biol* **18** (4), 422 (2006).

[171] Hurley, J. H., ESCRT complexes and the biogenesis of multivesicular bodies. *Curr Opin Cell Biol* **20** (1), 4 (2008).

[172] Rieder, S. E. et al., Multilamellar endosome-like compartment accumulates in the yeast vps28 vacuolar protein sorting mutant. *Mol Biol Cell* **7** (6), 985 (1996).

[173] Williams, R. L. and Urbé, S., The emerging shape of the ESCRT machinery. *Nat Rev Mol Cell Biol* **8** (5), 355 (2007).

[174] Bilodeau, P. S., Urbanowski, J. L., Winistorfer, S. C., and Piper, R. C., The Vps27p Hse1p complex binds ubiquitin and mediates endosomal protein sorting. *Nat Cell Biol* **4** (7), 534 (2002).

[175] Bache, K. G., Raiborg, C., Mehlum, A., and Stenmark, H., STAM and Hrs are subunits of a multivalent ubiquitin-binding complex on early endosomes. *J Biol Chem* **278** (14), 12513 (2003).

[176] Teo, H., Perisic, O., González, B., and Williams, R. L., ESCRT-II, an endosome-associated complex required for protein sorting: crystal structure and interactions with ESCRT-III and membranes. *Dev Cell* **7** (4), 559 (2004).

[177] Nickerson, D. P., Russell, M. R., and Odorizzi, G., A concentric circle model of multivesicular body cargo sorting. *EMBO Rep* **8** (7), 644 (2007).

[178] Bowers, K. et al., Protein-protein interactions of ESCRT complexes in the yeast Saccharomyces cerevisiae. *Traffic* **5** (3), 194 (2004).

[179] Bowers, K. et al., Degradation of endocytosed epidermal growth factor and virally ubiquitinated major histocompatibility complex class I is independent of mammalian ESCRTII. *J Biol Chem* **281** (8), 5094 (2006).

[180] Bilodeau, P. S. et al., Vps27-Hse1 and ESCRT-I complexes cooperate to increase efficiency of sorting ubiquitinated proteins at the endosome. *J Cell Biol* **163** (2), 237 (2003).

[181] Babst, M. et al., Escrt-III: an endosome-associated heterooligomeric protein complex required for mvb sorting. *Dev Cell* **3** (2), 271 (2002).

[182] Babst, M., Wendland, B., Estepa, E. J., and Emr, S. D., The Vps4p AAA ATPase regulates membrane association of a Vps protein complex required for normal endosome function. *EMBO J* **17** (11), 2982 (1998).

[183] Vajjhala, P. R. et al., Vps4 regulates a subset of protein interactions at the multivesicular endosome. *FEBS J* **274** (8), 1894 (2007).

[184] Kieffer, C. et al., Two Distinct Modes of ESCRT-III Recognition Are Required for VPS4 Functions in Lysosomal Protein Targeting and HIV-1 Budding. *Dev Cell* **15** (1), 62 (2008).

[185] Christoforidis, S. and Zerial, M., Purification and identification of novel Rab effectors using affinity chromatography. *Methods* **20** (4), 403 (2000).

[186] Horiuchi, H. et al., A novel Rab5 GDP/GTP exchange factor complexed to Rabaptin-5 links nucleotide exchange to effector recruitment and function. *Cell* **90** (6), 1149 (1997).

[187] Hama, H., Tall, G. G., and Horazdovsky, B. F., Vps9p is a guanine nucleotide exchange factor involved in vesicle-mediated vacuolar protein transport. *J Biol Chem* **274** (21), 15284 (1999).

[188] Esters, H. et al., Vps9, Rabex-5 and DSS4: proteins with weak but distinct nucleotide-exchange activities for Rab proteins. *J Mol Biol* **310** (1), 141 (2001).

[189] Peterson, M. R., Burd, C. G., and Emr, S. D., Vac1p coordinates Rab and phosphatidylinositol 3-kinase signaling in Vps45p-dependent vesicle docking/fusion at the endosome. *Curr Biol* **9** (3), 159 (1999).

[190] Mills, I. G., Jones, A. T., and Clague, M. J., Regulation of endosome fusion. *Mol Membr Biol* **16** (1), 73 (1999).

[191] Peplowska, K. et al., The CORVET tethering complex interacts with the yeast Rab5 homolog Vps21 and is involved in endo-lysosomal biogenesis. *Dev Cell* **12** (5), 739 (2007).

[192] Rieder, S. E. and Emr, S. D., A novel RING finger protein complex essential for a late step in protein transport to the yeast vacuole. *Mol Biol Cell* **8** (11), 2307 (1997).

[193] Raymond, C. K. et al., Molecular analysis of the yeast VPS3 gene and the role of its product in vacuolar protein sorting and vacuolar segregation during the cell cycle. *J Cell Biol* **111** (3), 877 (1990).

[194] Srivastava, A., Woolford, C. A., and Jones, E. W., Pep3p/Pep5p complex: a putative docking factor at multiple steps of vesicular transport to the vacuole of Saccharomyces cerevisiae. *Genetics* **156** (1), 105 (2000).

[195] Rothman, J. H., Yamashiro, C. T., Kane, P. M., and Stevens, T. H., Protein targeting to the yeast vacuole. *Trends Biochem Sci* **14** (8), 347 (1989).

[196] Nichols, B. J. et al., Homotypic vacuolar fusion mediated by t- and v-SNAREs. *Nature* **387** (6629), 199 (1997).

[197] Fischer von Mollard, G. and Stevens, T. H., The Saccharomyces cerevisiae v-SNARE Vti1p is required for multiple membrane transport pathways to the vacuole. *Mol Biol Cell* **10** (6), 1719 (1999).

[198] Cowles, C. R., Emr, S. D., and Horazdovsky, B. F., Mutations in the VPS45 gene, a SEC1 homologue, result in vacuolar protein sorting defects and accumulation of membrane vesicles. *J Cell Sci* **107 (Pt 12)**, 3449 (1994).

[199] Becherer, K. A., Rieder, S. E., Emr, S. D., and Jones, E. W., Novel syntaxin homologue, Pep12p, required for the sorting of lumenal hydrolases to the lysosome-like vacuole in yeast. *Mol Biol Cell* **7** (4), 579 (1996).

[200] Burd, C. G., Mustol, P. A., Schu, P. V., and Emr, S. D., A yeast protein related to a mammalian Ras-binding protein, Vps9p, is required for localization of vacuolar proteins. *Mol Cell Biol* **16** (5), 2369 (1996).

[201] Odorizzi, G., Babst, M., and Emr, S. D., Fab1p PtdIns(3)P 5-kinase function essential for protein sorting in the multivesicular body. *Cell* **95** (6), 847 (1998).

[202] Horazdovsky, B. F., Busch, G. R., and Emr, S. D., VPS21 encodes a rab5-like GTP binding protein that is required for the sorting of yeast vacuolar proteins. *EMBO J* **13** (6), 1297 (1994).

[203] McMahon, H. T. and Mills, I. G., COP and clathrin-coated vesicle budding: different pathways, common approaches. *Curr Opin Cell Biol* **16** (4), 379 (2004).

[204] Collins, K. M., Thorngren, N. L., Fratti, R. A., and Wickner, W. T., Sec17p and HOPS, in distinct SNARE complexes, mediate SNARE complex disruption or assembly for fusion. *EMBO J* **24** (10), 1775 (2005).

[205] Tall, G. G., Hama, H., DeWald, D. B., and Horazdovsky, B. F., The phosphatidylinositol 3-phosphate binding protein Vac1p interacts with a Rab GTPase and a Sec1p homologue to facilitate vesicle-mediated vacuolar protein sorting. *Mol Biol Cell* **10** (6), 1873 (1999).

[206] Salminen, A. and Novick, P. J., The Sec15 protein responds to the function of the GTP binding protein, Sec4, to control vesicular traffic in yeast. *J Cell Biol* **109** (3), 1023 (1989).

[207] Longtine, M. S. et al., Additional modules for versatile and economical PCR-based gene deletion and modification in Saccharomyces cerevisiae. *Yeast* **14** (10), 953 (1998).

[208] Janke, C. et al., A versatile toolbox for PCR-based tagging of yeast genes: new fluorescent proteins, more markers and promoter substitution cassettes. *Yeast* **21** (11), 947 (2004).

[209] Puig, O. et al., New constructs and strategies for efficient PCR-based gene manipulations in yeast. *Yeast* **14** (12), 1139 (1998).

[210] Shorter, J. et al., GRASP55, a second mammalian GRASP protein involved in the stacking of Golgi cisternae in a cell-free system. *EMBO J* **18** (18), 4949 (1999).

[211] Griffith, J., Mari, M., De Mazière, A., and Reggiori, F., A cryosectioning procedure for the ultrastructural analysis and the immunogold labelling of yeast Saccharomyces cerevisiae. *Traffic* **9** (7), 1060 (2008).

[212] Robinson, J. S., Klionsky, D. J., Banta, L. M., and Emr, S. D., Protein sorting in Saccharomyces cerevisiae: isolation of mutants defective in the delivery and processing of multiple vacuolar hydrolases. *Mol Cell Biol* **8** (11), 4936 (1988).